Republic of Iraq
Ministry of Higher Education and
Scientific Research
University of Babylon
College of Materials Engineering
Department of ceramic and building
Materials

Thermal investigation of ceramic oxide materials for coating of diesel engine piston

A Thesis

Submitted to the Department of ceramic and building Materials at College of Materials Engineering / University of Babylon in Partial Fulfillment of the Requirement for the Master Degree in Materials Engineering / Ceramic

By

Mohammed Kadhim Hussein Alwan

(B.Sc. In Materials Engineering)

(2002)

Supervised by

Prof. Dr. Elham Abdul-Majeed

2022 A.D

Prof. Dr. Hayder Kraidi Rashid

1443H

بسم الله الرحمن الرحيم

"ويسألونك عن الروح قل الروح من امر

ربي وما اوتيتم من العلم الا قليلا"

صدق الله العلي العظيم

الآية 85 ,الاسراء

Supervisors Certification

We certify that this thesis, entitled ***(*Thermal investigation of ceramic oxide materials for coating of diesel engine piston *)*** was prepared by the student **(**Mohammed Kadhim Hussein**)**, under our supervision , in partial fulfillment of the requirements for the degree of Sciences in Materials Engineering / Ceramic , at the Department of Materials Engineering / Ceramic

Supervisors

signature

Prof. Dr. Elham Abdul-Majeed

Date / / 2022

signature

Prof. Dr. Hayder Kraidi Rashid

Date / / 2022

Linguistic Certification

I certify that this thesis, entitled " **Thermal investigation of ceramic oxide materials for coating of diesel engine piston** ", was prepared under my linguistic supervision. It was amended to meet the style of the English language.

Signature:

Name:

Title:

Data / / 2022

Certification of the Examining Committee

We certify that we have read the thesis entitled " **Thermal investigation of ceramic oxide materials for coating of diesel engine piston** ", and as an examining committee, examined the student **(Mohammed kadhim Hussein)**, in its contents and that in what is connected with it, and that in our opinion it meets the standard of a thesis for the degree **of Sciences in Materials Engineering / Ceramic**

Signature
Prof. Dr. Samir Hamid Awad
Chairman
Date : / / 2022

Signature
Prof.Dr. Abdul Raheem Kadhim Abd Ali
(Member)
Date / / 2022

Signature
Asst. Prof. Dr. Hanaa .A. Al Kaisy
(Member)
Date / / 2022

Signature
Prof. Dr. Elham Abdul-Majeed
(Supervisor)
Date / / 2022

Signature
Prof. Dr**.** Hayder Kraidi Rashid
(Supervisor)
Date / / 2022

Signature
Prof.Dr. Mohsin Abbas Aswad
Head of ceramic and building material department
Date / / 2022

Signature
Prof .Dr. Imad Ali Disher
Dean of material engineering college
Date / / 2022

Dedication

To my family,

Mother and son soul

and

To All my teachers

Acknowledgements

First of all, profusely all thanks be for Allah Lord of all creation and AHLUl-Bayt (peace on them) Who enable me to achieve my dream.

I would like to express my gratitude to my supervisor , **Prof.Dr. Elham Abdul-majeed** and **Prof.Dr. Hayder Kraidi Rashid** for their guidance, advise and enthusiastic encouragement through this study.

I am very grateful to my brothers, sisters who backed me continuously, especially, **Asst. prof. Dr. yehya kadhim**.

My lovely wife and sons, I introduce my big thanks for their assistance , encouragement and support me during the time of preparing this work.

I also introduce my many thanks for ceramic and building material department teachers and laboratories staff for big help that timely introduce.

Finally , I express my great thanks and gratitude to the College of Materials Engineering and the University of Babylon for providing the laboratories and possible equipment to carry out the research in the best case.

Abstract

Diesel engines are used in many industrial applications in addition to those in cars. Developing diesel engines to be more efficient with less fuel consumption, low gas emissions, and high performance an objective of many researchers. Ceramic thermal barrier coatings (TBC) have been identified as the most promising method of developing diesel engines.

In this study, a new coating (TBC) as a single layer, attempting to replace a yttria stabilize zirconia coating that contains three layers to overcome many issues such as spallation. Beside owing lower thermal conductivity of new coating ,It improves combustion features, resulting in enhanced efficiency and economic and environmental performance of the diesel engine. The A304 alloy steel diesel piston was brought from oil products distribution company stores (OPDC) / Babylon branch. Eight coatings blends were prepared to investigate their properties using ceramic powder materials, that is, magnesium oxide (MgO), Aluminum oxide (Al2O3), Silicon oxide (SiO2), and zirconium oxide (ZrO2), at different percentages and were numbered (M1,M2,…M8). Two of these blends show the lowest thermal conductivity among others, namely, M4 which contain ($MgO=30\%, Al_2O_3=45\%, SiO_2=25\%$),and M7 which contain ($MgO=35\%, Al_2O_3=30\%, SiO_2=25\%, ZrO_2=10\%$).

Flame spraying was the technique adopted using an acetylene and oxygen mixture under a pressure of 0.6 bar and 5 bar for acetylene and oxygen, respectively. Furthermore, X-ray diffraction (XRD), scanning electron microscopy (SEM), and Atomic force microscopy (AFM) tests were carried out to identify and characterize the microstructure and morphology of the powders and coated layer. Thermal conductivity, coating layer thickness, porosity content , and adhesion strength are also tested to determine the thermal conductivity of the TBC coating

layer, which confirmed the thermal conductivity of M4 and M7 was the lower among other blends , which have the lowest values of 0.831334 W/m .c and 0.72186 W/m .c, respectively. The coating layer thickness was about 0.6 mm with a porosity content of about 15–20%.The highest adhesion strength of specimens was about 20 MPa, which was for the M7 blend.

The results are used in the simulation process using Ansys workbench 16.1 simulation software as a steady-state thermal condition. The model was built using the actual dimensions of the diesel piston and coating layer, and it was then simulated with an initial and boundary condition (700C as the operation temperature and 30C as the initial and environmental temperature).The model geometry was discretized and optimized until obtaining the best number of elements, which is (213514) elements and (303548) nodes with the quadratic shape. The obtained results confirmed the temperature was lowered at the piston crown surface after coating to (534 C^o and 513 C^o) for M4 and M7 specimens coated, respectively. That means the lower temperatures ranged between 165 C^o and 190C^o.

List of Contents

List of Contents

List of Figures

List of Tables

List of symbols

Symbol	Physical Meaning	Units
d	Disc or specimen diameter ……	mm
dt/dx	Temperature gradient over disc thickness…….	-
E	Thermal energy passed throw discs……	Watt
H_{coat}	coating layer thickness……	um
HV	Vickers hardness value……	gmf/m^2
I	Current ……	Amp
J	Heat flux ……	Watt
K	Thermal conductivity…….	$W/m.C^o$
P	Load that is applied on coated sample……	N
R	Radius of disc…….	mm
T	Temperature……	C^o
V_{coat}	Coating layer volume…….	mm^3
V	Electrical potential …….	volts
W	Weight of specimen……	gm

Abbreviations

APS	Air Plasma Spraying process
AFM	Atomic Force Microscopy
BC	Bond coat layer
CTE	Coefficient of Thermal Expansion
EB-PVD	Electron –beam physical vapor deposition process
EDS	Energy Dispersive spectroscopy
FEM	Finite Element Method
FS	Flame Spraying
IC	Internal combustion engine
LPPS	Low Pressure Plasma Spraying Process
LZ	Lanthanum zirconate
LHR	Low heat Rejection Engine
MgSZ (MSZ)	Magnesia stabilized Zirconia
MAO	Micro Arc Oxidation
M4	Symbol of the fourth blend
M7	Symbol of the seventh blend
OPDC	Oil products distribution company
SEM	Scanning electron Microscopy
SLPM	Standard Litter per minute (Flow Rate Gas measurement)
TBC	Thermal Barrier coating
TGO	Thermal Grown Oxide
TC	Top Coating Layer
VPS	Vacuum Plasma Spraying
XRD	X-Ray diffraction test
YSZ	Yttria stabilized zirconia

Chapter one

1.1. General view.

The right use of thermal insulation materials in internal combustion engine manufacturing helps increase the performance and service life of internal component while lowering maintenance costs. Furthermore, advanced insulation materials or surface engineering technologies may be used to improve the insulation capability of the engine components based on their temperature retention capacities[1].Material scientists observed that ceramic materials have high working temperatures and other good thermophysical and mechanical properties, so they selected them as TBC can be applied on metals or alloys operating under high temperatures[2]. TBC has generally been used in IC engines to protect components from high temperatures effects and oxidation, extending the engine's service life, optimizing the combustion characteristics and increase engine performance[3]. Many researchers reviewed many more ceramic materials. They summarized some types that have properties that make them suitable to be used as ceramic coatings, such as alumina, mullite, yttria stabilized zirconia, and some general structures like the fluorite structure (AB structure), and the pyrochlore structure ($A_2B_2O_7$). These materials are often applied using thermal spraying techniques like plasma spraying and EB-PVD. These two techniques are more commonly used[4].

1.2.Introduction

TBC are a multi-layer coating system with a distinct function for each layer[5].The topcoat layer, which is deposited on the intermediate layer, provides thermal insulation and is composed of ceramic materials with low thermal conductivity. The second layer is a bond coat, which is an intermediate layer that is applied directly to the metal surface. Its function is to protect the metal substrate from oxidation and enhance adhesion between the topcoat and the substrate surface. It's either a diffusion aluminide, like platinum aluminide, or an overlay coating, typically NiCoCrAlY.[6]

TBC are typically conducted in gas turbine engines for land power generation, aero-engine, marine, and diesel engine applications to reduce the surface temperature of the combustion chamber and the hottest component[7]. The majority of the heat generated during the combustion process is transferred to engine components via the piston in internal combustion engines. Engine coating with a ceramic thermal barrier can be used to improve the reliability and durability of diesel engine performance and efficiency. Cooling spends 30% of total energy loss, and it was determined that engine coating could be a viable solution[8].Fuel energy must convert to kinetic energy at the fastest possible rate to achieve better engine performance. The use of low heat-conducting ceramic materials to coat combustion chambers causes an increase in temperature and pressure in internal combustion engine cylinders. resulting in an increase in the engine efficiency[9].

Engineers tend to use computer abilities, which make calculations easier and more accurate, to achieve their objectives with less effort, cost, and time. Ansys, is a computer program build on basis of finite element method for all purpose of engineering analysis which has the power to analyze a wide range of various engineering problem, it is the preferred analytical software used by design

engineers. Drawings, preprocessing, solutions, and post- processing are all included in a single, comprehensive package[10]. Ansys generates and solves equations that control the behavior of materials or components being analyzed. After that, results are showed with graphical charts or tables. This analyzing method is generally utilized to create and improve a system that's very hard to calculate by hand[11].

In this thesis, ANSYS Workbench 16.2 software in a steady-state heat transfer system is used. The initial thermal and physical material properties are entered of new designed material. The structural model was initially built using the program abilities of a design modeler and then analyzed thermally.

1.3 Statement of the Problem

The large fleet of fuel tankers that are owned by the oil products distribution company consume large quantities of fuel, which has an economic effect on the company and an environmental effect on society ,therefore, this problem was addressed by researching to improve the performance of the tankers carrier engines, which operate with diesel. reduce the fuel consumption which mean less cost that were spend on fuel in addition to enhance the gas emissions characteristic that result from fuel combustion.

. To find out , coherent, compatible, thermal protective materials alternative to conventional materials while matching the specifications of lower-temperature engines such as diesel engines at the lowest cost and having better features, diesel engine enhancements are focused always on increasing the performance and efficiency of the engine, in addition to reducing fuel consumption and gas emissions. These developments are achieved through improving the fuel burning characteristics in the combustion chamber.

The thermal insulation is one of the important approaches in order to achieve this target which depends on utilizing low thermal conductivity materials such as ceramic. For the aforementioned purposes, the piston crown, piston rings, cylinder wall, manifolds, exhaust and intake valves are all coated with ceramic material by a different researchers.

1.4 The Aim of The study

The goal of a thesis is to prepare an effective coating layer suitable to deposit on diesel engine components. The new coating layer should has a good thermal reduction and is cost-effective to be used on the diesel engine piston crown to reduce the energy spend on engine cooling and improve the combustion process and gases emission type. This type of coatings will benefit the oil products distribution company and the community. When mixed with other oxides (SiO_2, Al_2O_3, ZrO_2, etc.), magnesium oxide (MgO), which has excellent thermal and mechanical properties, becomes a suitable choice to study as a new coating for diesel engines. Using MgO with other oxides as a thermal protective layer on the piston crown is being investigated.

1.5 Thesis Structure

This thesis is divided into five chapters that detail the research effort done, the results obtained, conclusions, and suggestions.

The first chapter includes an introduction and a broad overview of Thermal Barrier Coatings (TBC). It also includes the topic of the current study and the thesis framework.

A theoretical basis and the application fields of TBC are provided in chapter two. Which is divided into seven subdivisions that cover a wide range of TBC. It also covers the structure of TBC, The most common ceramic materials used in

TBC processing, as well as the properties that these materials must have in order to be suitable choices, the important manufacturing processes used to manufacture TBC, the advantages of employing it in diesel engine, and a brief overview of the significance of simulation in validation the results we obtained.in addition to, literature survey of some researchers that were worked on this type of coating.

Chapter three provides an explanation of the experimental work, starting with material characterization, mixtures preparation, the coating process, and the manipulated conditions, as well as the characterization of TBC layer. XRD, SEM, SEM-EDS, AFM tests, the thermal conductivity tests, micro-hardness and adhesion tests, coating layer thickness, roughness, porosity content, piston model building by Ansys and meshing process with boundary condition application .they are included in this chapter.

Chapter four describes the results obtained, which are represented in graphs and their interpretations, as well as performing the comparison with ANSYS program data.

The conclusions and recommendations are put in the last chapter, that is, chapter five, followed by appendices containing all of the related information to the thesis and not told in the preceding chapters.

Chapter Two

Theoretical part

2.1 Introduction

This chapter of the thesis reviews the nature of the TBC used to coat a diesel engine piston, as well as a definition of its constituent layers, the types of materials used to achieve it, and the most common methods of its application, in addition to a simple introduction to the ANSYS program that was used to perform a simulation process to show the thermal gradient of the coating layer.

2.2. Thermal barrier coating system (TBCs)

IC Engine development, worldwide rising fuel prices, and environmental considerations drive material engineers to look for new ways to improve the features of IC engines. The thermal barrier coating system (TBCs) is one of the most effective solutions for increasing the power of various engine[8].

(TBCs) system is used to reduce heat transfer to the surface of any metal component that is subjected to extremely high temperatures. It is made up of different layers, each with a definite function to perform, from outer to inner, top coat, bond coat. The first layer is made of ceramic materials with low thermal conductivity typically from (zirconate ceramics, mullite, alumina, earth oxides and other ceramic material) which protects the component and reduces heat arrival. This layer is known as the topcoat layer which is deposited on the intermediate layer called bond coat[6]. The bond coat, the important second layer in order , is composed of a super alloy (MAlY, where M = Ni, Cr, Co) that provides a rough interface between the other two layers (top coat and substrate), therefore, enhancing the adhesion between them as well as reducing the thermomechanical stresses as a result of the high coefficient of expansion that has conformed somewhat to the

substrate alloy composition [6,9].The substrate surface, the final layer, is sometimes steel alloys or super alloys like Ni, Cr alloys that must be best prepared for coating[13],[14]. As a result of the bond coat oxidation, a thin thermally grown oxide (TGO) layer composed of alumina (Al_2O_3) arises at the TC/BC interface, causes spallation, or the final failure of the coating[15,6, 7].

TBC has some benefits when utilized in a diesel engine. Heat can be retained inside the engine, thermal fatigue and shocks can be avoided. Additionally, by minimizing heat flux into the piston and reducing fuel consumption, a piston can be guarded against corrosion damage, thermal stress, also reducing high temperature carbon emissions. Moreover, TBC can retain so much more heat within the engine even with low-quality fuels. Therefore, TBC may be beneficial in achieving more economical engine performance [16,17].

Flame spraying , Air plasma spraying (APS), electron beam-physical vapor deposition (EB-PVD), and High velocity oxy fuel (HVOF) are commonly used technologies to apply the ceramic top layer. Other techniques for applying TBC include sol-gel, solution precursor plasma spraying (spps), which are rarely used[16,18,19].

2.3 Properties for TBC materials

The work conditions, design, and function of TBC are the number of TBC layers, microstructure desired, and substrate metal type impose constraints on the coating materials selection [9]. Table2.1 specifies the significant features of the ceramic coating of the TBC system[17,20,21].

Table 2.1: Ceramic Materials Requirements for TBC [21]

features	**status**	**explanation**
Thermal conductivity	low	Thermal conductivity is inversely related to temperature decreases.
Phase	No change	In a thermal cyclic process, phase transition is substantially damaging
Thermal expansion Coefficient	High	The substrate and bond coat on which the TBC is applied must expand in a similar manner.
Melting point	High	the temperature of operation is very high
Oxidation resistance	High	Strong oxidizing working conditions
Strain tolerance	High	Strong oxidizing working conditions imposes large strain ranges

The topcoat layer materials should have low thermal conductivity to transfer significantly decreased heat through the topcoat layer into the beneath layer, furthermore, to be resistant to high working temperatures without melting, the topcoat materials ought to have a high melting point [17].

Strain compliance is needed for the material to resist the strains related to thermal expansion difference between the topcoat layer and bond coat or the substrate during heating and cooling cycling. If there is no strain compliance, for example, as a result of a lower modulus of elasticity, the high elastic difference might create extremely high stresses and result in sudden failure on cooling[15]. On the other hand, since TBCs' essential duty is as a thermal barrier. The highly offensive thermomechanical conditions in which they must operate necessitates that they also fulfill other stringent performance requirements. In internal combustion engines, TBC coatings must be capable of resisting continuous exposure to high temperatures in an oxidizing environment. To meet those criteria, refractory oxides are the concentrate of looking for novel and alternative TBC materials[21].

2.4.Ceramic materials for thermal barrier coating

Because of its low thermal conductivity, moderately high coefficient of thermal expansion, and suitable toughness, 6–8 wt% YSZ is the most commonly used topcoat material. Other ceramics used as TBC materials besides YSZ include mullite, Forsterite, Al_2O_3, TiO_2, CeO_2+YSZ, La_2 Zr_2O_7, Spinel, perovskites, and pyrochlore [7],[20]. Several topcoat materials have been reviewed for diesel engine applications over the decades. Most of these materials is explained in figure2.1 below[18].

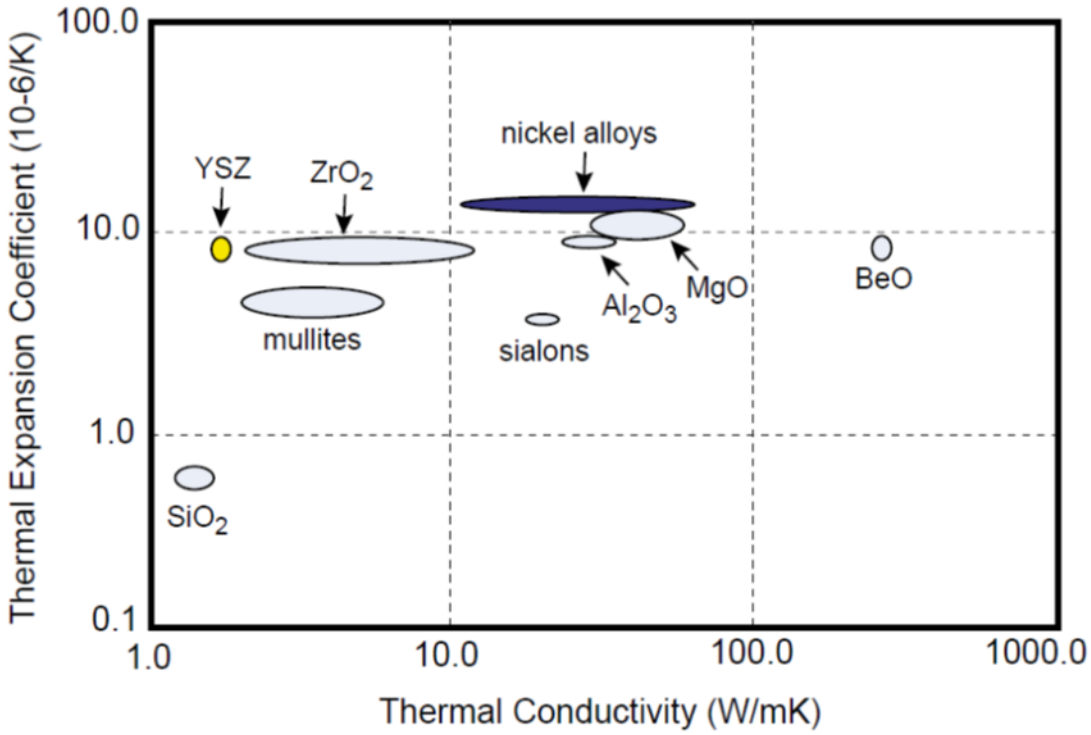

Figure 2.1:. distribution of TBC materials based on thermal properties [18,22]

2.4.1 Magnesium oxide (MgO)

Magnesia (Magnesium oxide ,MgO) is found in nature as the metamorphic mineral periclase, which is produced by the breakdown of dolomite ($CaMg(CO_3)_2$). Magnesium carbonate ($MgCO_3$) and magnesium hydroxide [$Mg(OH)_2$] are the two most common origins of MgO. magnesium-rich brines and Seawater may both be used to make magnesium oxide [23].

MgO has a molecular weight is (40.32 gm/mol) with a density 3.65 gm/cm3 crystallizes in a cubic structure with a melting point of 2800 degrees Celsius and an ionic bond [24]. The bulk of magnesia is utilized in refractories in the iron and steel industry, where the material's basic oxide characteristics are required. Magnesia can resist the extreme heat of converters up to (1,700°C) [25]. Another important application of magnesium oxide is as an insulator in heating systems. The thermal conductivity and electrical resistance of periclase (MgO) at high temperatures are key feature in this application. Periclase has still another using where employed in thermocouple insulation. Because the great majority of these are used in nuclear applications [24].

2.4.2 Alumina (Al_2O_3)

Alumina is extremely hard and chemically inert. When compared to yttria-stabilized zirconia, it has a higher thermal conductivity and a lower thermal expansion coefficient. Coating hardness can also be increased by spraying an outer layer of alumina onto YSZ coatings [18]. Because of its low oxygen diffusivity, alumina arises gradually at elevated temperatures, so it was designed to act as an intermediate barrier located between the bond coat and the topcoat, so that it protects the underling substrate from oxidation. [16,4].the alumina properties are shown in Fig 2.2.

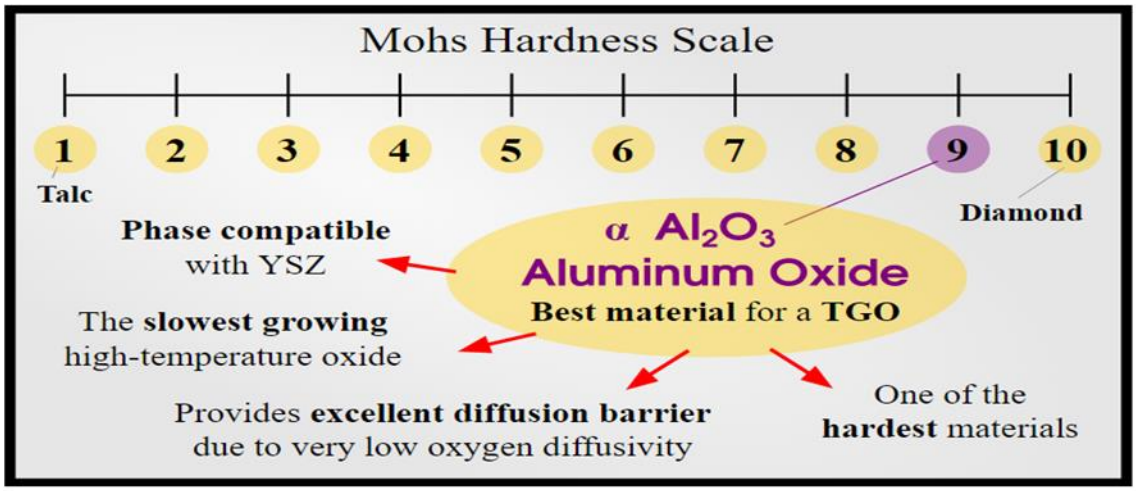

Fig 2.2: α -AL_2O_3 features which make it suitable for use as TBC material.[8]

2.4.3.Mullite ($3AL_2O_3.2SiO_2$)

Mullite is a compound of alumina and silica with a chemical formula ($3Al_2O_3$. $2SiO_2$). Compared with yttria-stabilized zirconia it has a higher thermal conductivity and much lower coefficient of thermal expansion (CTE), as well as being much more oxygen resistant. Mullite's low thermal expansion coefficient is an advantage over yttria-stabilized zirconia. Engine tests conducted with both materials show that the mullite coating in the engine lasts extremely longer than the zirconia coating. Mullite is a great TBC material alternative to zirconia especially for applications like diesel engines, where component temperatures are lower than in gas turbines blades or vanes[26], However, can summarize its positive and negative characteristics as[20]

Positive characteristic

- thermal conductivity is Low
- High resistance to oxidation
- High corrosion resistance
- Appropriate thermal shock resistance below 1270k̊

Negative characteristics

- Crystallization temperature rated between 1023 k̊ and 1273 k̊
- The coefficient of thermal expansion is very low.

2.4.4. Forsterite (Mg_2SiO_4)

Forsterite is a mineral with the chemical formula Mg2SiO4 that can be found in nature, incorporated in igneous rock. It has a melting point of around 1750 °C, therefore, it has a low heat conductance around 2.4W/m.k at (1000C̊) and high coefficient of thermal expansion (CTE) reach to 9.5×10^{-6}/C̊ [27,28]. it allows better coordination with the substrate. Coating a layer of hundreds of microns, it exhibits excellent thermal shock resistance[18]. It is particularly useful for low loss dielectrics and in designs where the coefficient of thermal expansion must match the metal-ceramic bond[29].Steel-making refractories for back fillers, crucible boards, and ladle protective linings for dolomite brick, roof brick, and electric arc furnace integrity linings are among its most widespread purposes. Forsterite is used in alloy plants and glass reservoir regenerators in industrial furnace applications[27]. Because of its good CTE can be used as a bond coat in multilayer TBCs systems[30].

2.4.5. Zirconia (ZrO2)

Zirconium dioxide (zirconia) is available in three structure types. They are Monolithic (m), tetragonal (t), and cubic (c). The monolithic structure is unchanging between ambient temperature and 1170C̊, but above 1170C̊, it transforms into a tetragonal structure. The stable structure up to 2379C̊ is tetragonal, after which it transforms into a cubic structure[9]. A metastable tetragonal phase is formed as a result of rapid cooling during the coating processes.

When heated to high temperatures, the tetragonal phase decomposes into a two-phase mixture of the tetragonal and cubic phases via diffusion. When the tetragonal phase later converts to the monoclinic phase, the coating may spall due to the volume Change , However, The tetragonal phase in a diesel engine is expected to be stable at relatively low temperatures[16]**.**fig 2.3 represent the phase diagram of zirconia .

Table 2.2: thermal and thermodynamic properties of zirconia [6]

Thermodynamic features	**value**
Boiling temperature	4300 C̊
Enthalby of phase change(t to m)	4.83x104 J/Kg
Melting Enthalby of Zr_2O_3	7.08x105 J/Kg
Vaporization Enthalby	5.23x106 J/Kg

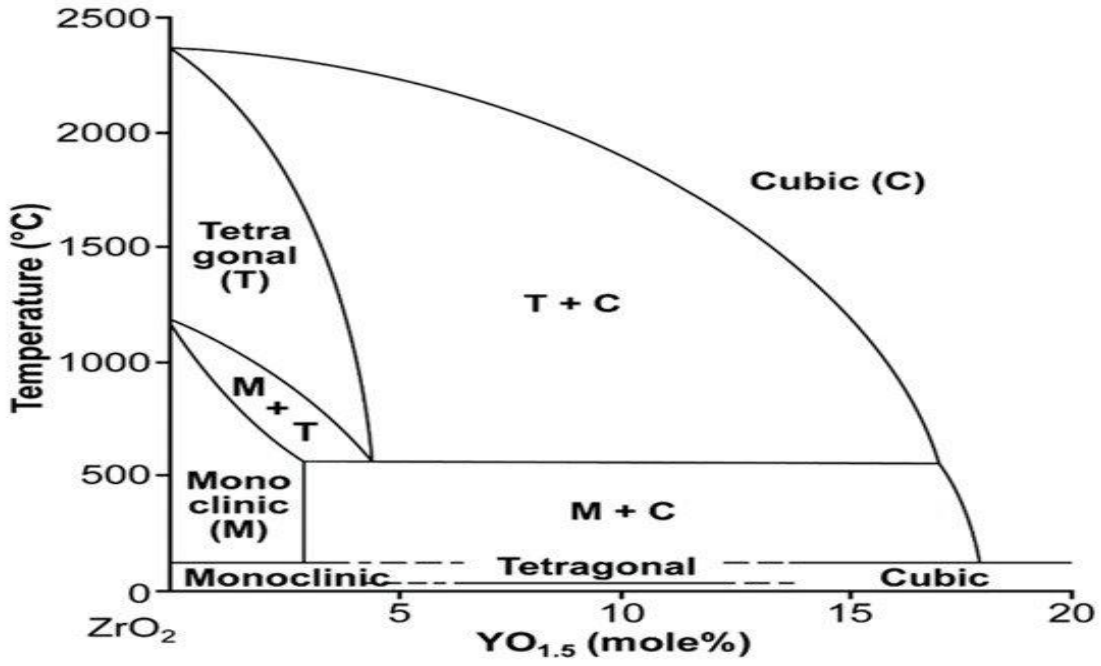

Figure 2.3: Phase diagram of ZrO2-Y2O3 system [31].

2.4.6 Lanthanum zirconate ($La_2Zr_2O_7$)

Lanthanum zirconate has a pyrochlore-structure, which has fracture toughness that is close to YSZ, and its thermal conductivity at higher temperatures is approximately 20% less than that of YSZ. Lanthanum zirconate has a thermal expansion of 9.1x10–6 K–1 at 30–1000°C, which is lower than that of YSZ and may result in higher stresses in the coating due to a larger thermal expansion mismatch with other layers in the TBC system. Thermal cycling studies of LZ and YSZ/LZ coatings, on the other hand, have yielded encouraging results. As a result, in diesel engine applications, this should not be a problem[16,20].

2.5.Surface Engineering

Surface engineering encompasses all scientific and technical problems connected with the manufacture of surface layers prior to end use or service (technological layers) or during service (service-generated layers), on or under the surface (superficial layers) or on a substrate (coatings), with properties differing from those of the material. depending on the type of effects utilized to form surface layers techniques of formation may be generally divided into six groups (mechanical, thermo-mechanical, thermal, thermo-chemical, electrochemical and chemical, and physical).[32]

2.5.1.Thermal spray technologies

Thermal spray is a method that applies a focused thermal source to melt or soften coating material (powder, wire) while process gases or fine particles jet are used to propel the coating material directly to the substrate surface. When the heated energetic particles collide with the surface of the component to be coated, they harden quickly. As more particles collide with the surface, a deposited layer thickness will increase. Thermal spraying may be used to make coatings out of

almost any substance that melts without degradation and creates a stable liquid phase. Despite the fact that a sprayed substance directly impacts a substrate as molten or partially melted, the temperature of substrate can be kept near ambient. [33]. Devices are used to achieve this function are usually called guns or torches [7,19]. It is obvious that only regions of parts that have easy accessibility for coating and are located on the track of the jet may be coated using thermal spraying; hence, it is difficult to cover entirely industrial components with complex designs. consequently, the major constraint is that thermal spraying is a "line of sight" process in comparison to other coating application processes[33].Thermal and kinetic energy can be provided into particles during transferred from nozzle to surface of substrate by two mean ,directly, as in electric arc spraying, or indirectly, as in plasma jets or flame process[19]. Thermal spraying techniques that are used in industrial process can be generally divided into two categories as follows[33].

The important properties of thermal spraying approaches were showed in Table 2.3

- Combustion(flame)
- Electrical (plasma)
  - The combustion spraying technologies are:
    - Flame spraying
    - High velocity oxy-fuel spraying (HVOF).
  - The plasma spraying technologies are:
    - Atmospheric plasma spraying (APS),
    - Low pressure plasma spraying (LPPS),
    - Vacuum plasma spraying (VPS).

Table2.3: thermal spraying parameters and properties[19], [33]

Deposition process	Gas type	Typical temperature c^o	Typical particle velocity ($m.s^{-1}$)	material feed rate ($g.min^{-1}$)	Coating density (%)	Bond strength MPa
Flame spraying	O_2, C_2H_2	3500	50-100	30-50	85-90	7-18
HVOF	CH_4,C_3H_6, H_2,O_2	5500	200-1000	15-50	>95	68
Plasma spraying	Ar,H_2 ,N_2,He	15000	200-800	25-150	90-95	>68
Wire Arc	Air, N_2, Ar	>25000	50-100	150-2000	80-95	10-40
Vacuum plasma spraying	Ar ,H_2,He	12000	200-600	25-150	90-99	>68

2.5.1 Flame spraying (FS)

The first thermal spray method, flame spray, was created in 1917 and is still in use [19,34]. It was first employed for low-melting metals like tin or lead, afterward it was expanded to include additional refractory metals and ceramic materials [35].Today it is one of the most cost-efficient coating processes for applying ceramic coatings for applications in automotive, aviation, power plants and other applications[36].

Flame spray produces heat by utilizing the chemical energy of burning fuel gas. The most widely used torch is the oxy-acetylene torch, it employs acetylene and oxygen to attain very high temperatures of flame, Feedstock which takes the form powder, rod, or wire is introduced directly to the rear of nozzle or to the flame from an outer can lies above. The flame spray torch contains gas distribution channels through the torch body and gas blending holes at the nozzle tip. Nozzles are used to form the jet pattern. Air caps sometimes are fixed to wire- and rod-fed torches which result in a concentrated air stream to atomize the molten wire or rod

tip. Wires or rods are mechanically drawn across the nozzle center into the heating region .Powder is injected into spray torches by one of the following methods (carrier gas or gravity feeding). Powder cans or bottles are immediately attached to and on top of the torch in gravity-fed systems. A pressure valve regulates the pace at which powder is fed into the torch's body, where it is sucked by the gases that flow through it [19,37]. The flame temperature varies depending on whether the fuel is among the gases that are commonly combined with oxygen to create a flame. Acetylene, natural gas, hydrogen, propane, methyl-acetylene propadiene stabilized, and other synthetic fuels and hydrocarbons are the gases that are that are the most commonly used.an oxy-acetylene flame may reach over 3000 °C [19,36].

In the flame, coating materials either melts entirely or becomes sufficiently soft. A gas jet accelerates the particles or droplets into the substrate surface where they are stick as a coating layer[34].The best adhesion strength of coting layers is in the range of 15 MPa of ceramic material coatings to 30 MPa for metals and alloys coatings. Porosity percentages range from 10% to 20%, while typical thicknesses range from 100 to 2500 μm [35,38]. There are two forms of flame spray technique, these are powder flame spraying and wire or rod flame spray method which will explained below[19,35,37].

2.5.1.1 Powder flame spraying

This type of flame spraying described in Fig 2.4 is mainly suitable for spraying ceramics, metals and cermet (ceramic oxide in metals matrix) as coating material [9].When a wire or rod cannot be created from a substance, a canister is connected to the top of the oxy-acetylene torch to allow powder to be gravity feed[37].Powders have a number of properties that make them appropriate or

inappropriate for regular feeding, However, it must have normal size distribution, easy to flow, uniform shape (spherical is preferred). The particles should have a size of 5–100 µm with a narrow distribution is preferred, that allow good flowability. The morphology of the particles affects their feedability, sprayability, and porosity[19]. The high temperature required to melt the powder material is provided by the combustion of an oxygen-fuel gas. The molten particles or semi molten are then transported to the substrate surface by a compressed carrier gas or air sometimes. With in-flight speeds of 50 m/s, flame temperatures are reach to 3000°C [36,37]. This process may be used to coat bearing supports, axle and shaft pivots, compressor pistons, cam shafts, bushes, rings and sleeves, hydraulic cylinders and pistons [9].

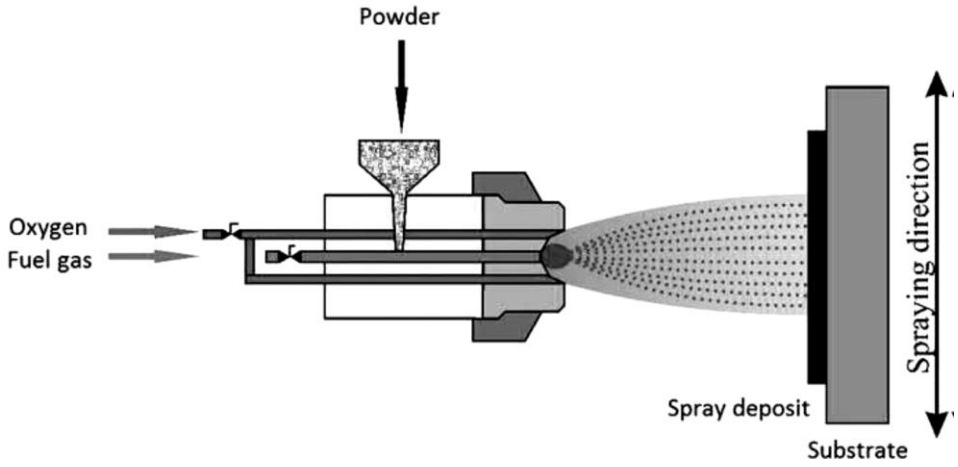

Fig 2.4: Schematic representation powder flame spraying [38]

2.5.1.2 Wire/Rod flame spraying

The wire/rod flame spraying method shown in fig 2.5 another manner to powder flame spraying. It is used for materials with high melting points or when required to deposit composite material such as ceramics (especially oxides), refractory metals, and composites ,However ,By regularly providing the feedstock

(wire or rod) into the special designed torch, the wire/rod apex is completely fused and sprayed with an oxy-fuel gas mixture in addition to compressed air to produce fine molten droplets which are consequently build up on the substrate surface forming layer of coating[19, 34,37]. the major benefits of wires and rods compared with powders are that the feedstock is totally melted along with the atomizing air jet, resulting in finer droplets and denser coatings.[19]. The preferred dimensions of rods are of 500 mm in length and ranging from 4.75to 7.94 mm in diameter. The one significant limitation of rod feeding is stopping during rod changes and integrating rods end to-end. However, It is used when materials to be coated are extremely difficult to form or very fragile, such as ceramics, which are unable to be shaped into wires (. on the other hand, Continuous wire supply is the preferred feed for several metal coatings., Flame wire spray uses wires with diameters ranging from 0.5 to 5 mm. Larger, stronger wires, generally with a diameter of >2 mm. When compared to other thermal spray methods, ceramic coatings by rod flame spray have very low residual stresses and may be sprayed in very thick areas. Many component or element can be covered by rod/wire flame spray coating technique such as “hydraulic piston pins, various bearings, shafts, wearing surfaces of axles, piston segments, synchromesh, crank shafts, clutch pressure plates” [9,19,34,35].

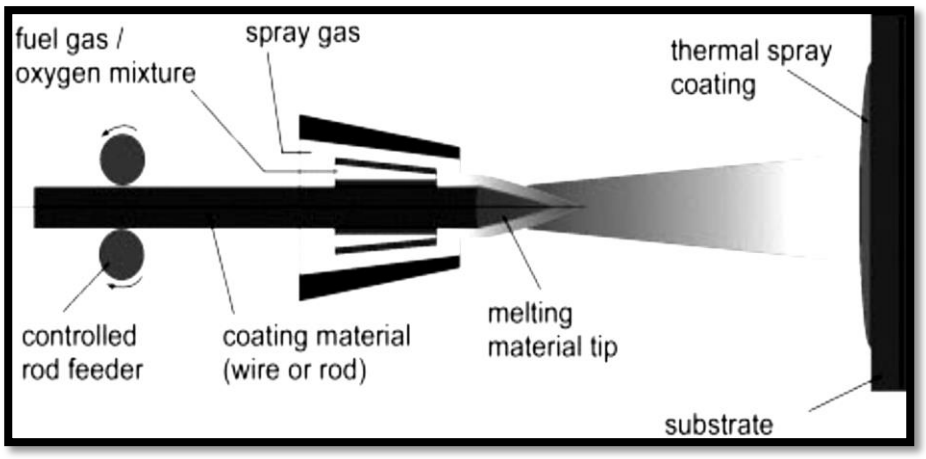

Fig 2.5:schematic shape representing wire/ rod flame spraying system [34].

2.5.1.3. Coating parameters

Some parameters should be adjusted before and through the coating operation especially the material to be coated, torch setting, substrate, and flame spray gases, those are explained as follows[19,34,35,39].

- The spraying distance that separates the nozzle tip from the component surface is favored to be in the range of 100-200mm.Adjusting the spray distance guarantees that the coating is applied uniformly over the desired area and thickness.
- Angle of impact: the angle of the spray flow with respect to the part's surface, usually, 90° ± 20° is an adequate deviation if necessary.
- Component surface temperature:
  - For spraying ceramics upon metals, the temperature of component surface should maintain between 373 and 473K to reduce residual stresses.
- spraying gas flow rate and fuel /oxygen ratio:
  - Flame and carrier gas flows rate being best at rang of 3 to 5 slpm.
  - Fuel-to-oxygen ratio being a significant parameter in flame spray processes and the best ratio is 1/1.1.

- Feedstock characteristics that common for powder and wire/rod :
  Chemistry, melting point, particle size, rod/wire dimension and coefficient thermal expansion (CTE).
- Torch to substrate velocity: the relative speed between the torch movement and the substrate.
- flame temperature and velocity: Flame spraying temperatures of about 3000 °C and in-flight particle velocities of less than 100 m/s are commonly obtained.

2.5.2 High velocity oxy-fuel process (HVOF)

HVOF is a process in which the fuel gas and oxygen are burned and give the powder particles high speeds, melt them, and propel them toward a substrate surface in order to deposit coating layers. The HVOF process achieves supersonic speeds of over 1800 m/s and flame temperatures of over 2800 °C. High powder speeds are a key benefit of the HVOF process since they enable the deposition of coatings with lower porosity levels of less than 1% and enhance adhesive bonds between the coating layer and the substrate surface. The best field of use of the HVOF technique includes materials as a powder with a lower melting point (e.g. metals) and those that are exposed to thermal decomposition at higher temperatures. (E.g. ceramics and ceramic oxides) [33]. The fuels gases are mostly used in High velocity oxy-fuel technique include (acetylene, hydrogen, propane, propylene and kerosene). The process results in a very dense, excellent adhesive coating, making it attractive for many applications. Both powder and wire feedstock can be sprayed [19]. This is because the particles in a comparatively cool flame have a limited dwell period[40]. The powders used for HVOF spraying give different coating properties according to their method of manufacturing, initial characteristics (composition, shape,

morphology, etc.) and parameters of spraying. The following types of powders are mainly used for HVOF spraying:

- Metals and metallic alloys
- Cermet (e.g. consisting of carbides and metallic matrix)
- Oxide ceramics.

HVOF coatings sprayed by these powders have a wide range of applications, such as Automotive, pulp and paper industry, power plants, petroleum and petrochemical industry, machinery, and aircraft industries [33]. The benefit of utilizing HVOF ,regardless of its being appropriate for applying dense coatings, is that a low oxides content in coatings due to the reduced spraying temperature making it wanted for TBC bond-coat implementations[7] .

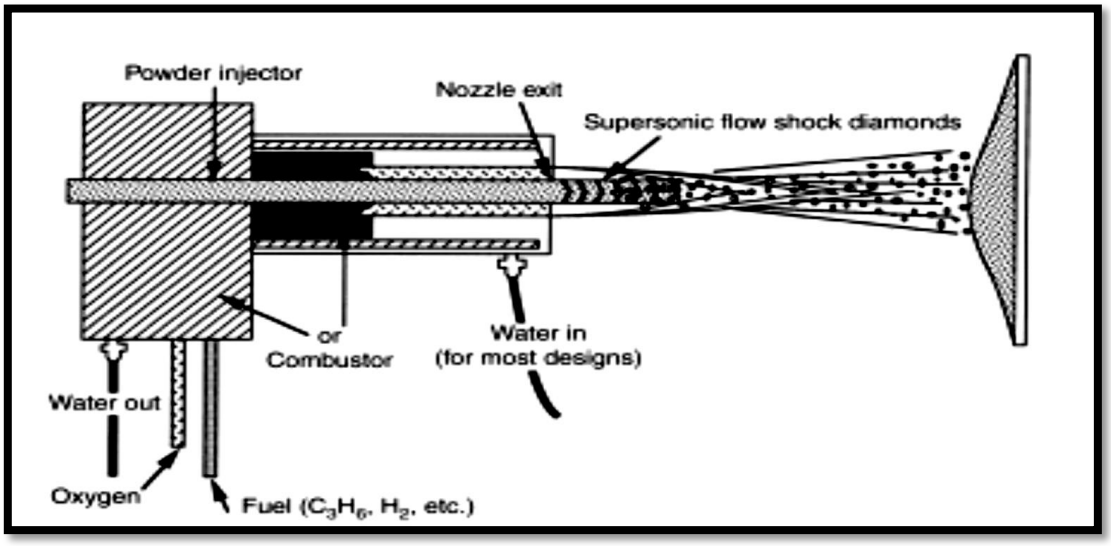

Fig 2.6: High velocity oxy-fuel process features [19].

2.5.3. Air plasma spraying (ASP)

Air plasma spraying (APS) for ceramic coatings is the same as that for metallic coatings, with the exception that ceramic materials have higher melting temperatures, which needs some modifications. The feedstock material, in the form

of powders, is introduced into the higher temperature zone of the plasma using a carrier gas. The powder's particle size is typically between 10 and 40 μm. particles larger than (40 μm) tend to melt partially. Particles smaller than 10 μm, on the other hand, are unable to reach the plasma and are trapped in the cooler periphery. The majority of the bonding between the coating material and the substrate is mechanical. The adhesion mechanism is provided by the interconnecting of the depositing elements with the substrate roughness topography[6]. The plasma jet melts the particles and accelerates them towards the substrate. On contact, the molten particles flatten and form splats. A lamellar coating forms when more splats touch the surface. During the solidification of the splats, cooling rates can reach 105K s–1, resulting in lateral solidification and grain growth that is primarily perpendicular to the substrate[16].

APS coatings with typical microstructure, the porosity creates some lateral strain compliance the plasma spraying technique’s susceptibility to operating environments, as well as a large number of customizable parameters, requires optimizing the process for both applications and materials. The following are some of the characteristics that recognize plasma spraying from other coating methods[41].

1. APS is fundamentally a cold process because the source of heating is remote from the substrate, and the temperature of the substrate’s surface can be saved at the lowest level
2. Spraying can be done with almost any substance that can be produced as a powder and is chemically unchanging at high temperatures.
3. The coatings are made up of lamellar layers. Every molten particle seals in the imperfections of the surface during impact, mechanically anchoring it to the covering. As a result, the coating adheres well.

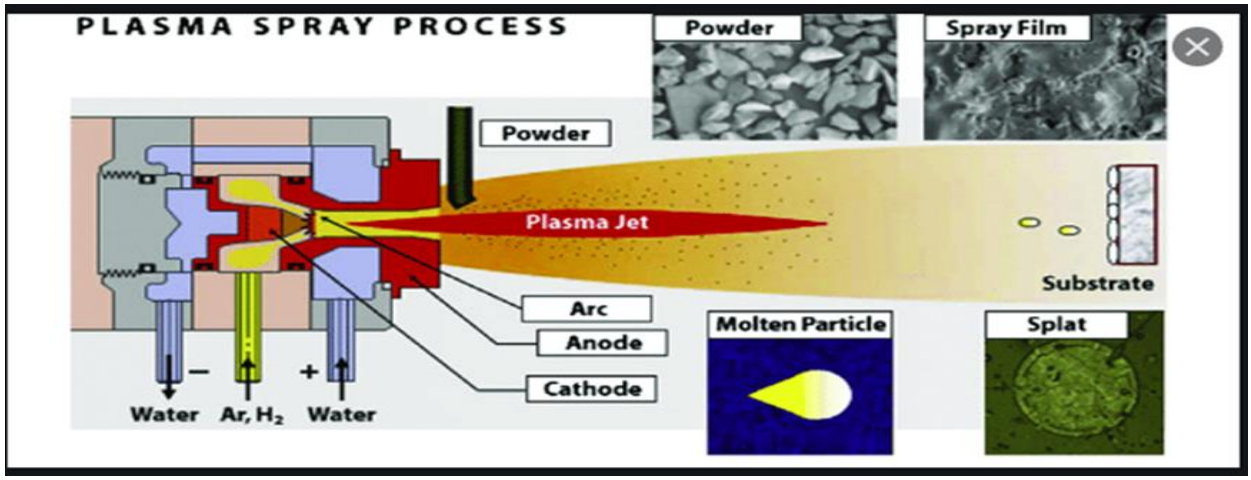

Fig 2.7 : Plasma spray process drawing explain the key elements of the plasma torch [42]

Controlled-atmosphere deposition approaches help thermal spray procedures the most. Plasma spray research has centered on spraying in a controlled environment. These advancements were founded on the idea that coating oxide inclusions may be decreased or eliminated if inert gases were used instead of air as the surrounding environment, which mixes into the plasma spray jets ,The impurities of coating oxides could thus be minimized or deleted[19].

2.6. Applying TBC on diesel engine advantages

A piston is one of the most significant components of an IC engine, since it converts the chemical energy produced by fuel combustion into mechanical energy. As a result of a combustion, the piston is subjected to high temperatures [43].TBC coatings are used in diesel engines for parts that are susceptible to high temperature conditions. Coatings on piston crowns are commonly applied to reduce the amount of combusted fuel in order to lower emissions and improve engine efficiency, while also enhancing the performance of the engine and extending the life of the

component [12,19,44]. Low thermal conductivity coating materials, such as ceramic, can help attain these aims. Mullite, forsterite, 8YSZ, MgSZ, spinel, alumina, and other ceramics are frequently used as TBC in diesel engine coatings[6,12].They also revers the heat from TBC surfaces leading to rise the temperature of the combustion chamber, resulting in evenly and early explosions [19,43] .

Coatings are applied on diesel engine parts normally have a thickness of 0.5 to 1 mm and are only implemented to surfaces that are not exposed to other metal touching or experience a detrimental sliding wear [19,30].Many researchers investigating the effect of coating thickness in range of 0.4-1.6mm on thermal conductivity ,emissions, performance of diesel engines, particularly the coatings that applied on piston crown , show that the combustion characteristics and engine performance are enhanced at lower TBC thickness [8,12,43,45].

Thermal spraying techniques are the most commonly used methods to apply ceramic coating materials, which are called TBC system. For the top coat, which is always from MgO-ZrO_2, YSZ, Mullite, etc., Air plasma spraying or flame spraying is preferred, depending on the substrate material to be coated. On the other hand, High velocity oxy-fuel (HVOF) is the technique adopted for applying the bond coat since it produces a high coating layer property[6,9,19,35].

The findings of FCS Inc. company, USA, after ten-years of actual experiments have been summarized as follows: the advantages of TBCs for diesel engines comprise lowering fuel consumption (up to 11%), prolong engine service life by up to 20%,rise an energy by up to 10%, decreased the emissions, diminished particulate formation, allow using low-octane fuel, low motor noise, high operation temperature of component by around 100C , valve life become longer , and the cost of maintenance will be low[6]. The economics for commercial

application are appealing since data suggests that such coatings improve engine performance and extend the duration between rebuilds. There is also a lot of evidence that diesels processed in this way reduce pollutants such as hydrocarbons and NOx [46,47]. There are many applications in diesel engines other than pistons that are coated with TBC, such as manifolds, intake and exhaust valves, turbochargers, piston rings, and cylinder walls. Each of them has positive gain on the engine's part weight, cost, life and environmental effect that are mentioned above[9, 18, 19,47].

2.7. TBC modeling and simulation

The Finite element Method (FEM) is a computer-based numerical method for simulation of the process that a part or a system can be subjected to. It may be used efficiently to compute thermal stresses, thermal flux, thermal conductivity, temperature gradient, and a range of other material properties such as mechanical and electrical. Using the finite element method, a body is divided into countless small fundamental blocks or components. To analyze the behavior of a single element, an essential set of equations that explain the feature to be calculated can be used. These equations are grouped together to form a broad set of equations that characterize the component's behavior[10,48]. For more detailed information about equation that were used in this study can see reference [49]

Modeling represents the steps in which the part or component is constructed. An engineering model is a numerical shape of a project based on real dimensions and geometry. These are taken from the component under design or analysis within a computer-aided design program [50].

The simulation is the process of testing thermal, mechanical, electrical, or any other boundary conditions on a model, which then gathers the analysis data as a process output in order to assess. [51].

ANSYS is a commonly utilized program for simulation and analysis of a wide range of issues in a variety of engineering sectors all over the world [10]. ANSYS provides a developed toolset and abilities that enable engineers to finish their work in a timely, low-cost, and efficient way. ANSYS software has many useful features, as well as a broad range of facilities and an connected with practically any CAD drawing application, such as AutoCAD drawing software, Creo package , and Solid work program….etc. However, ANSYS' solver technologies are among the best in the industry[11]. Finally, ANSYS has released the Workbench feature, which facilitates the software's use by using a Graphic User Interface (GUI). The basic steps employed when modeling and simulating any project are generally similar, so that can be summarized as follows [48].

1. Building a model with a shape and dimensions close to real.
2. The properties of the project's material that are related to the feature that would be tested should be included at the beginning of the modeling process.
3. Discretizing the model into connected tiny elements according to model nature, this is what is called meshing.
4. Input the boundary conditions required for simulation in the next step.
5. Carrying out the simulation process to extract the results and represent them graphically or in the form of diagrams.
6. assessing the results, repeating the simulation process with modified data if they are not in the acceptable limits .

2.8 Literature survey

Wu et al 2021 reviewed a modifying ZrO_2-based ceramics and looking for novel ceramic materials and technologies. It had discovered that by modifying the doping, thermal stability, mechanical properties, the thermal conductivity and other properties of conventional ZrO_2-based ceramics could be significantly upgraded. Pyrochlores, magnetoplumbites, and rare-earth tantalates have been prioritized for research and development of recent ceramic materials. Finally, the improvement trajectories of developed top ceramic coatings were proposed, which combine doping correction with preparation technology to adjust and restrict the structure property of high-performance new ceramic materials[52].

Balamurugan et al 2020 study the difference in stresses between the conventional piston and ceramic coated piston with various thicknesses (0.2, 0.3 & 0.35mm) using ANSYS program. The Piston is coated through deposition YSZ or MSZ. The piston had drawn in accordance to the procedure and specifications provided, as well as the data handbooks. FEM is the approach have been used according to three main stages are Pre-processing stage, Solution and Post processing. The analysis determined the Deformation, Stress, Stress Intensity, Temperature and Heat Flux of designed piston before and after coating for each thickness. Make an assessment to choose a suitable thickness of coating .the results showed the rise in the maximum temperature on the piston crown, the von-Misses stress decreases while increases the coating thickness increases. As a result, yttria stabilized zirconia is a better material coating with 0.35mm thick[53]

Rajesh and Naven Reddy 2016 investigated the temperature distribution in the ceramic coated Aluminum alloy piston using ceramic materials such as Zirconia stabilized with magnesium oxide, Mullite, and Alumina. The maximum

surface temperature of an uncoated aluminum alloy piston was compared to that of a ceramic coated one using the ANSYS workbench 10 program and the model is drawn using solidworks software. Researchers found that the surface temperature of the ceramic-coated piston is higher than that of the uncoated piston. The coating layers of magnesia stabilized zirconia (MSZ), mullite, and finally alumina have different temperatures ($377C^0$, $360C^0$, and $357C^0$) compared to 295C for the uncoated piston. The coated and uncoated pistons were tested under virtual operating conditions within ANSYS workbench 10 simulation program[54].

Jun Gou and colleagues 2016 try to predict the thermal contact resistance of rough surface for two case .They analyze the thermal contact resistance of gap with air and vacuum state at steady state heat flux, respectively. Numerical model of rough surface was built based on experimental measurements that were performed of Ti alloy specimens . The thermal computations are carried out using the 3D solid element with 8 nodes. To specify contact area pairings, the 3D 4-node surface to surface contact element is employed. The contact elements are attached to the surfaces of underlying solid elements and share the same geometric properties as the linked surfaces. ANSYS code is used to analyze the thermal resistance of contact area. Researchers was found that the temperature distribution of contacted area with air was much uniform compared with vacuum case[55].

Dudareva et al 2015 investigated the effect of different micro arc oxidation coatings applied to the bottom of Al-12Si-Mg-Cu-Ni alloy pistons on its thermal properties. Layers of Alumina have thicknesses (60 μm, 100 μm, 120 μm and 160 μm) were deposited on aluminum alloy piston bottom using MAO with alkaline electrolyte of distilled water, KOH (2.5 g/l), and Na2SiO3 (2.5 g/l).It was

been found that the most active MAO- Alumina layer thickness of 100μm could give the best piston thermal protection[56].

Pinninti 2015 presented a numerical study of the temperature and thermal stress distribution on the aluminum and SiC piston crown base material. The magnesia stabilized zirconia coating is performed using a plasma spraying process with various thicknesses (0.4 mm, 0.8 mm, 1.2 mm, 1.6 mm) respectively. After that, the temperature variations at the surface of the piston are investigated in addition to the thermal stresses at the substrate/bond coat and bond coat/topcoat boundaries. The researcher compared these results with those obtained from the uncoated piston. By using the general-purpose package software ANSYS, the simulation process was conducted.

For all thicknesses of coatings and for coated pistons compared to uncoated piston, the highest degree of thermal distribution is concentrated in the center and the rim of the piston crown. Consequently, The combustion chamber temperature was raised to the highest value by means of TBC, in opposition to the base material surface temperature that was reduced. The results showed that thermal stress is linked to coating thickness. The largest stress that causes spalling of the TBC is generated at the bond coat/topcoat interface[45].

Widyastuti and colleagues 2014 studied using alumina and silica powder mixtures in different ratios for coating the rocket's nozzle of AlSI 4340 alloy as a thermal barrier coating. The deposition technique used to perform their work is flame spraying with multiple plies manner . As a coating material, Al_2O_3-SiO_2 powders were employed. Al_2O_3 powders had a particle size of 89.67 μm and SiO_2 particle size were 56.59 μm,. Researchers focused on investigation of the composition that produces the best adhesive strength and which blends meet this

property. The results emphasize that the best blend was 80% Al_2O_3 with 20% SiO_2 by two plies of about 20 μm thickness for each ply, which caused it to form a mullite phase with an adhesive strength of 16 MPa[57].

Dinesh Kumar and his group 2013 reported the utilizing of ceramic top coat materials to improve the engine combustion characteristics through coating the piston head of a two stroke petrol engine of AlSi alloy with varying thicknesses of zirconia and titania separately. They were used plasma spraying process to achieve their work .The bond coat consist of NiCrAl was deposited firstly . Four pistons were taken for experimentation. Each two piston were coated with different top coat ,that is, ZrO_2 and TiO_2 powders, which were sprayed at various thickness layers(0.25,0.20mm) respectively. The ZrO_2 TBC produced superior outcomes than TiO_2 TBC, according to the findings of the experiments. Generally, using TBC enhance the fuel consumption, NOx and CO emissions, and efficiency of engine[58].

Al-Namie et al 2012 studied flame sprayed ceramic coating effects on exhaust gas temperature, performance and Gases emissions of diesel engine worked on diesel fuel and biodiesel mixtures. Using diesel fuel and biodiesel blends, a four-stroke, single-cylinder, direct-injected diesel engine was tested at unvarying speed and under various load conditions. The combustion chamber, intake and outlet valves of the engine were coated by ceramic materials. Two different ceramic materials were using to be coated on piston, cylinder head and valves which are (350-400) μm of YSZ with (50-100) μm of 4NiCr5Al as a bond coat for top of piston and (280-320) μm of Sic and (40-80) μm of 4NiCr5Al as a bond coat for cylinder head and (210-240) μm of Al_2O_3 and (30-60) μm of 4NiCr5Al as a bond

coat for inlet and exhaust valves. The flame spraying was the technique that used. The calculations exhibited that a drop in brake specific fuel consumption of 19.29 % , 15.91 % , 14.65 % and 7.06 % , an increase in brake thermal efficiency of 23.68 % , 19.77 % , 16.51 % and 6.32 % , the enhance in exhaust gas temperature of 9.01 % , 7.22 % , 15.7 % and 11.42 % , the reduction of CO emission of 18.57 % , 20 % , 20.5 % and 27.77 % , the lessening of HC emission of 28.97 % , 43.9 % , 38.88 % and 36.41 % for diesel respectively[59].

Shrirao and Pawar 2011 Test The effect of mullite coating (Al_2O_3= 60%, SiO_2= 40%) on a direct injection diesel engine. The tests were performed on an uncoated standard engine and a low heat rejection (LHR) engine with and without a turbocharger. The results displayed that the LHR engine with turbocharger had a 2.18 % reduction in certain fuel consumption, a 12% raise in exhaust gas temperature, a 22.05 % decrease in CO emission, and a 28.20 % reduce in HC emission when compared to a standard engine at full load[60]

Samadi and Coyle 2009 introduced a new thermal barrier coating appropriate to be deposited on the diesel engine piston considering the different operating conditions than the turbine blade. Thick, multilayer film with a thickness of about 1 mm based on the traditional refractory system, $Al_2O_3.SiO_2.MgO$. The attractive properties of the phases generated from this system, i.e., forsterite, spinel, and mullite, have thermal and thermo-mechanical properties that fulfill the requirements of the thick film desired. First, forsterite (Mg_2SiO_4) was coated, which has a high CTE match with the metal substrate, then deposited the spinel phase to integrate the function of forsterite into a uniform thermal transition from metal to ceramic material, and finally, mullite was used as a topcoat. The thickness of the individual layers was optimized using numerical models to generate the least

amount of stress under operational circumstances while maintaining the appropriate temperature gradient. The results show that the new multilayer system is the best for coating diesel engine pistons due to lower stresses induced in heating and cooling cycles, in addition to lower cost when compared to the zirconia system[30].

2.9 Summary of literature survey

Many researchers worked to investigate the effects of depositing oxide stabilized zirconia materials experimentally on diesel engine pistons at different thicknesses and percentages, and others studied stresses, strains, and temperature distribution over TBC. All of them gave different results based on the material used. In this study, a mixture of ceramic materials was designed and deposited on an ICE piston, producing an alternative ceramic coating layer without the need to deposit a bond coat. The coating layer produced has good thermal, mechanical, and physical properties. Table 2.4 is a summary of all the studies above in a more convenient format to understand.

Table 2.4. summary of a researchers works

Researchers	work	results
Wu et al 2021	reviewed a modifying ZrO_2-based ceramics and looking for novel ceramic materials and technologies	It had discovered that by modifying the doping, thermal stability, mechanical properties, the thermal conductivity and other properties of conventional ZrO_2-based ceramics could be significantly upgraded
Rajesh and Naven Reddy 2016	investigate the temperature distribution in the ceramic coated Aluminum alloy piston using ceramic materials. The maximum surface temperature of an uncoated piston was compared to that of a ceramic coated one using the ANSYS workbench 10 program	Researchers found that the surface temperature of the ceramic-coated piston is higher than that of the uncoated piston.
Jun Gou and colleagues 2016	tried to predict the thermal contact resistance of rough surface for two case , with air and vacuum state at steady state heat flux	Researchers was found that the temperature distribution of contacted area with air was much uniform compared with vacuum case
Dudareva et al 2015	investigate the effect different coatingsthickness(60,100,120)µm of Alumina applied to the bottom of Al-12Si-Mg-Cu-Ni alloy pistons on its thermal properties	found that the most active Alumina layer thickness is 100µm to give the best piston thermal protection
Pinninti 2015	presents a numerical study of the temperature and thermal stress distribution on the aluminum and SiC piston crown base material by using Ansys program	The results emphasize that the best blend was 80% Al_2O_3 with 20% SiO_2 by two plies of about 20 µm thickness for each ply
Widyastuti 2014	studied using alumina and silica powder mixtures in different ratios as a thermal barrier coating by flame spraying, focused on investigation of the composition that produces the best adhesive strength	The results emphasize that the best blend was 80% Al_2O_3 with 20% SiO_2 by two plies of about 20 μm thickness for each ply

Dinesh Kumar and his group 2013	Studied the effect of using ZrO_2 and TiO_2 on engine combustion characteristics through coating the piston head with different thickness layer.	The results found that the ZrO_2 TBC produced superior outcomes than TiO_2 TBC
Al-Namie et al 2012	studied ceramic coating effects on exhaust gas temperature, performance and Gases emissions of diesel engine worked on diesel fuel and biodiesel mixtures	The calculations exhibited enhancing in all combustion properties with different percentage
Shrirao and Pawar 2011	Test The effect of mullite coating (Al_2O_3= 60%, SiO_2= 40%) on a direct injection diesel engine	The results displayed that the LHR engine with turbocharger had a 2.18 % reduction in certain fuel consumption, a 12% raise in exhaust gas temperature, a 22.05 % decrease in CO emission, and a 28.20 % reduce in HC emission when compared to a standard engine at full load
Samadi and Coyle 2009	Applied multilayer thermal barrier coating based on $Al_2O_3.MgO.SiO_2$ system with a thickness 1mm as three layers (forsterite and spinel as bond coat with mullite as top coat	The results show that the new multilayer system is the best for coating diesel engine pistons due to lower stresses induced in heating and cooling cycles, in addition to lower cost when compared to the zirconia system

CHAPTER THREE

EXPERIMENTAL WORK And Numerical Simulation Process

3.1.Introduction

This chapter explains the preparation steps for the feedstock materials and samples used. In addition ,it contains the equipments description that are used in the coating process and the practical method which was followed for coating the samples of steel alloy, as well as tests that were conducted, such as XRD, SEM, SEM-EDX, micro-hardness, coating thickness, roughness of the coating layer, and other required test. These steps were described in the figure 3.1 below.

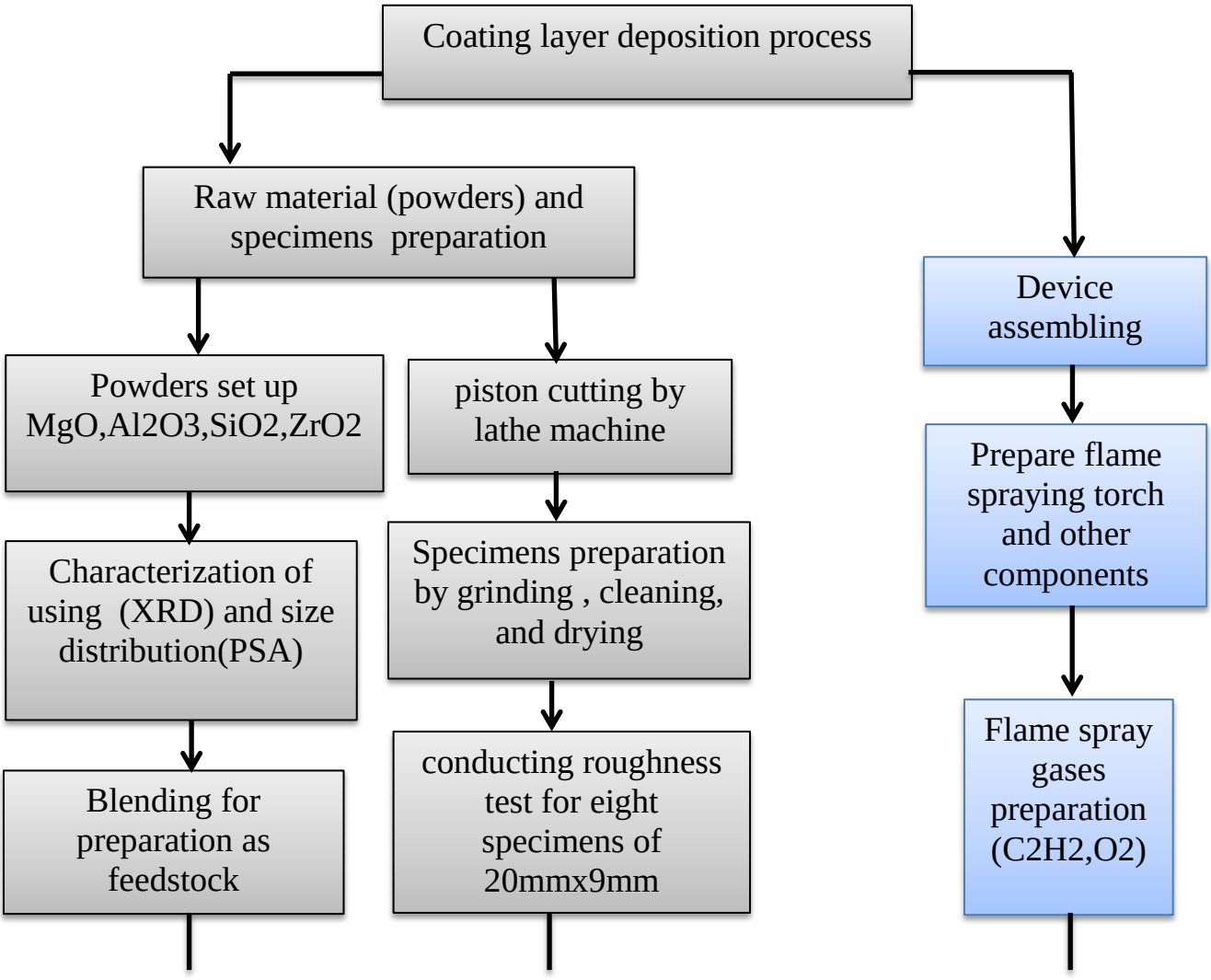

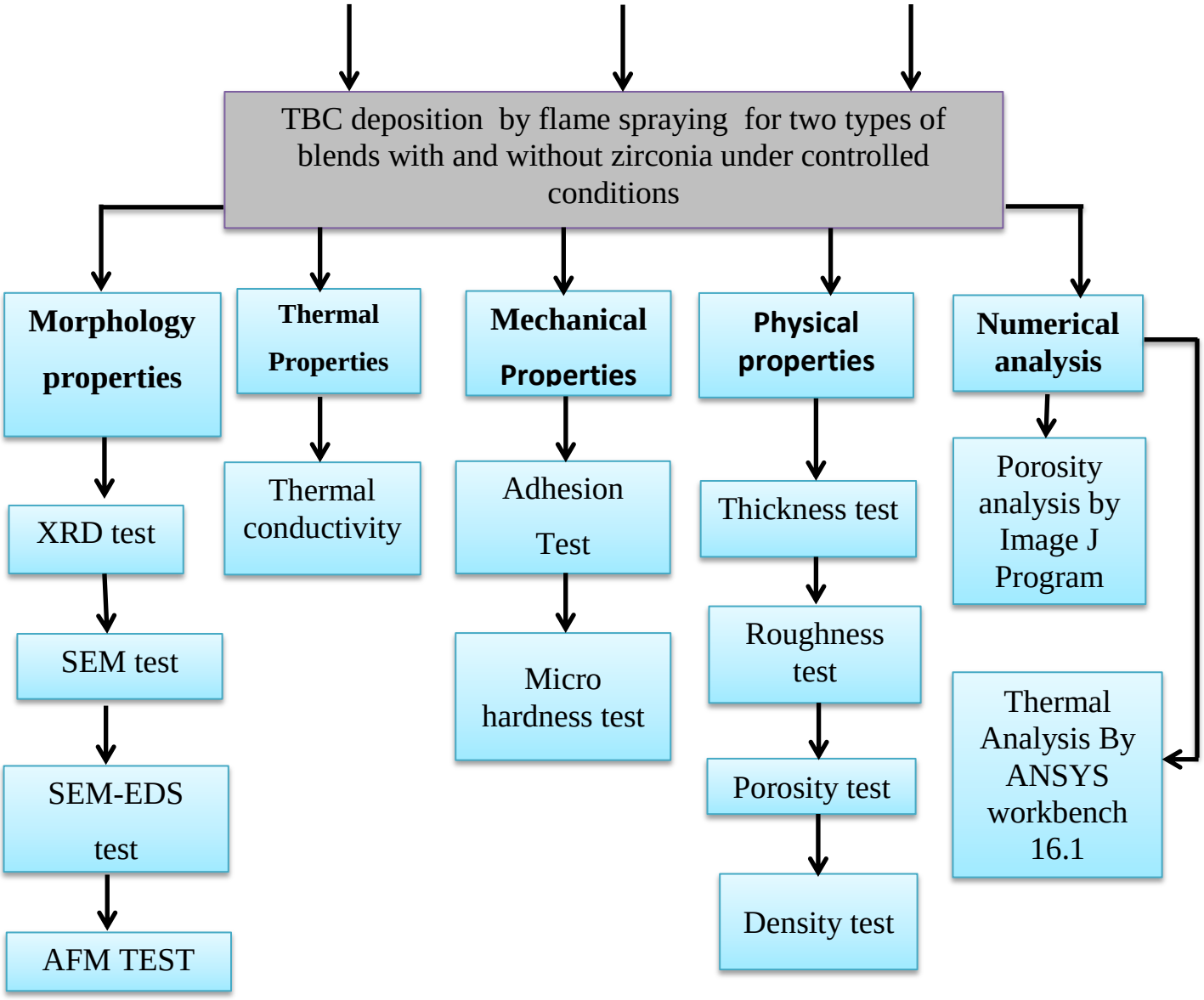

Fig 3.1: Flow chart of thermal barrier coating preparation and spraying process

3.2. Powders and specimens preparation

3.2.1. powders used

Four types of powders were used in this study for synthesis TBC these are, magnesia, alumina, silica, and zirconia in micro size. They were imported from China and their physical and thermal properties are summarized in the table below.

Table 3.1 : Properties of Powders used to prepare blends

Material	**Density g/cc**	**Coefficient of thermal expansion CTE x 10-6 µm/m.C^0**	**Thermal conductivity K W/ m. K**	**Young modulus E (GPa)**	**Melting Point °C**
MgO	3.54	9	30	270	2800
Al_2O_3	3.89	9.10	10.5	370	2054
SiO_2	2.65	0.75	1.5	74.8	1753
ZrO_2	6.5	12.2	2.7	250	2626

3.2.1.1 X-ray diffraction (XRD) test

in order to identify and checking the as received powders ,the XRD characterization test was performed using X-ray diffraction test (Type XRD-LAB6000, Shimadzu) in Babylon University / College of Materials Engineering / Department of Ceramics Engineering and Building Materials Laboratories, diffraction patterns obtained from XRD test approved the types of four powder, namely, MgO, Al_2O_3 , SiO_2, ZrO_2 .

3.2.1.2 Particle size Analysis (PSA)

This test was conducted to determine the particle size of powders that will be used in the spraying process, where particle size is an important parameter affecting powder feeding and in-flight state, as well as the melting behavior of particles during spraying. Bettersize 2000 laser particle size analyzer device that is used in test ,"The Bettersize 2600 utilizes laser diffraction technology. There are 92 photoelectric detectors to convert light signals from the scattering spectrum to electrical signals, which are transmitted into an intelligent software that can be derive the complete particle size distribution". it is working with water as a dispersant medium. the results for powder explained in the next chapter.

3.2.2. Specimens preparation

A304 alloy steel piston ,the substrate were selected of heavy duty diesel engine type Scania DC12 brought from oil products distribution company stories (OPDC) / Babylon branch. chemical composition analysis was conducted in the laboratories of the industrial and metals ministry/Dora and the results are shown in table 3.2. Eight specimens shown in Fig 3.2 of (Φ20mm x Φ9mm) were obtained by machining. After that, the specimen preparation processes such as grinding, cleaning with ultrasonic and acetone were carried out in Babylon University/College of Materials Engineering /Department of Ceramics Engineering and Building Materials Laboratories .

Table 3.2: Chemical composition of alloy steel piston (ASTM A304 4140H)

Element %	C	Si	Mn	P	S	Cr	Mo	Ni	Al	Cu	Fe
Percentage %	0.427	0.193	0.747	0.0082	0.0091	0.961	0.217	0.0191	0.0245	0.234	BAL

Furthermore the specimen were cleaned with acetone and dried with air, then ground with alumina emery paper (150 grit). On the other hand, the roughness of the specimen surface was tested semi-manually by the surface roughness test device. in the College of Materials Engineering/Department of metals Laboratories. Surface roughness is an important factor that affects coating layer adhesion on a substrate surface. This in turn affects the service life of the thermal barrier coating Finally, they were saved in plastic bags inside can after being cleaned with acetone and dried by air another time to be ready for coating.

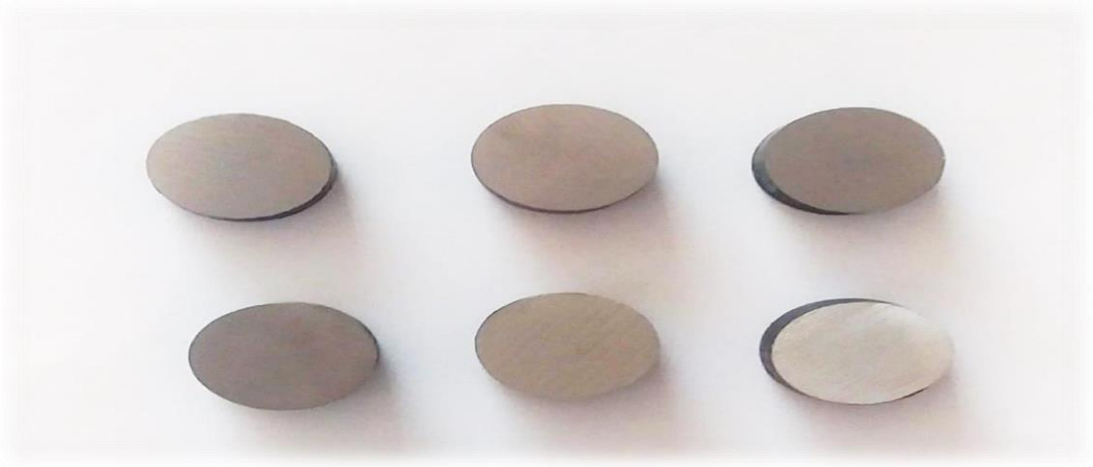

Fig 3.2 : prepared specimens of A304 4140H alloy steel before coating

3.3.Flame spraying system

A flame spray system shown in Fig 3.3 was consisting of several parts and should be installed to set up the first step of the spraying operation. However, the process may be conducted fully automatically or may be achieved manually, as in the study. The device is composed of :

1. Flame spraying torch with a different nozzles, which contains a can at the top. It is considered the main part in the system.
2. Two bottles contain gases, usually (O2, C2H2) that are mixed in specific ratio to generate the flame,
3. Pipes, flowmeters, flashback arrestors, regulators to adjust the gas pressure.

4. workbench for fixing the workpiece during operation
5. The ventilation and cooling system, if necessary.

3.4 .Coating Deposition

3.4.1 blends

Eight blends of 5 gm wt% were prepared with percentages explained in table 3.4, the first four specimens containing Mgo, Al_2O_3, SiO_2, and the others containing zirconia in addition to components of the aforementioned blends, namely, MgO, Al_2O_3, SiO_2. Table3.3 show the composition of the blends.

Before mixing, the PSA was performed. The particle size ranged from about (51µm) for silica powder as a maximum limit and (4.4µm) for Zirconia powder as a minimum limit. After that, the blends were calculated and weighed by using a four-digit sensitive balance then divided into two groups , group1 and group 2. Zirconia was added to the second group for comparison purposes because it is considered the backbone feedstock in almost all research when manufacturing and applying the TBC. Powders were mixed using a rotary mixer at the College of Materials Engineering/Department of Ceramics Engineering and Building Materials Laboratories. However, wet mixing operations continued for six hours at a speed of 20 rpm for all blends.

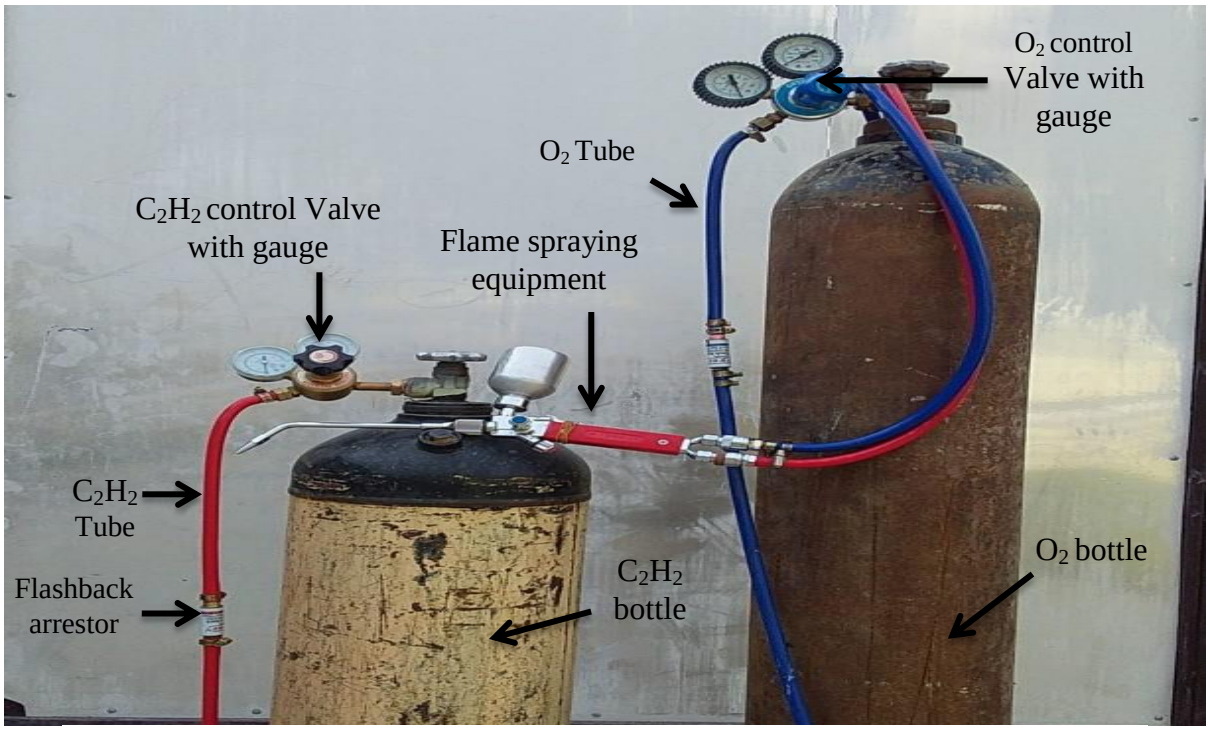

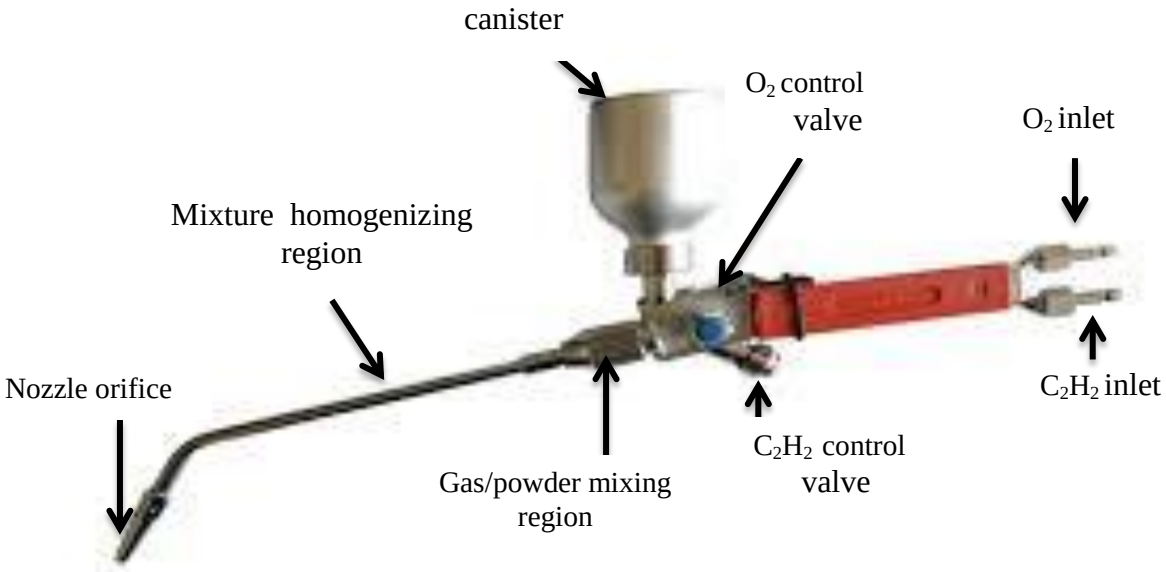

Fig 3.3 . Flame spraying equipment

Ethanol is the wetting solution added at a weight percentage of 0.1 wt% mixture in order to prevent the agglomeration process from happening to feedstock material as it descends from the bottle to the mixing area of the device [19].

In all blends, the MgO was the pivotal oxide, then it's effect on the conductivity property of the TBC was studied, so the powder percentage was varied depending on the MgO percent.

Table 3.3: describe the weight percent of all Oxides in blends

Specimen No / **oxides**	**M1**	**M2**	**M3**	**M4**	**M5**	**M6**	**M7**	**M8**
MgO	**45**	**40**	**35**	**30**	**40**	**37.5**	**35**	**32.5**
Al_2O_3	**30**	**30**	**35**	**45**	**30**	**30**	**30**	**30**
SiO_2	**25**	**30**	**30**	**25**	**25**	**25**	**25**	**25**
ZrO_2	**0**	**0**	**0**	**0**	**5**	**7.5**	**10**	**12.5**

3.4.2.Device installation

The device was assembled in Iraq from a spraying torch of the type QH1/H manufactured by Shanghai Welding & Cutting Tool Works, which was imported from China. Two bottles were filled with oxygen of high purity (99.9%) for medical use and with acetylene (C2H2) of high purity also (99%).Pipes and other related tools are installed to gases bottles and spraying torch tightly. Safety and integrity equipments were utilized during spraying process.

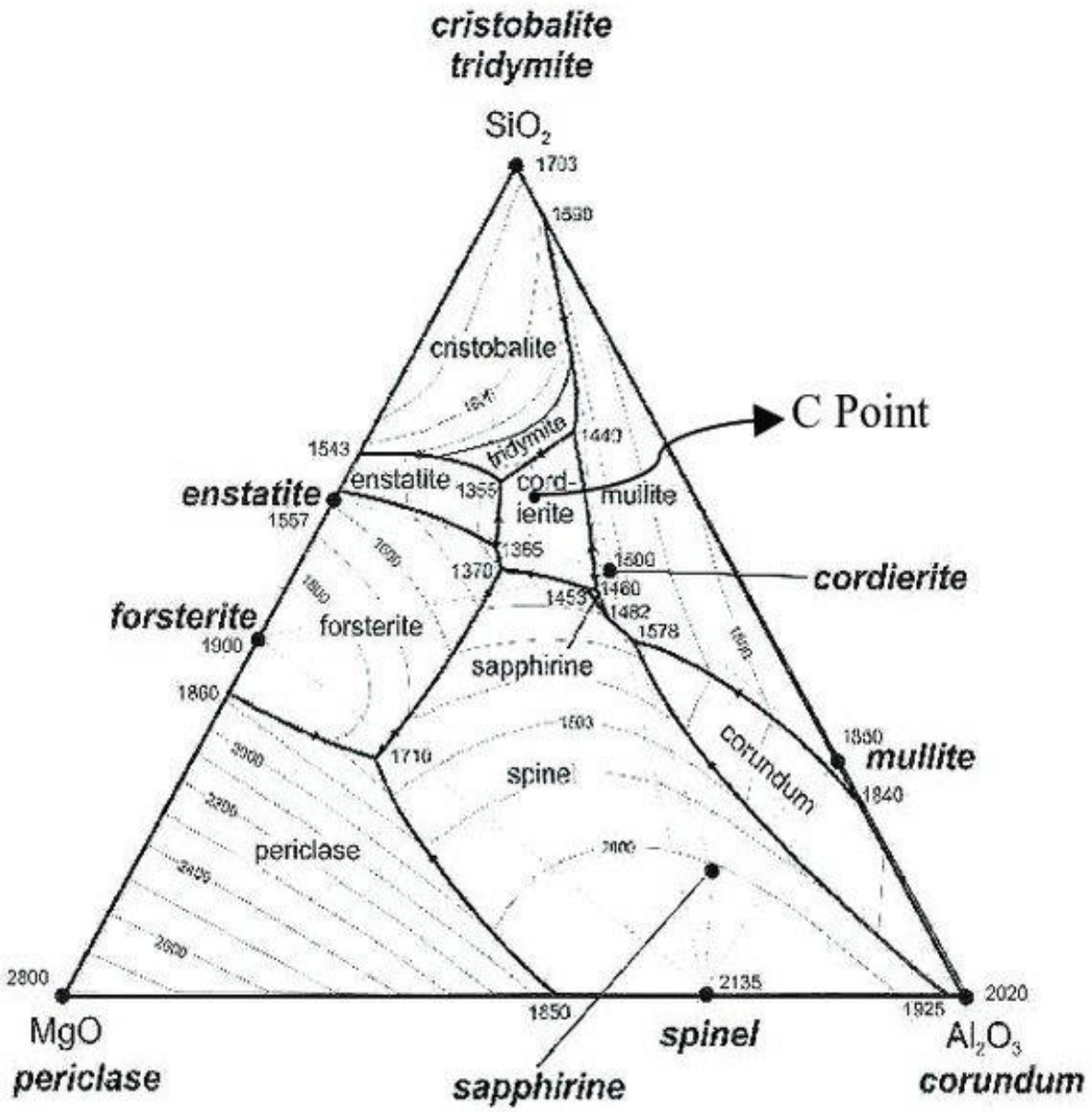

Fig 3.4: Ternary phase diagram of MgO-Al_2O_3-SiO_2 system

.

3.4.3. Spraying process

To perform the spraying process, many parameters must be adjusted in order to achieve the best possible results. These parameters are the spraying distance, pressure of gases, spraying angle, spraying time period, and flame temperature. However, the coating operation was achieved as follows:

1. Specimen holding on clay brick above the workbench.
2. Adjust gases pressure at 5 bar of oxygen and 0.6 bar of acetylene.
3. The spraying distance was about (80–90)mm from the nozzle opening to the surface of the substrate.
4. 85^0-90^0 was the angle of the nozzle at spraying.
5. 0.3 mm was the nozzle opening was used through spraying.
6. Substrate surface roughness before coating was (Ra = 1.598um) as a rated value of eight specimens obtained from three reading of each specimen .
7. At the time of spraying, the temperature of the substrate surface was save it at 150–200 °C where measured by IR thermometer gun.
8. Time of deposition was 15 sec with pausing time about 5 sec until pass finished.
9. Spraying was conducted at several passes till get the acceptable thickness (cover all over the surface of specimen).
10. Leave's the coated specimen to cool slowly in air.

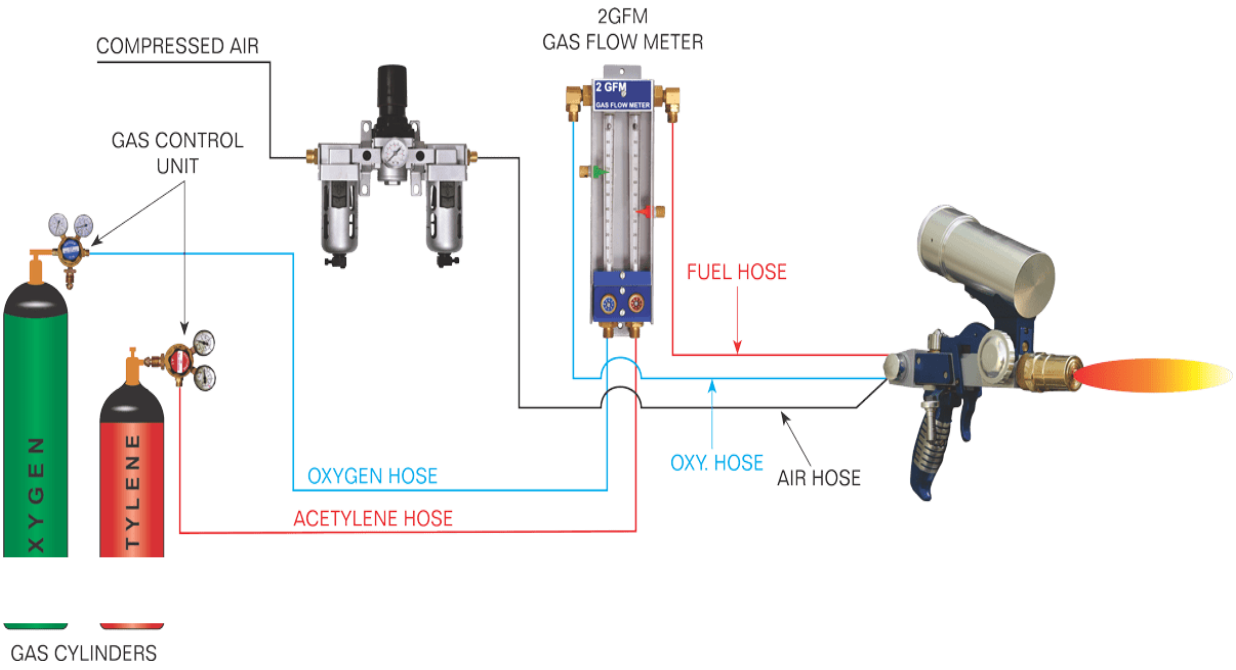

Fig 3.5 Schematic of thermal spray equipments installation

Fig 3.6: four coated specimens

3.5. Coating layer Characterization and Tests

This study investigates thermal conductivity property of TBC layer .thermal conductivity and other characterization tests were achieved. such as XRD test, SEM test, SEM-EDS test, thermal conductivity test, ,micro-hardness and adhesion test, TBC layer thickness, roughness, and porosity evaluation test. after that ,thermal conductivity was validated by simulation operation with ANSYS multipurpose package software.

3.5.1.Morphology characterization test

3.5.1.1 X-Ray diffraction (XRD) Analysis

The X-ray diffraction test is used to determine the crystal structure of solids, as well as phase identification and other analysis options, after a reaction occurs between electrons incident with atoms of crystalline materials, which are generally distributed regularly and repeatedly. X-ray diffraction test for powder (Type XRD-6000, Shimadzu) was conducted in Babylon University / College of Materials Engineering / Department of Ceramics Engineering and Building Materials Laboratories and in university of Technology /nano- technology center/X-ray laboratory for TBC coating layer.

3.5.1.2 SEM and SEM-EDS test

3.5.1.2.1.SEM test

It is a type of electron microscope that produces images of a sample by scanning it with a focused beam of electrons in a wide range of magnifications, about from (X10) to (X500,000) which is 250 times more than the magnification of the best optical microscopy . The electrons interact with atoms in the sample, producing various signals that can be detected and that contain information about the sample's surface topography and composition. The most common mode of

detection is by secondary electrons emitted from atoms excited by the electron beam while back-scattering electrons (BSE) reflected from the sample provides information about the distribution of different elements in the sample [59]. The SEM instrument INSPECT S50 at University of Technology /Nanotechnology center was used to investigate the structure of the surface coating of TBC.

3.5.1.2.2. SEM-EDS test

The SEM-EDS technique, which provides both qualitative and quantitative information, is used to identify the amount and type of element in materials based on the X-ray spectrum emitted by the specimen. Electron beams with high energy can energize the release of X-rays in numerous variant ways by striking the atoms of a sample. However, the atom that gets hit by an electron (from an electron beam) releases an electron primarily located in an interior position (inner shell (K) shell). To restore the stability of an atom, an electron travelling from a higher-energy shell in the atom fills this "vacancy' right away. Consequently, electrons in high energy orbitals may emit X-rays to release part of their energy. The associated X-ray leaves the material and collides with the detector, causing a charge pulse. The instantaneous current is then transformed into a voltage pulse whose amplitude reflects the detected X-ray energy. lastly, the voltage pulsing produces a digital signal. The cumulative digital signal builds a count, which in turn generates a typical X-ray spectrum with the primary peaks overlaid on the background after the test is complete[61].

3.5.1.3. Atomic Force microscopy Test

In order to observe the resulting surface profile and determine if the coating layer of flame spraying have a suitable roughness or it is need to post treatment ,the

AFM test was performed in Babylon University / College of Materials engineering /polymer and petrochemicals department laboratories.

3.5.2 .Thermal properties tests

3.5.2.1 Thermal Conductivity k

Thermal conductivity is a parameter that indicate to the amount of thermal insulation of a material. The thickness of the layer was deposited in the this study was 600 microns, and the thermal conductivity was tested using a device known as a Lee disc. device exist in university of technology / applied physics department laboratories. The device was produced by Griffin & George in England.

The apparatus is a small device that is electrically heated and is used to verify the thermal conductivity of poor conductors. The device consists of three 12mm thick discs of brass, in addition to an electric heater inserted between the first disc and the second one. 4mm terminals are used to connect the heater. Between the second and third discs, an insulating substance that is to be tested is put. with the assistance of a screw made of a substance that has a high thermal resistance. A hole is made on the upper rim (at the thickness face) of each disc which is used to put the thermometer. A 6 volt and 0.25 ampere supply is applied to the heater that generates heat, which is then transferred to the discs in turn, reaching the third disk after passing the sample. at a repeatedly constant period time, the temperature of each disk is measured until the second and third disc attain a balanced temperature. The relationships were used to calculate the thermal conductivity of coating layer are:

$$J = k\, dt/dx \qquad \text{…….. (1)}$$

Where J is the heat flux that is determined from equation

K is the thermal conductivity of a sample to be tested

dt/dx is the temperature gradient over disc thickness

heat recipients by the first disk (d_A) is calculated using relationship below

$(\pi r^2 + 2\pi r\, d_A)\, E\, T_A$ .....(2)

And if $(\pi r^2 + 2\pi r\, d_A)\, \mathbf{E}\, T_A + 2\pi r\, d_S \times \mathbf{E} \times ½ (T_B + T_A)$ …….(3)

Represent the amount of heat transferred through sample, However, heat recipient and lost in the sample equal to half of the addition for the two values of equation (2) and (3). because the thermal conductivity that passed through sample is

$\pi r^2 k (T_B - T_A/d_s)$ ……(4)

So that value of **E** can be computed depending on

$H=VI= \pi r^2 E (T_A+T_B) + 2\pi r E [d_A T_A + ds/2 (T_A+T_B) + d_B T_B + dc\, Tc]$……..(5)

Where (**E**) is the heat energy amount that passed through disc's Area. Since (**E)** is a known value, therefore, the K value can be calculated from equation as follows:

$k (T_B - T_A/ds) = E [T_A + 2/r (d_A + ds/4) T_A + ds\, T_B /2r]$……(6)

where

E is thermal energy passed throw discs

T_A and T_B are the temperatures of disc A and B respectively

R is the radius of disc A,B,C

And d_A, ds are the diameter of A and Sample respectively.

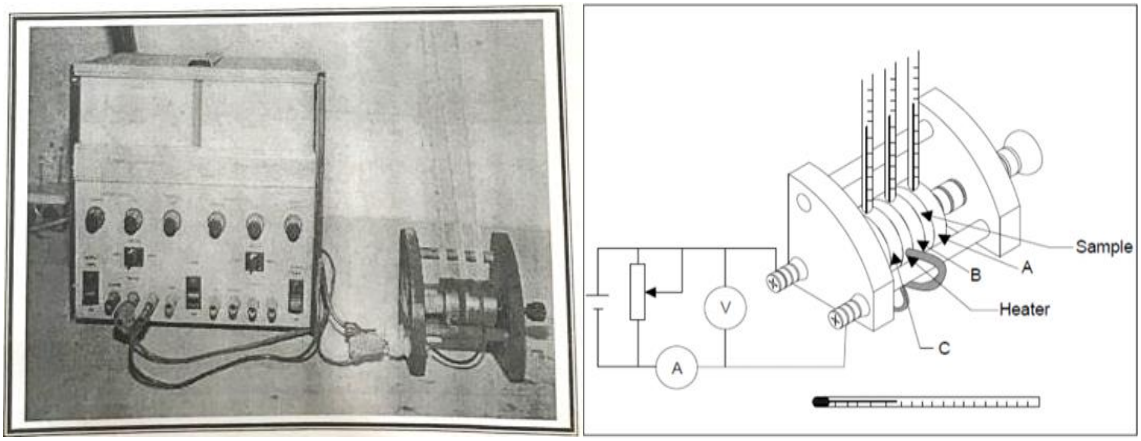

Fig 3.7: a) Lee disc apparatus. b) component of device.

3.5.3 Mechanical properties tests

3.5.3.1. Adhesion test

The adhesion test of 6 coated specimens was carried out to evaluate adhesion strength by using the microcomputer controlled electronic universal testing machine that was found in the faculty of materials engineering/polymer and petrochemical department laboratories according to the specification ASTM C 633-01 . The dolls were glued to the coated specimens by epoxy adhesive from (MAGPOW company with item code SK-1122). which is consist of two component that were mixed at the same amount . the mixture was spread over the coating layer . The assembly was left for 24 hours to reach the highest strength as the manufacturer's instructions, and was fixed to the testing machine tightly. The load was applied at a rate of 1 mm/min (the lowest rate of the machine)until the dolls detach from the specimens. At that moment, the failure load was recorded in (kN). Finally, the adhesion strength determined as a result of the failure load divided by the area of the specimen coated surface.

3.5.3.2 Micro-hardness test

The coatings were tested using a (TH–717 digital micro-Vickers hardness tester) with a total amplification of 400X and a load of 300 gm with a dwell time of 15 seconds in accordance with ASTM C 1327-03 specifications. In this study, the examination was carried out at Babylon University-College of Materials Engineering/Department of Ceramic Engineering and Building Materials. Vickers hardness (HV) is expressed in terms of the contact area of the indenter and is computed from the relation:

HV=1.8544(P/d2) …….. (1)

Where P is the load applied in gram force, and d is the average diagonal length of the indentation impression measured in micrometers (although the hardness number units are expressed in units of kgf /mm2 rather than the equivalent (gf/m2) [62].

3.5.4. Physical properties tests

3.5.4.1. Coating layer thickness measurements

Coating layer thickness measurement is achieved using a coating thickness gauge meter of model TT260 from Time Company. The values of the thicknesses of the coating layers were given as a rate of three measurements for each specimen. That is, thickness of M4coating layer was (640µm) and thickness of M7 coating layer was(609µm) .All readings were done in Babylon University/College of Materials Engineering /polymer and petrochemicals department laboratories.

3.5.4.2. Roughness test

The Roughness of specimens surfaces were measured after coating layer was measured using the profilometer device that was found in the faculty of material engineering/metals laboratories .Three test points were adopted for every measurement, they have been taken on the same line , consequently, The rate of these three measurement was the roughness of the specimen. The results has been confirmed by AFM test .Results of roughness test and AFM showed the low level of coating layer surface roughness as well as the tow techniques results was convergent as will see in the results discussion chapter.

3.5.4.3.Porosity test

Porosity is one of the most important features of the TBC which has to be measured .there are many approaches to determine porosity, However, Archimedes

approach is the widely used in evaluation of porosity. but this method generally able to determine open pores more than other type of porosity .

To determine the porosity of the coating layer, the Archimedes technique is used. In addition to the porosity data acquired via the traditional methodology, namely the Archimedes method, image analysis of the digital micrographs generated from the SEM was performed, where the results of porosity were so close to the Archimedes test, They were created in the ImageJ program by the National Institute of Health (USA) using the threshold method for measuring porosity percent and porosity size. This method adopted from many researcher, The processed images were detailed in the figure 4.27 and the measurements for both samples M4 and M7 were about (22.6 And 12.39 μm) respectively. These results were so closed to Archimedes method.

3.5.4.4.Density Test

Density of samples are measured through weighing the samples before and after coating then subtracting the weights to get coating layer weight which is used with it's volume to determine the densities depending on the equations below.

$$W_2 - W_1 = W_{coat} \quad \text{.....(1)}$$

$$V_{coat} = \pi\, d\, H_{coat} \quad \text{.....(2)}$$

where W1,W2 are the weight of specimen before and after coating respectively, and d is the specimen diameter and H is the coating thickness, hence

$$\textbf{Density} = W_{coat} / V_{coat} \text{.....(3).}$$

3.6. Simulation by ANSYS program

Simulation process of temperature gradient is performed at the topcoat/substrate interface using the general purpose program package, Ansys

workbench, of ANSYS Software Company that is installed firstly. The simulation process is achieved as the following sequence. Starting with sketch drawing composed of piston body addition to overlaid thermal barrier coating with a thickness of (600μm) as a rated value ,then making a model by revolving it 180 degree ,finally creating a mesh of the model with repeated optimizing process until get the optimized mesh, after that, applying the boundary conditions of initial and operating temperature at the surface of topcoat material, and piston surfaces . coupling method was utilized to attach the two bodies in the analysis step , at the end, the results attained were gathered and has been showed as a contour. These steps will be detailed as in below:

3.6.1. Modeling

The design of the piston model depended on the dimensions that are taken from the Scania DC12 piston heavy duty diesel engine. The piston design was implemented by the modeler program that is built into the ANSYS workbench package. The piston was manufactured from the A304 alloy steel, so its properties are considered to be the properties of the piston model. The coating layer was added to the piston model with the same properties that were obtained from the experimental data. The thickness of the coating layer that was added to conduct the simulation was taken for two coatings (M4, M7) as the rated value of the coatings, which was 600 μm.

The coating technique used converts some sprayed particles to a melted or semi-melted state, which then fills the valleys of the rough substrate surface. This realistic state that arises during coating results in full contact. When the final model was drawn, a continuous interface was considered because of full contact between the coating layer surface and the substrate surface. The two surface coupling

methods were used to connect the two surfaces during thermal analysis for the above reasons.

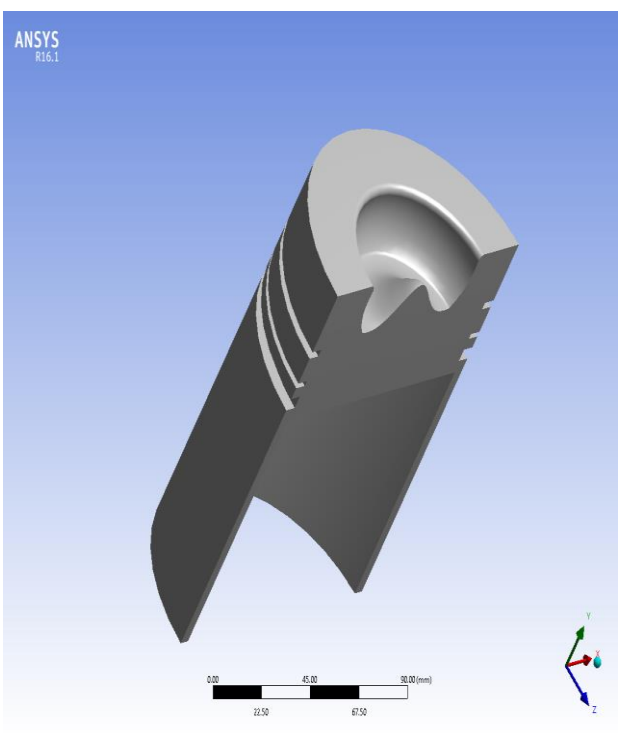

A

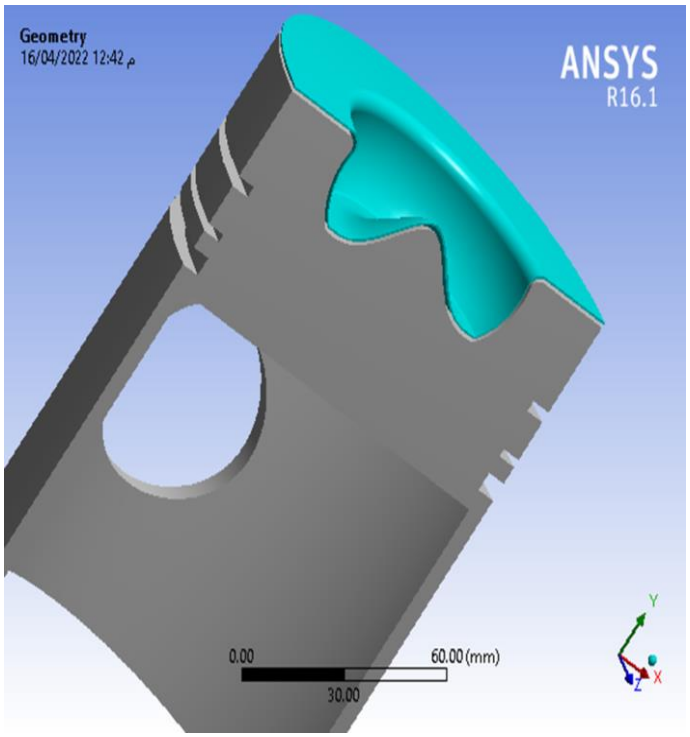

B

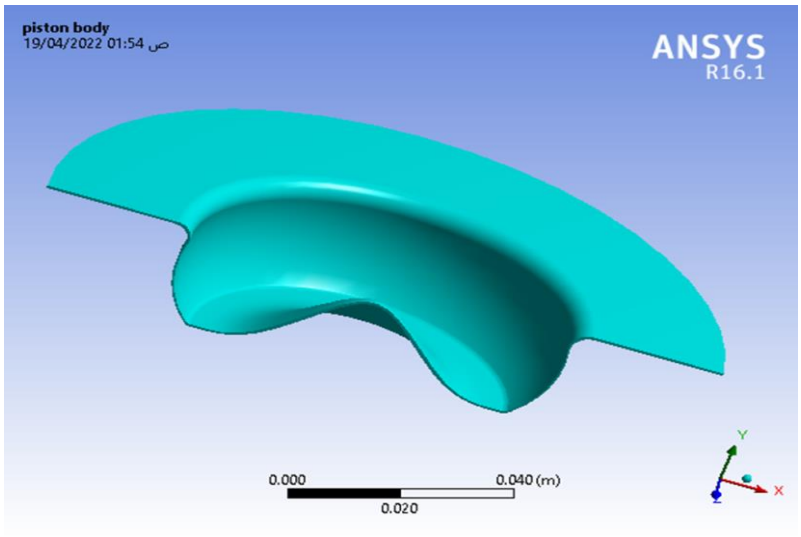

C

Fig 3.8 depicts the model of (A) uncoated piston , (B) coated piston and (C) coating layer.

Table 3.4: Mechanical and Thermal properties of piston material

Density gm/cm3	Thermal conductivity W/m. c^0	Thermal Expansion $1/c^0$	Elastic Modulus GPa	Melting Point C^0	Heat Capacity J/Kg. c^0	Poison's ratio
7.9	43	$1.4*10^{-5}$	215	1529	502	0.29

Table 3.5: properties of coatings that are adopted in simulation

Samples	Specific Heat capacity j/kg.c	Thermal conductivity W/m.c	Density kg/m^3 (average)	Thickness (μm)
Coating layer (M4)	46.2834	0.831334	$7.03967x10^{-6}$	640
Coating layer (M7)	42.3760	0.72286	$6.745497x10^{-6}$	609

3.6.2. Meshing

Before starting the simulation process, the discretization of the model into many smallest elements is achieved and is the most significant step. This discretization operation in ANSYS WORKBENCH is called meshing. The meshing process is optimized until it attaining the suitable number of elements and nodes that ensure the result doesn't change as the number of elements is increased. The relationship between the elements number and temperature was represented in figure 3.6 b below that describes the optimized state of the mesh. The model was discretized for (213514) elements and (303548) nodes. The procedure of meshing passing through the following track.

1. Mesh ordinary created as the first step with a size and shape which was selected automatically by mesh program.
2. Sizing mesh is achieved in details view and the setting varied to (fine relevance center ,high smoothing, fast transition, and fine span Angle)
3. Made a face meshing of the coating layer (top and bottom surface of coating layer) and the crown top surface .
4. Refinement step is conducted in order to enhance the quality of mesh of the surfaces in the step above .
5. Second refinement is performed at the same surfaces above till obtain the best quality of mesh as the program was indicated.

6-finally the mesh optimization was accomplished at the number of element (213514) and (303548) nodes as was explained in the chart below.

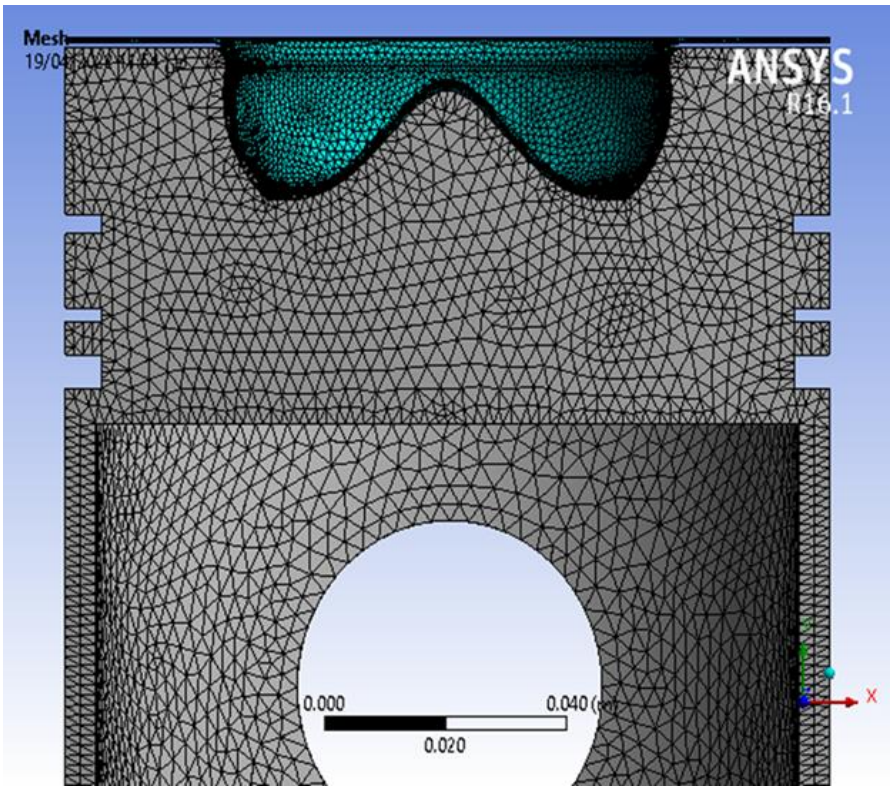

A

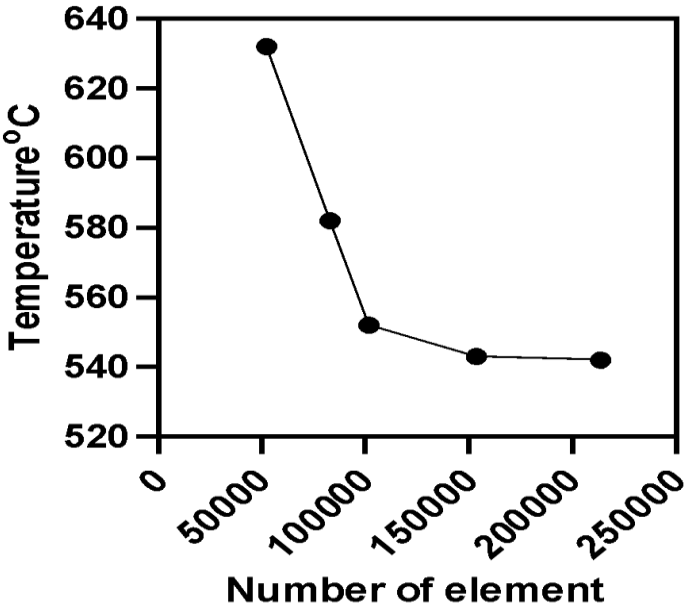

B

Fig 3.9 (A) represent the mesh distribution over entire piston body and coating layer and (B) which describe the optimized state of the Mesh optimization

3.6.3. Applying Boundary Condition

The simulation process in this thesis is focused on calculating the temperature and directional heat flux distribution on the coating layer and piston crown in order to investigate the thermal reduction of the novel ceramic coating layer. This means that the boundary condition represents only the temperature of combusted gases at the combustion time, which is the maximum temperature needed to emphasis the thermal reduction of the thermal barrier coating layer that we applied, in addition to the initial temperature of the engine that it started with. The simulation is performed of the two types of coatings which have the lowest thermal conductivity such that their properties are entered within the model properties in an engineering data cell of the steady state thermal program. The specimens (M4, M7) and piston crown material properties are presented in tables 3.4 and 3.5. The boundary conditions that were used were.

1. Gases Temperature at the combustion time is 700 C^0 applied on the upper surface of coating layer only.
2. initial temperature is 30C^0
3. Thermal conductivity (K) of coatings (M4 and M7) is shown in table 3.5.
4. Convection coefficient at the outer and inner surfaces was increasing as the temperature increases starting with 3.8 $KW/m^2.C^o$ .which is shown in figure 3.9
5. The coupling method is used for thermal connected between coating layer and piston surface. This method neglected Gthe air gap that may occur between coating layer and piston surface. Therefore, all amount of heat flux that exposed on the coating layer will transferred to piston surface.
6. Temperature of the bottom surface of piston crown was 50 C^o.
7. All boundary condition above was used in the bare piston thermal analysis too.

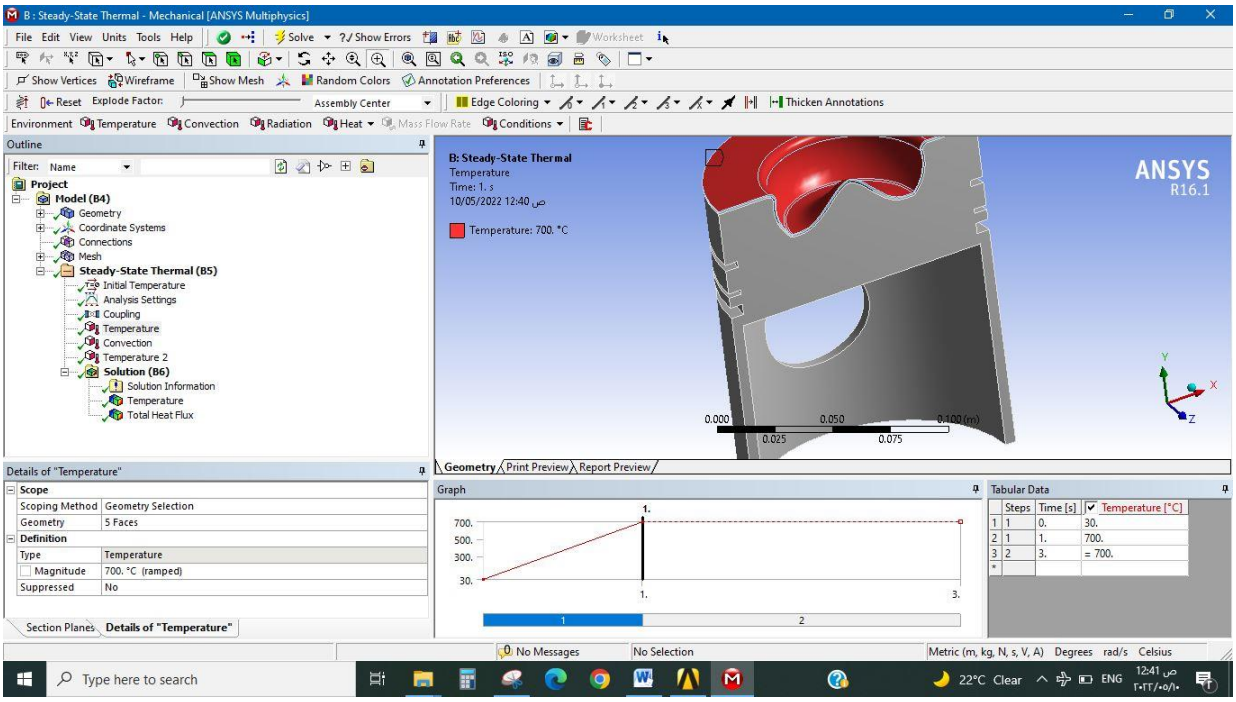

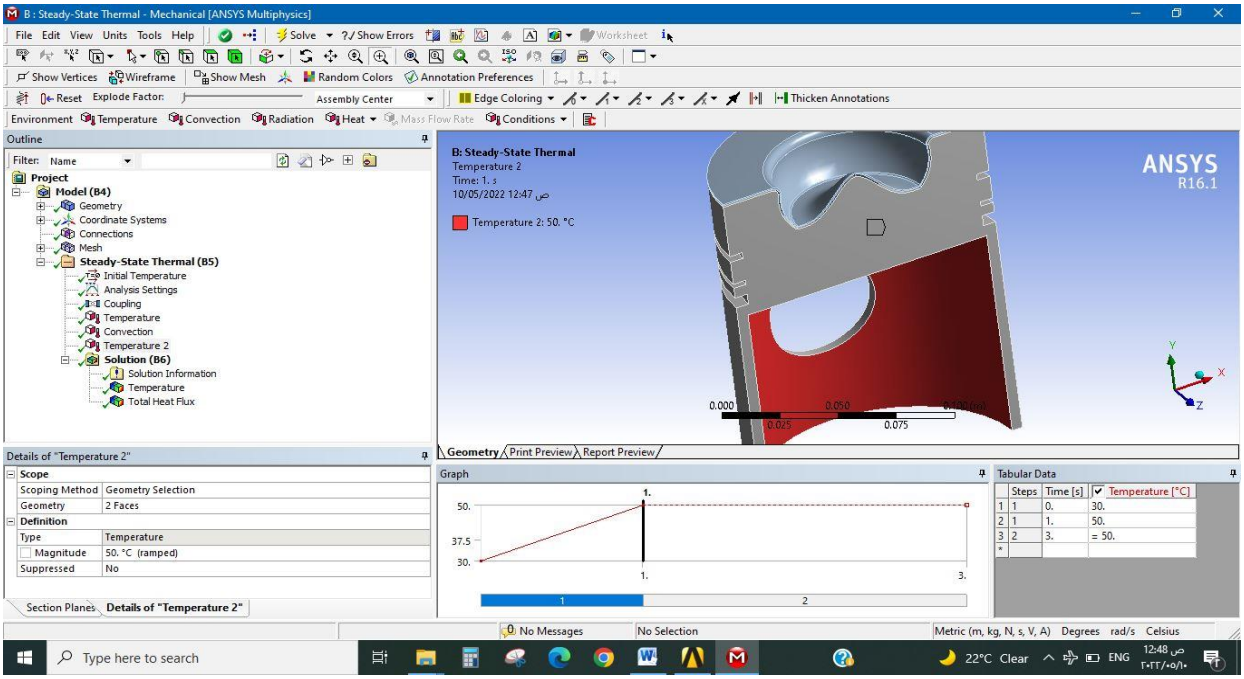

Fig 3.10 shows the initial and boundary condition applied on piston crown and coating layer surface.

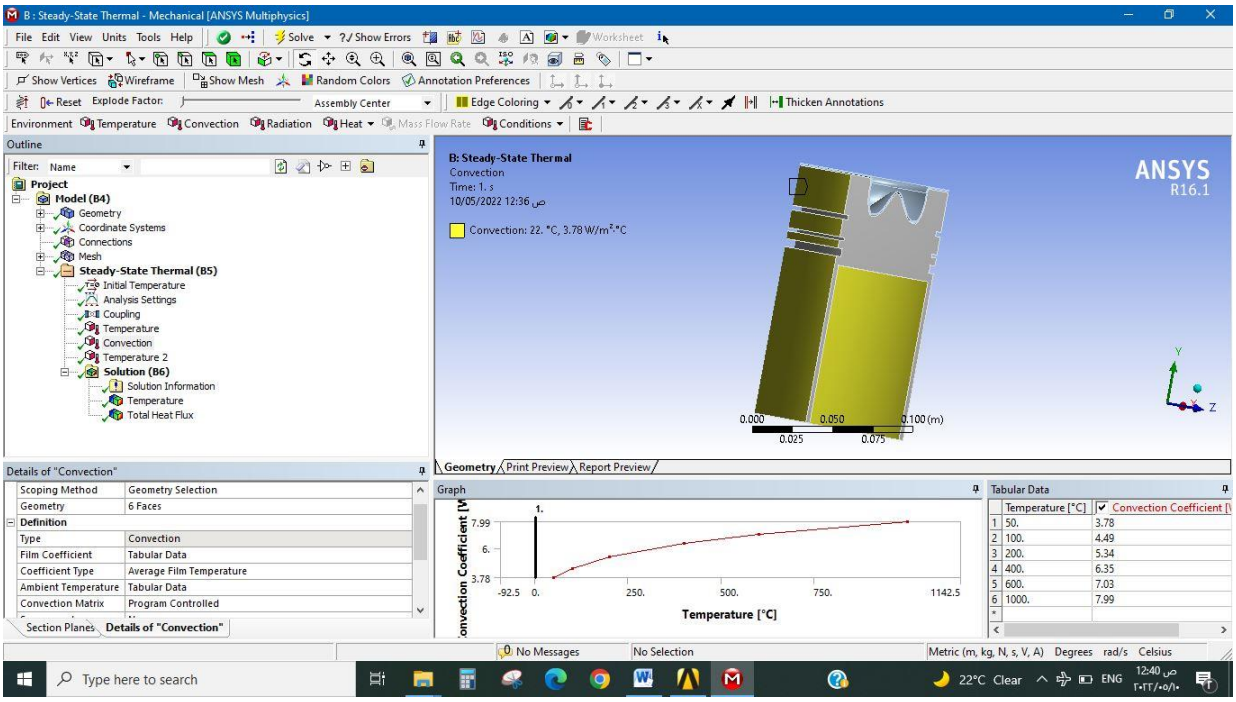

Fig 3.11 represent the convection heat values that varying with temperature

3.6.4 Assumptions of thermal Analysis simulation process

1. Coating materials are isotropic.
2. Perfect bond between coating layer and substrate surfaces.
3. Coating layer and substrate are perfect elastic materials.
4. Heat transfer occurs only by conduction and convection without radiation and in steady state method.

CHAPTER FOUR

RESULTS AND DISSCUSSION

4.1. INTRODUCTION

This chapter discusses the results of experimental work and characterization tests such as the XRD, SEM, AFM and Thermal Conductivity tests, as well as porosity, density, and thickness tests. Finally, the obtained results were discussed here. Besides, Numerical Analysis of thermal conditions by using numerical simulation program, ANSYS program which describes the temperature distribution on coating layer and piston body.

4.2. Powder characterization

4.2.1 X-Ray diffraction of Powders

The XRD test was conducted for the feedstock powders to specify the type of powders. Figures (4.1-4.4) represent the x-ray diffraction patterns for MgO ,Al_2O_3, SiO_2, and ZrO_2, that were compared with standard patterns which are identified by id numbers of (amcsd 0000503,RRUFFID=R060020, RRUFFID=R040031, RRUFFID=R110112) respectively, They demonstrated that the powders are as prescribed above, all of which have crystalline phases (as evidenced by the high intensity of their peaks), and are Compatible with the primary conditions required to be used as feedstock material in this study.

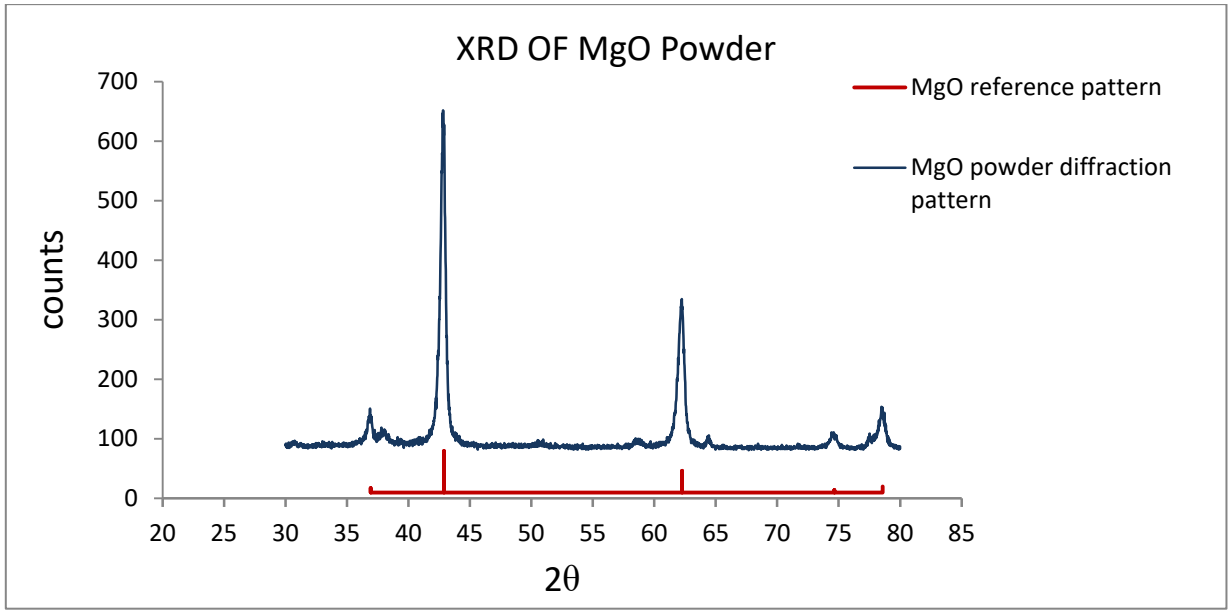

Fig 4.1 XRD pattern of MgO powder

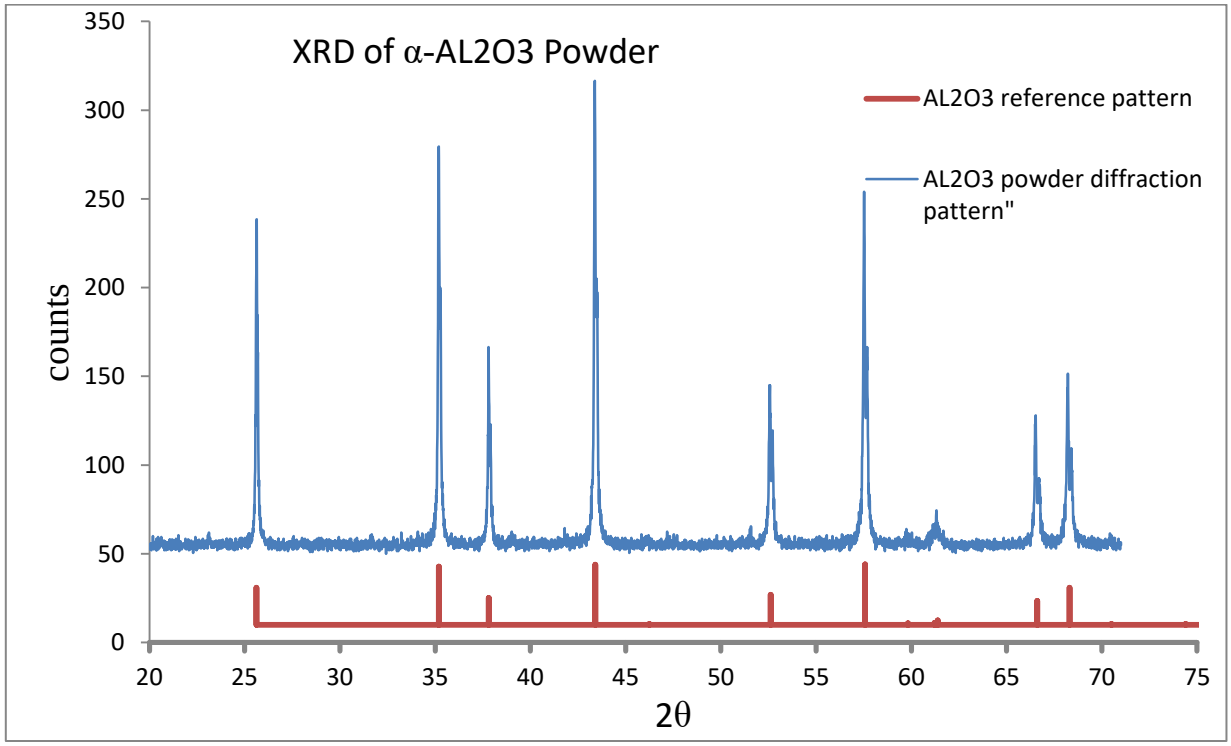

Fig 4.2 XRD pattern of α-AL_2O_3 powder

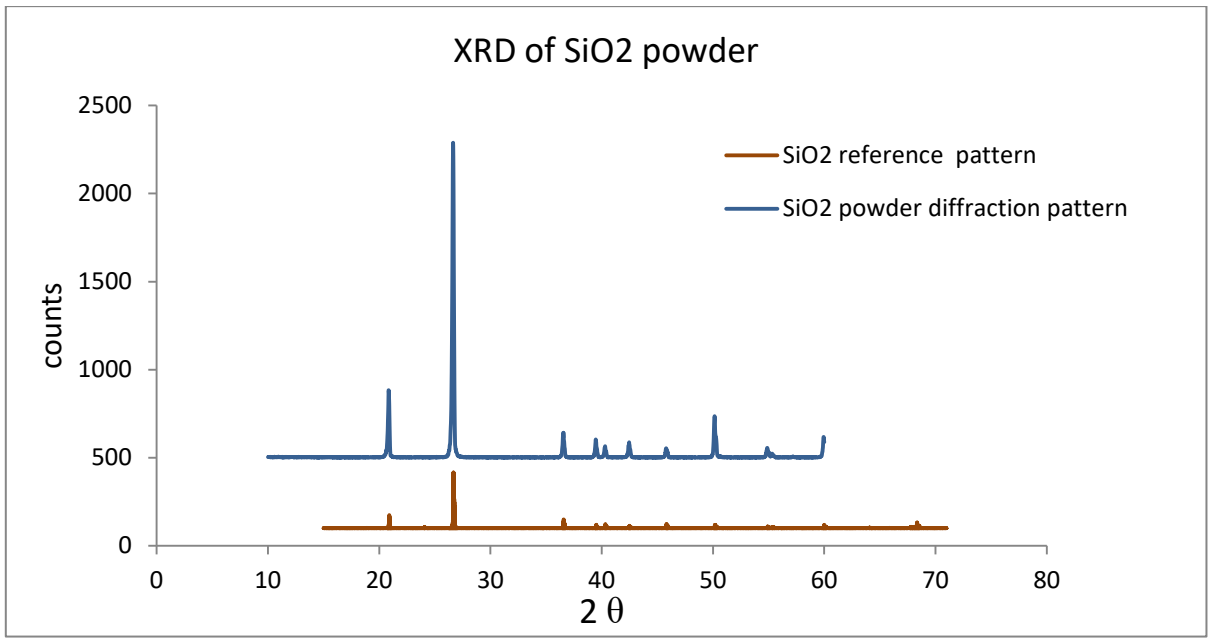

Fig 4.3 XRD pattern of SiO_2 powder

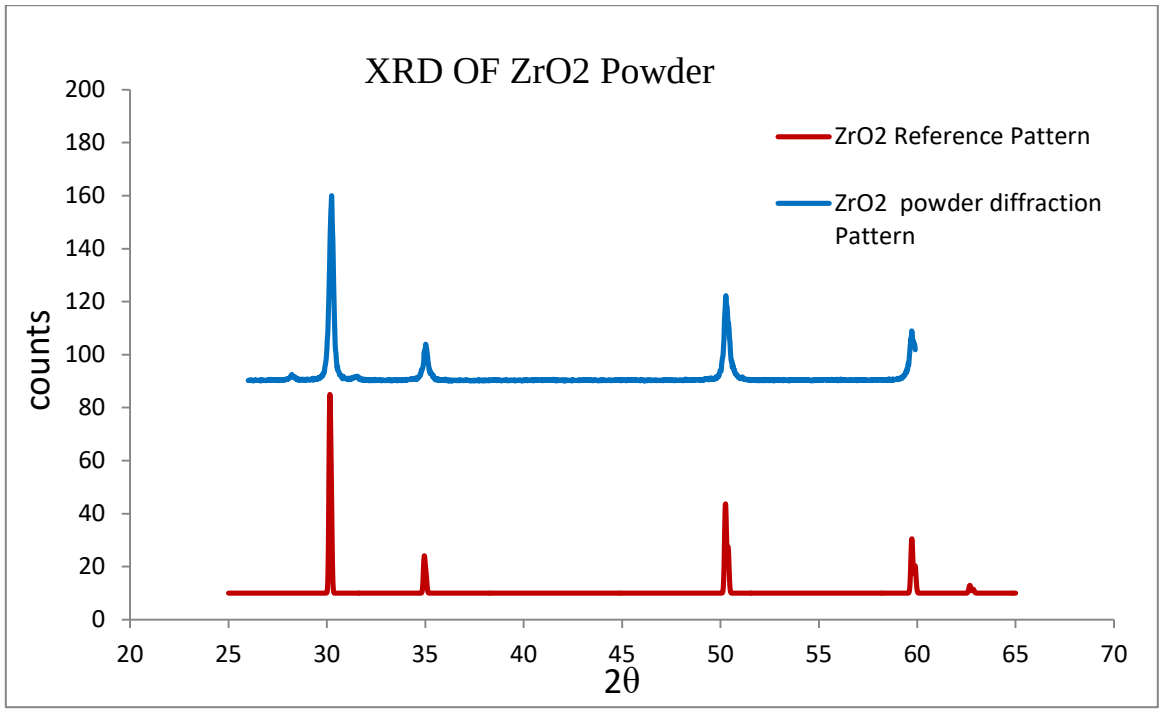

Fig 4.4 XRD pattern of ZrO_2 powder

4.2.2. PSA Results

Before coating, identifying the size of particles that would have been used in coating process was an important issue, The distribution of particle size has a clear effect on the feeding rate of the powder to the nozzle of the spray gun. If the distribution is wide, the problem of agglomeration of fine powders will generate problems in feeding the powder during the completion of the work, but if it is large in size, it will go out from the path of the torch during the transition to the surface of the substrate, and a defect will occur in the coating process. In this study, the particle size distribution was acceptable, as shown by the distribution schematics in Fig 4.5-4.8

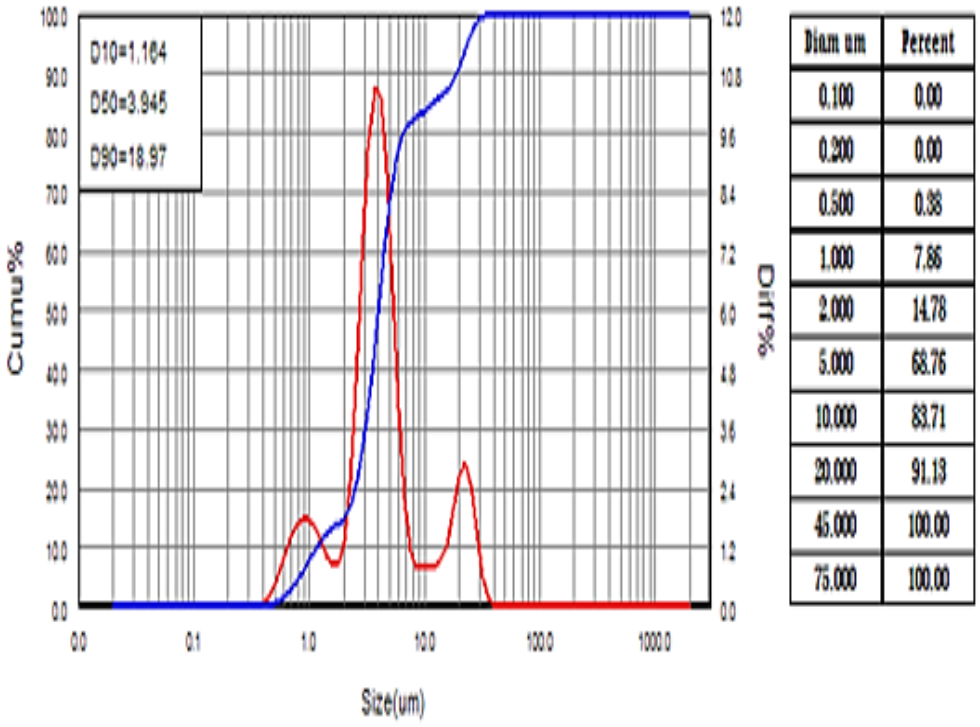

Diam um	Percent
0.100	0.00
0.200	0.00
0.500	0.88
1.000	7.86
2.000	14.78
5.000	68.76
10.000	83.71
20.000	91.13
45.000	100.00
75.000	100.00

Fig 4.5: PSA results of MgO powder

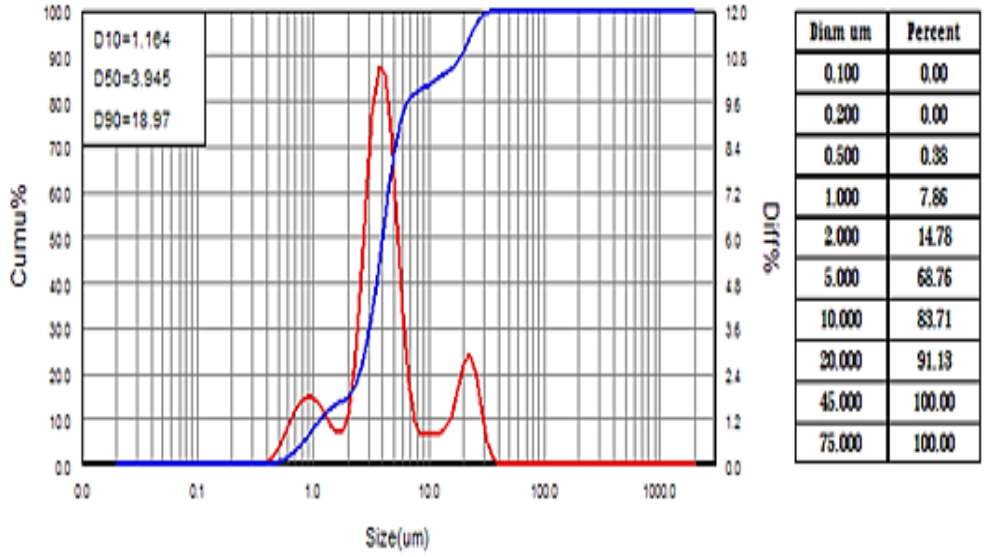

Diam um	Percent
0.100	0.00
0.200	0.00
0.500	0.38
1.000	7.86
2.000	14.78
5.000	68.76
10.000	83.71
20.000	91.13
45.000	100.00
75.000	100.00

Fig 4.6 PSA results of Al2O3 powder

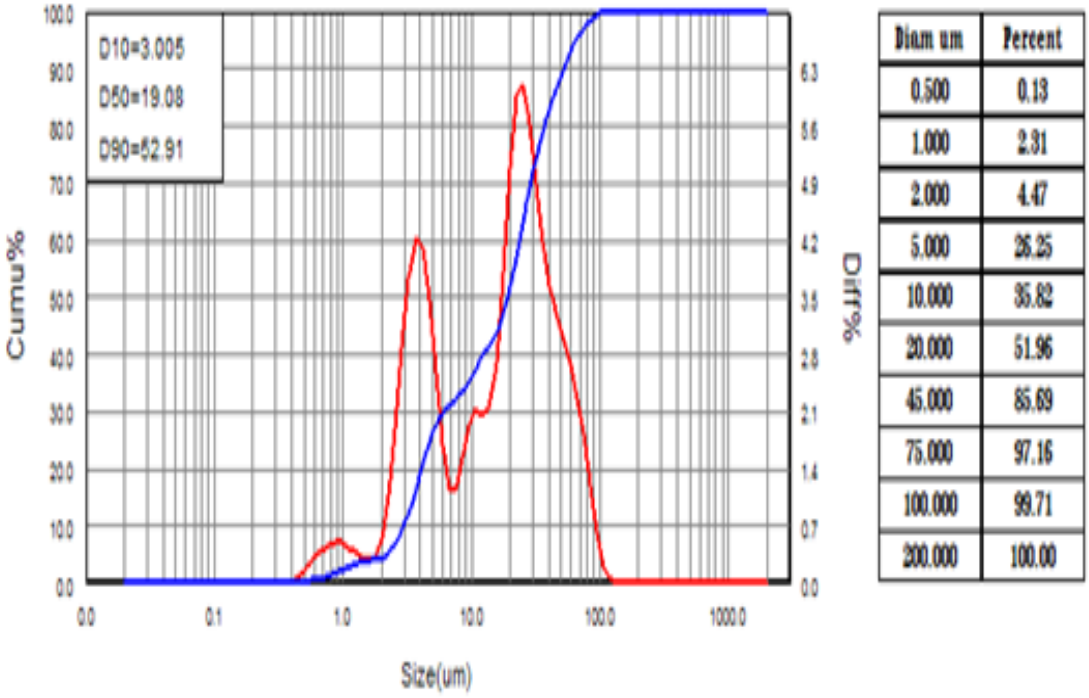

Diam um	Percent
0.500	0.13
1.000	2.31
2.000	4.47
5.000	26.25
10.000	35.82
20.000	51.96
45.000	85.69
75.000	97.16
100.000	99.71
200.000	100.00

Fig 4.7 PSA results of SiO2 powder .

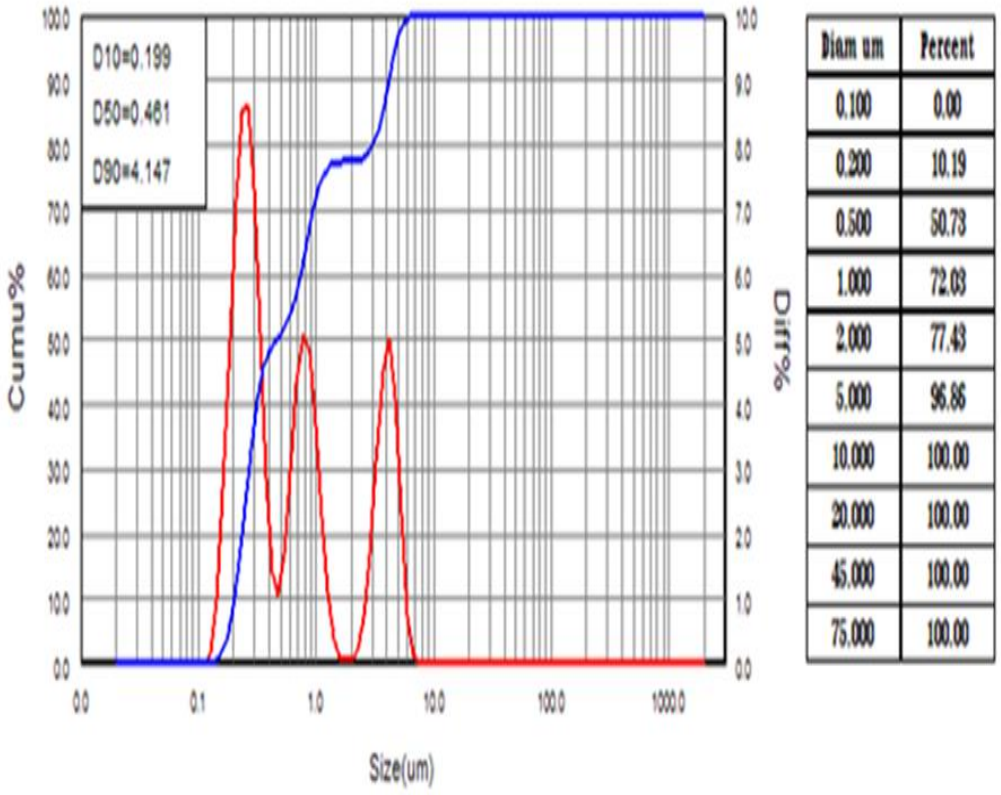

Diam um	Percent
0.100	0.00
0.200	10.19
0.500	50.73
1.000	72.03
2.000	77.43
5.000	96.86
10.000	100.00
20.000	100.00
45.000	100.00
75.000	100.00

Fig 4.8 PSA results of ZrO2 powder

4.2.3.Specimen roughness

The roughness of the substrate was measured by a profilometer device after preparing operations were completed, because it affects the adhesion of the coating layer (TBC) at the substrate surface. The roughness results of all specimens are represented in fig. 4.9, it is clear that they had micro-scale values. this amount of roughness gave the TBC coating layer a good bond with the substrate surface without the need to deposit a bond coat layer.

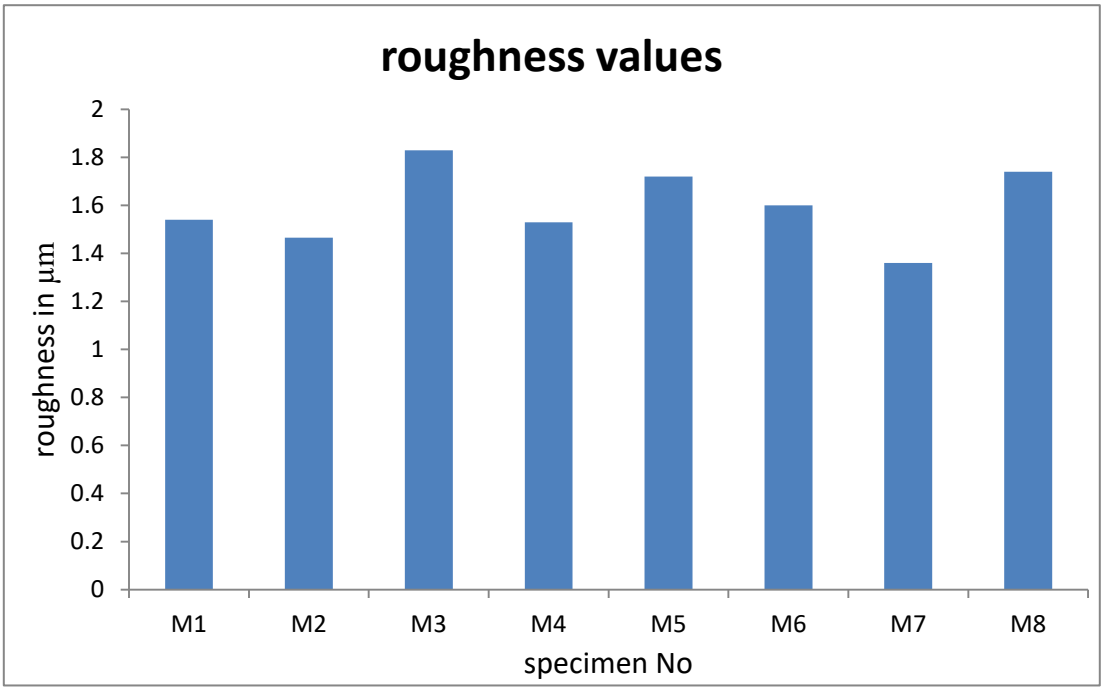

Fig 4.9: roughness values of substrates before coating .

4.3. Coating layer characterization

4.3.1. Coating layer Morphology

4.3.1.1 X-ray diffraction test

This test was performed for the as-sprayed samples that had the lowest thermal conductivities (M4, M7) only; in order to determine coating layer phases after the coating process was carried out. The X'pert HighScore software from MalvernPanalytical company was used for analyzing, However, The resulting peaks identification were conducted by matching phases peaks with their standard JCPDS data files that were built in the software library. Figures (4.10 and 4.11) exhibit the X-Ray Diffraction patterns of the as- sprayed coatings for samples (M4. M7) only.

The phases show in Fig 4.10 indicate to formation a bonding phase of silicate compounds like perovskite ($MgSiO_3$) and Sillimanite (Al_2SiO_5) with a semi-melted particles of magnesite and silica that implanted in this matrix .the existence of silicates bonding phase gave an good adhesion with substrate, in addition to other coating components themselves.as well as high hardness of phases included, This information was agreed with references. [58,59].

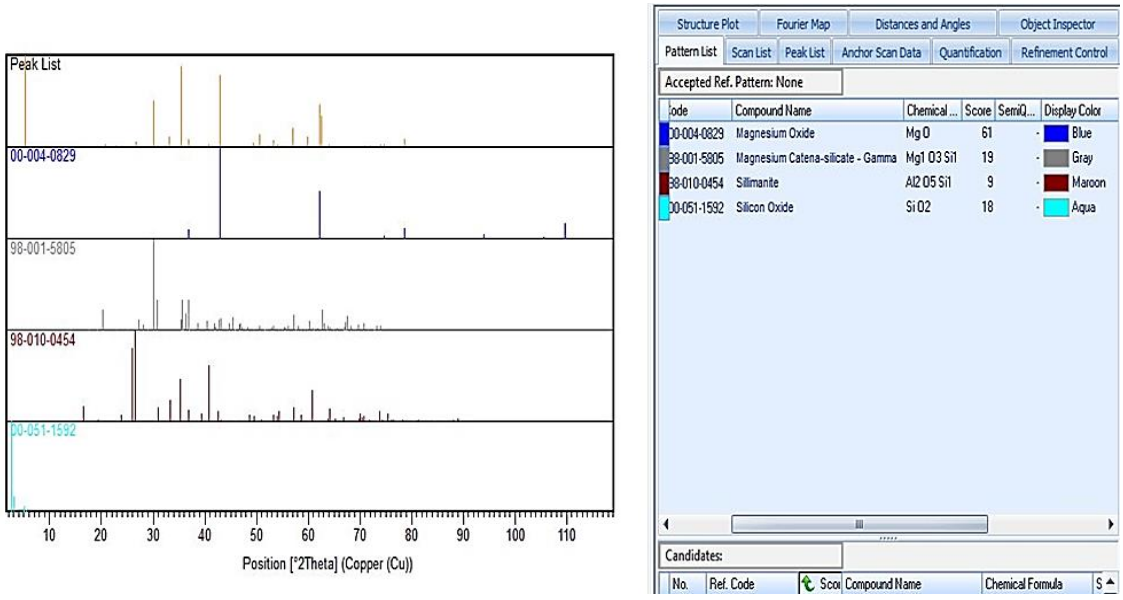

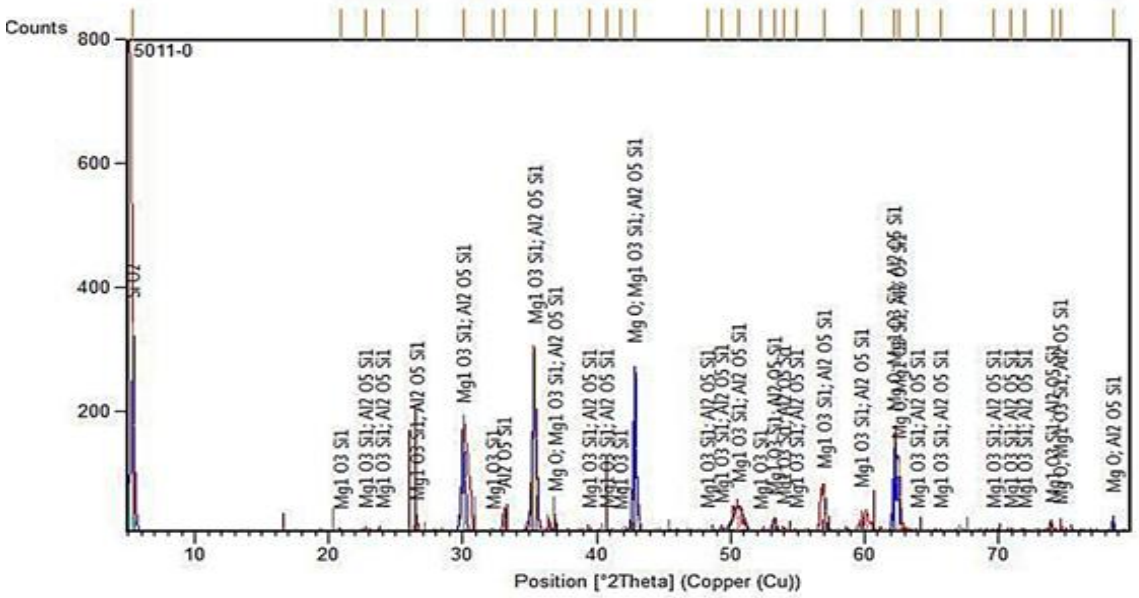

Fig 4.10: XRD Analysis of M4 coating layer .

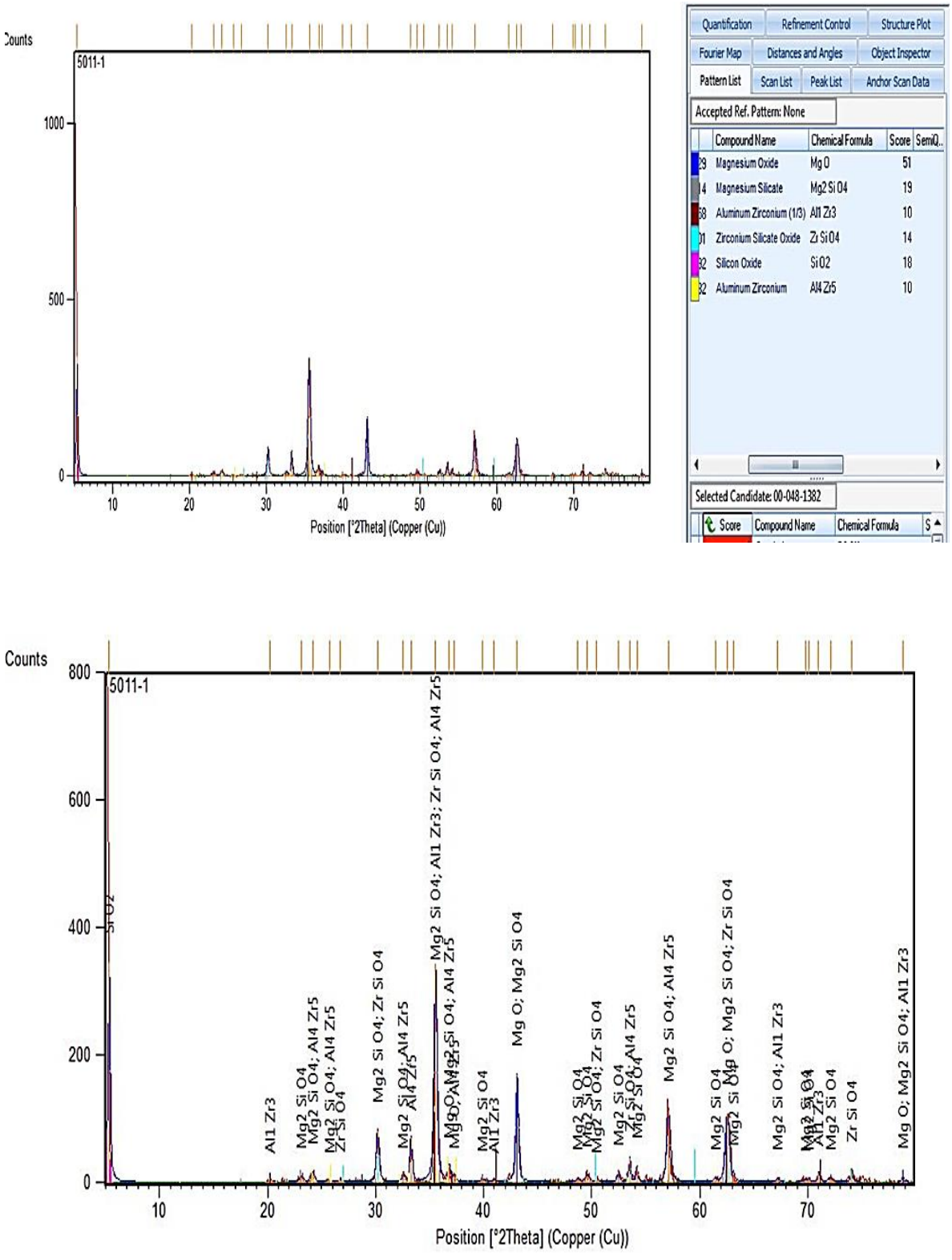

Fig4.11: XRD Analysis of M7 coating layer.

4.3.1.2 Scanning Electron Microscopy (SEM)

Morphologies and microstructures of the surface of coated samples have been studied depending on the micrographs that were obtained from scanning electron microscopy for the two samples (M4, M7). The lamellar structure of the coating layer, its porosity, cohesive among sprayed powders, and uniformity, as well as a cross section of the coating layer, is also shown in the micrographs below.

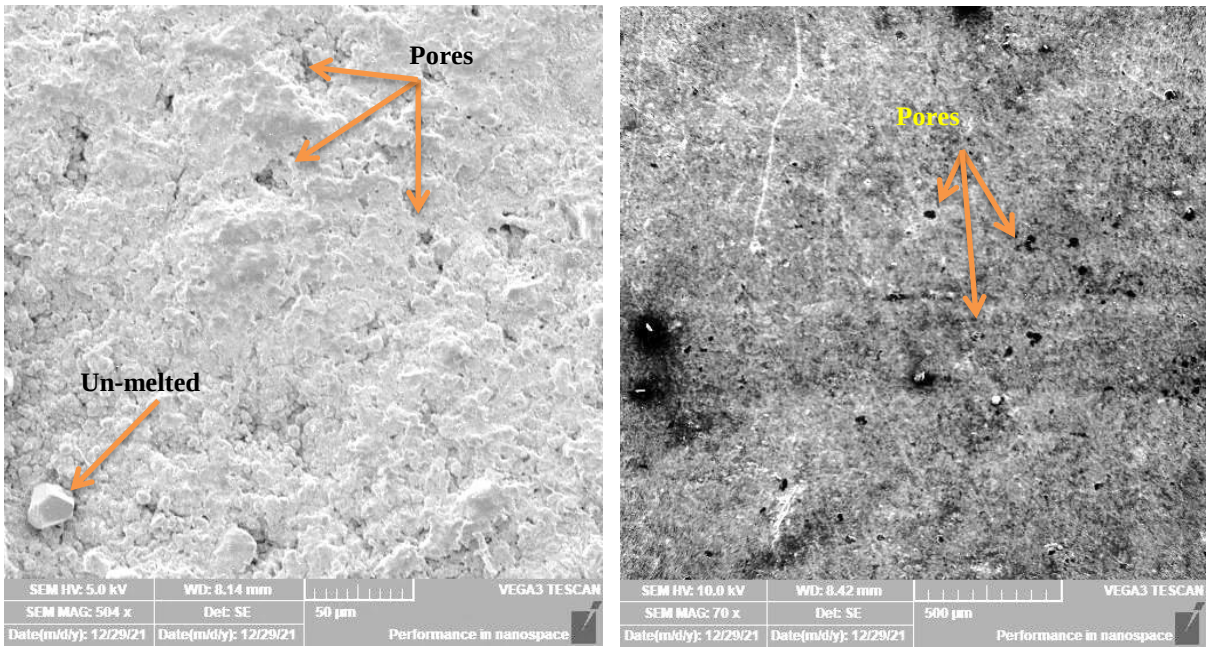

A B

Fig 4.12: SEM images of coating surfaces :(A) M4 specimen and (B) M7 specimen

Fig 4.12A shows clearly the pores in the surface of the M4 as-coated sample, which have the optimized blend induced by rapid cooling that does not allow the particles to completely melt at the surface, these pores have two types, namely, open pores that are located at the surface and closed pores that result from shadowing. The shadowing always accompanies the layered structure that is induced either by the powder/substrate impacting angle being less than 90^{o} or by

accumulated particles that haven't had time to melt, resulting in inter-lamellar pore[2, 19].Fig 4.12B exhibits the M7surface, which contains zirconia, high cohesive coating structure that was confirmed by micro-hardness readings and diffused particles, and a lower pore number than the M4 surface sample, with some un-melted particle spreading, in addition to the particles that melted and semi-melted that attached together well, as well as the peaks and valleys that caused the roughness.

These features may be caused by the high temperature of the flame and the rapid cooling that produced accumulated particles resulting in a lamellar structure, as seen in Fig 4.12B and Fig 4.13A.

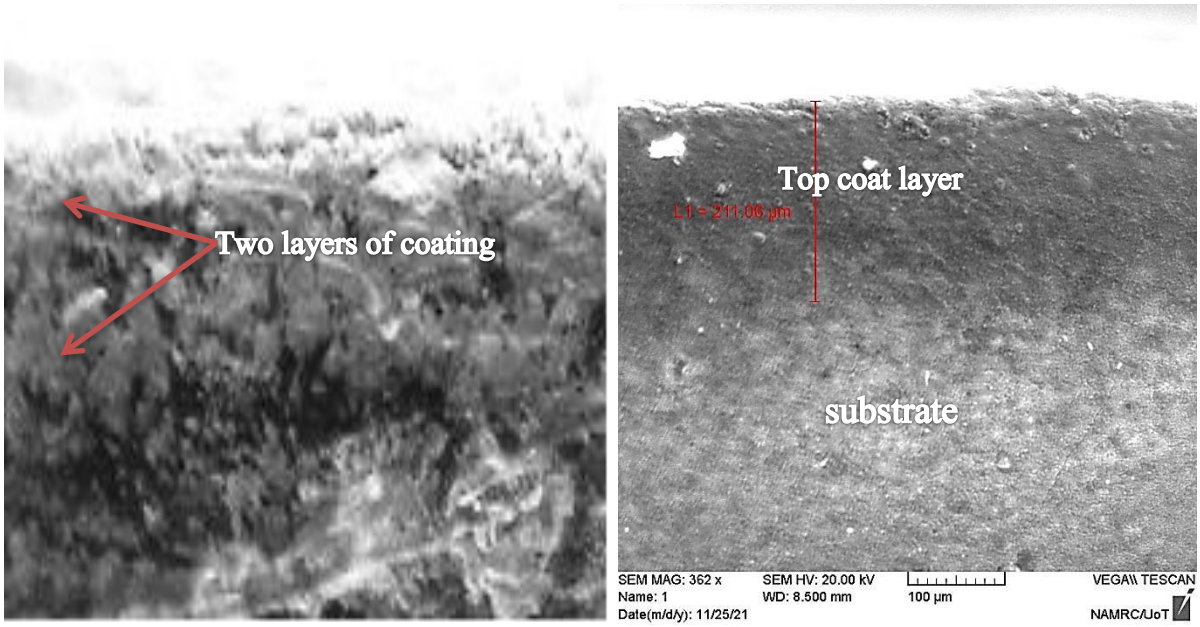

A **B**

Fig 4.13 SEM images for the coating surface cross section of M4 specimen

In Fig 4.13A , an evidence for the high adhesion between the coating layer and substrate has confirmed by adhesion test results .the coating layer and substrate is explained in the Fig 4.13B

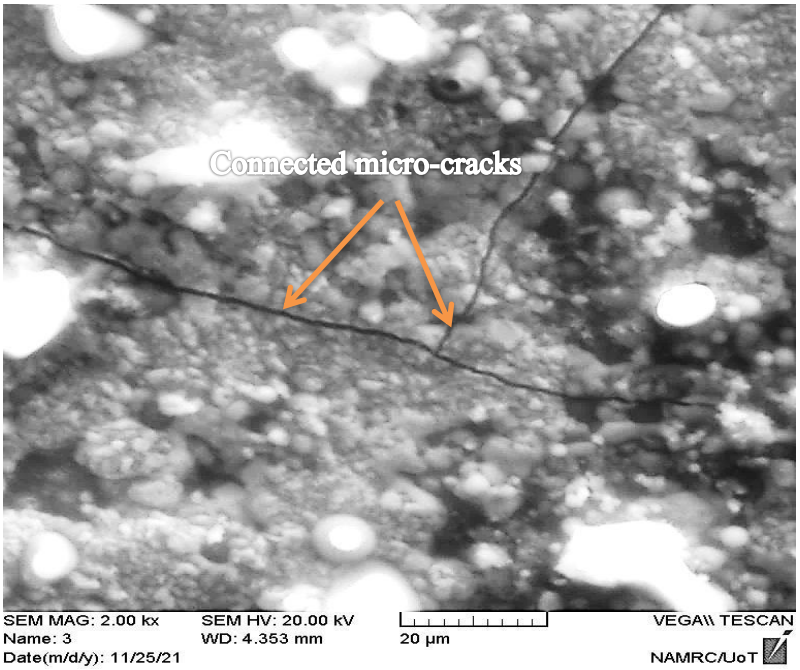

Fig 4.14 Micro-cracks connected with a nano-pores in M4 sample

Also, a small number of micro-cracks could be observed in the M4 porous coating layer as shown in Fig 4.14. They may have resulted from volumetric variation in enstatite that was an orthorhombic structure with a volume (836.39 A^o) to clinoenstatite, a monoclinic structure of a volume (415.36 A^o) during cooling [4, [63, 64]. as well as the difference in overall coefficient of thermal expansion between the ceramic top coat and substrate.

The low percentage of enstatite phase in the coating layer and the presence of phases that have a coefficient of thermal expansion close to metal values included in the topcoat ceramic layer, like forsterite ($9.5x10^{-6}$) in M7 sample , can be another reason for lower number of cracks present in the top coating layer.

4.3.1.3.SEM-EDS test

The SEM-EDS test was performed to determine whether or not the powder materials used existed and how much of each element was presented. The test shows the existence of an excellent amount of magnesium, which is the major element used in this work. In addition to the silicon and aluminum, it has a ratio compatible with the percentage that is used in blends. The presence of oxygen, which is found in high concentrations because the spraying process were performed in an open environment, as well as, it was essentially included in all compounds entering the coating process. The existence of a high oxygen percentage is evidence of the high oxidation resistance of the coatings during service because of their crystals being saturated with it. In addition to oxygen, carbon was the new element seen in EDS analysis, despite not being the input element. The flame containing acetylene was the main source of carbon presence. it didn’t enter into any phase composition. Finally, the results obtained from the EDS test conformed to what was obtained by the XRD test.

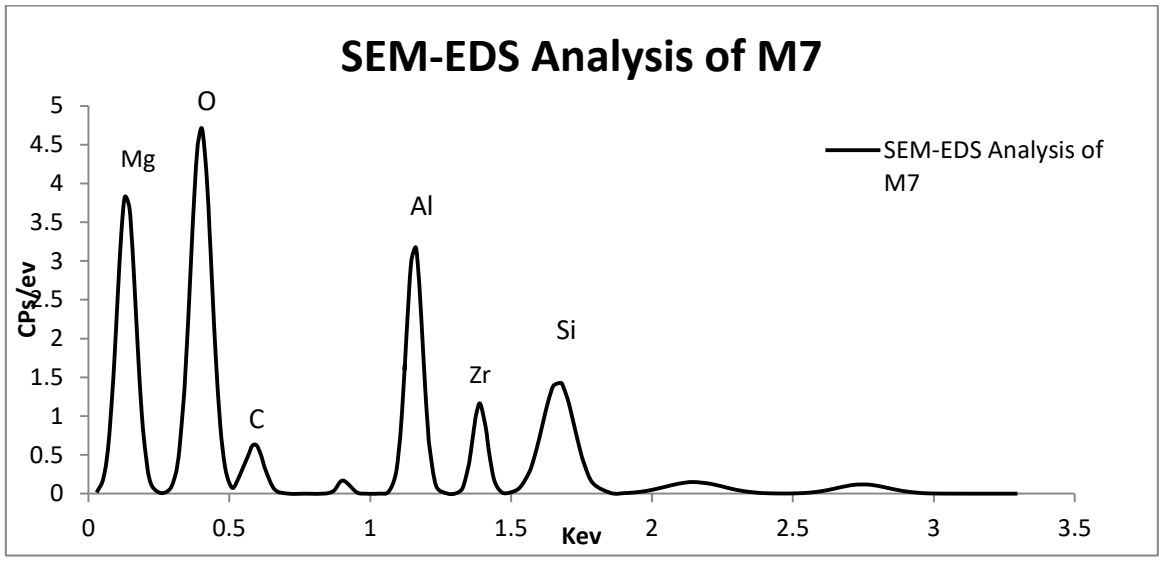

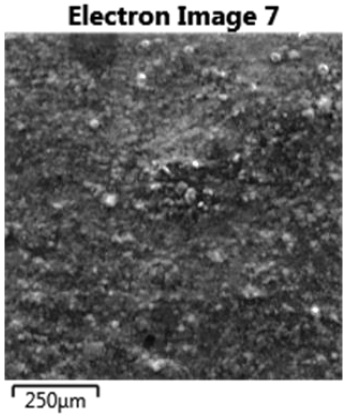

العينة M7

wt%	Element
5.88	c
33.29	o
21.26	Mg
17.56	Al
13.16	Si
8.85	Zr
100	total

Fig 4.15 SEM-EDS analysis of sample M7

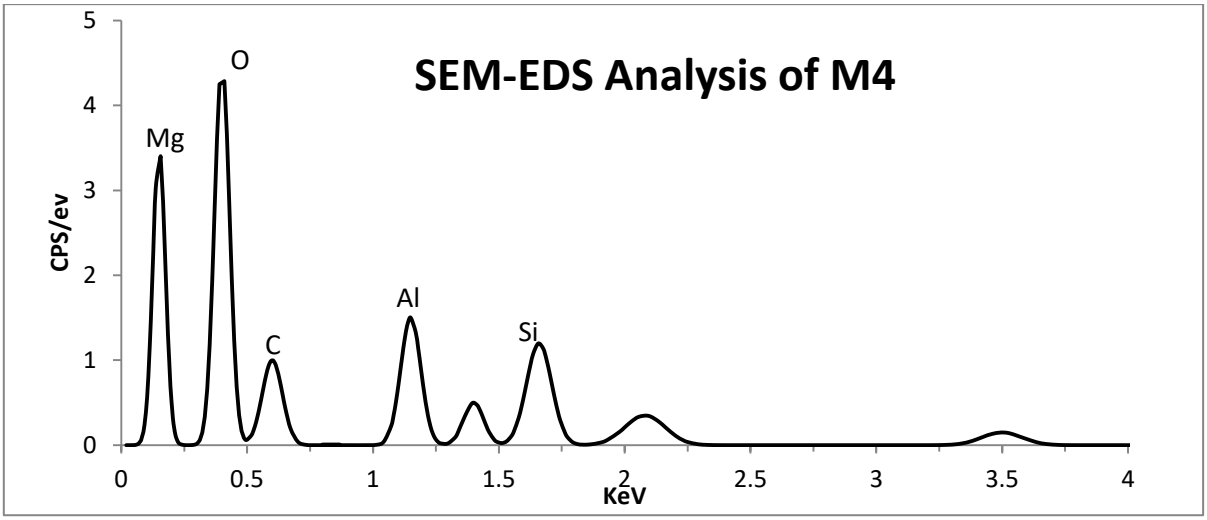

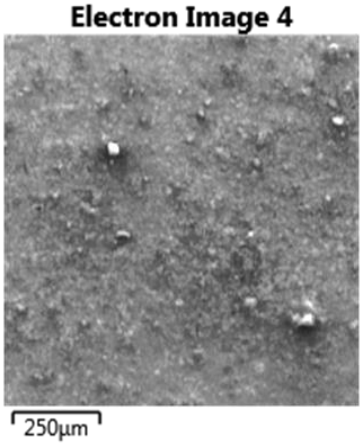

wt%	Element
4.89	c
38.23	o
25.26	Mg
17.21	Al
14.41	Si
100	total

Fig 4.16 SEM-EDS analysis of sample M4

4.3.4. Atomic Force Microscopy (AFM)

Figures 4.17 and 4.18 explain the profile in 2D and 3D graphs of two sample surfaces .The profile of the coating surface is revealed through conducting the AFM test. It emphasizes that the roughness of the sample surface of M4 is nearly that of the M7 sample at about (0.258 µm and 0.200 µm for M4 and M7,

respectively), though the coating process conditions are the same except for the zirconia contained in the sample M7 that reduce the surface roughness slightly . This may take place as a result of the handy achievement process where the operator is not fully in control of the circumstances during spraying. However, the roughness property of two samples is low as they were tested in the as-sprayed state.

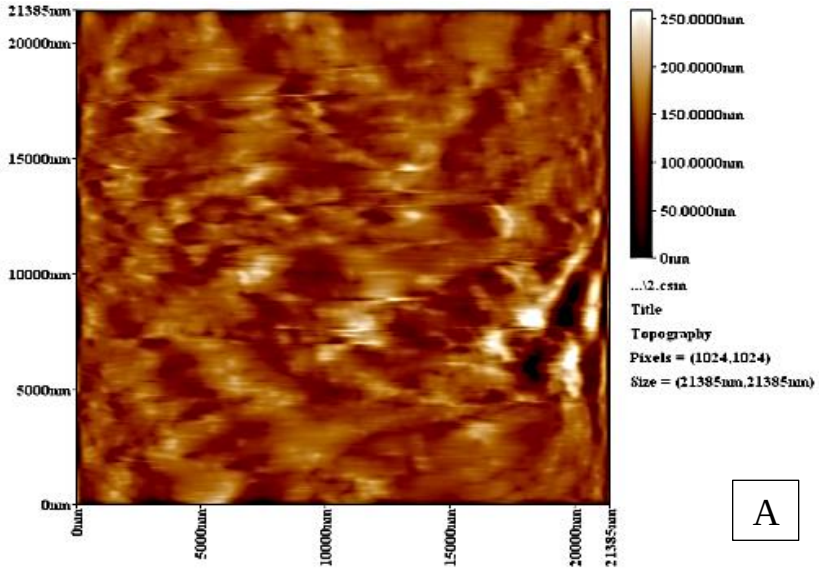

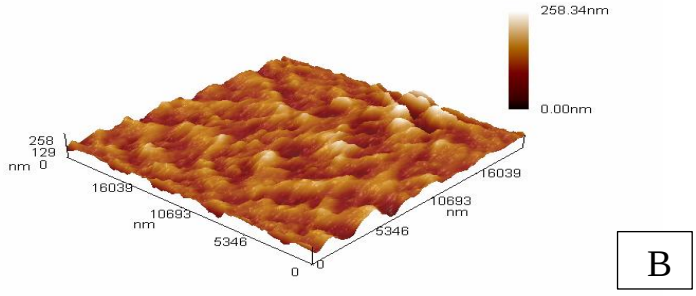

Fig 4.17 AFM of surface profile of the sample M4

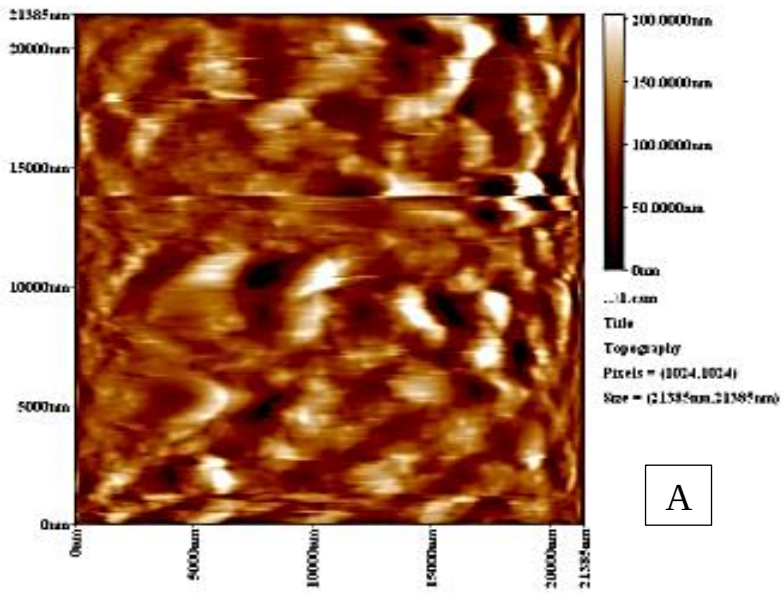

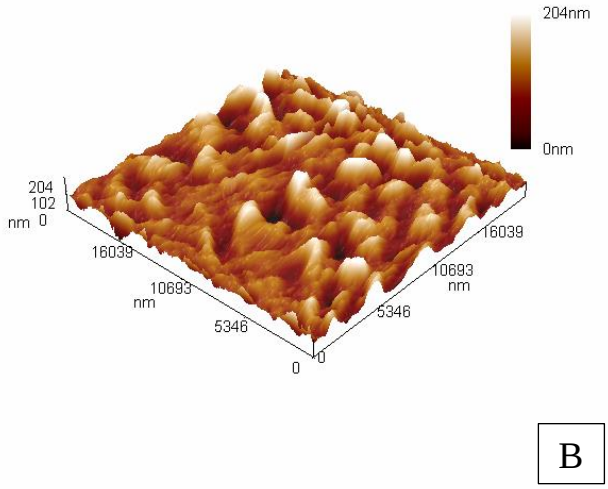

Fig 4.18 AFM of surface profile of the sample M7

4.3.2.Thermal conductivity results

The thermal conductivity of all coated samples is experimentally measured, both with and without zirconia, as can be seen, thermal conductivity values are convergent. Their values explained that the samples (M4, M7) have the lowest thermal conductivity as shown in Fig 4.19 due to porosity content which is approach to 20% ,and 15% for (M4, M7) respectively that were confined the air inside that have a lowest thermal conductivity, the fluorite crystal structure of SiO_2 (silica) and perovskite structure of magnesium silicate $MgSiO_3$ resulting from powder fusion and reaction during spraying as refer in the X-ray patterns, they play a crucial role in lowering thermal conductivity ,these structures were always prefer as TBC coating required to be deposited as indicated in many studies such as[21, 52, 65, 66].

Reactions of the base materials or feedstocks result in the formation of new phases, such as forsterite ($MgSiO_4$), Sillimanite (Al_2SiO_5), and Aluminum zirconium ($AlZr_5$, $AlZr_3$) and Zirconium silicate oxide ($ZrSiO_4$),and result in a new complicated structure which are more complicate than their origin powders [29]. Therefore, it may consider another main reason to reducing thermal conductivity of TBC coating that obtained in this research. In the lamellar structure , the Flame spray method is characterized by its lamellar structure, the presence pores with trends normal to the heat flow reduce the thermal conductivity of the ceramic coating also[67].

The mass and radius mismatch of the cations result in great lattice distortion and strong phonon scattering in materials. Lattice distortion might be one of the main reasons that resulting in the reduced thermal conductivities [52,66,68,69] . However, in this study ,cations used have a big difference like (Mg^{+2}=0.86 A^0,Al^{+3}=0.675 A^0, Si^{+4}=0.54 A^0) and (O^{-2}=140A^o) .

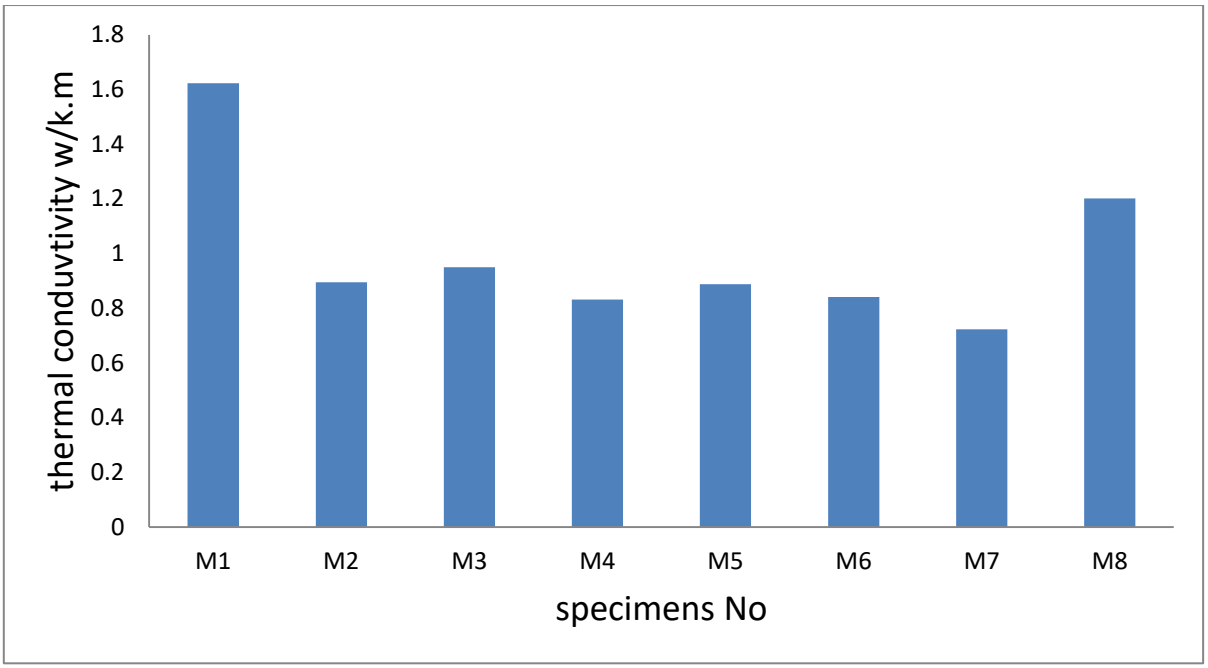

Fig 4.19 Results of thermal conductivity measurements

4.3.3.Mechanical Properties

4.3.3.1. Adhesion test results

The results of adhesion test showed that the coating layer had an excellent adhesion strength lies in the range (14MPa to 24MPa) ,the maximum value was for the M7 sample .the zirconia particles that filled the pores which had a small size resulted in an increase of the contacted Area that is in turn rise the strength of adhesion of sample M7. the suitable roughness of the base

surface of the all specimens including M4 specimen supported the anchoring of the coating with the substrate surface . The coating displayed both adhesive and cohesive failure. This is due to the high binding strength that occurs at the TC/BC contact [70].

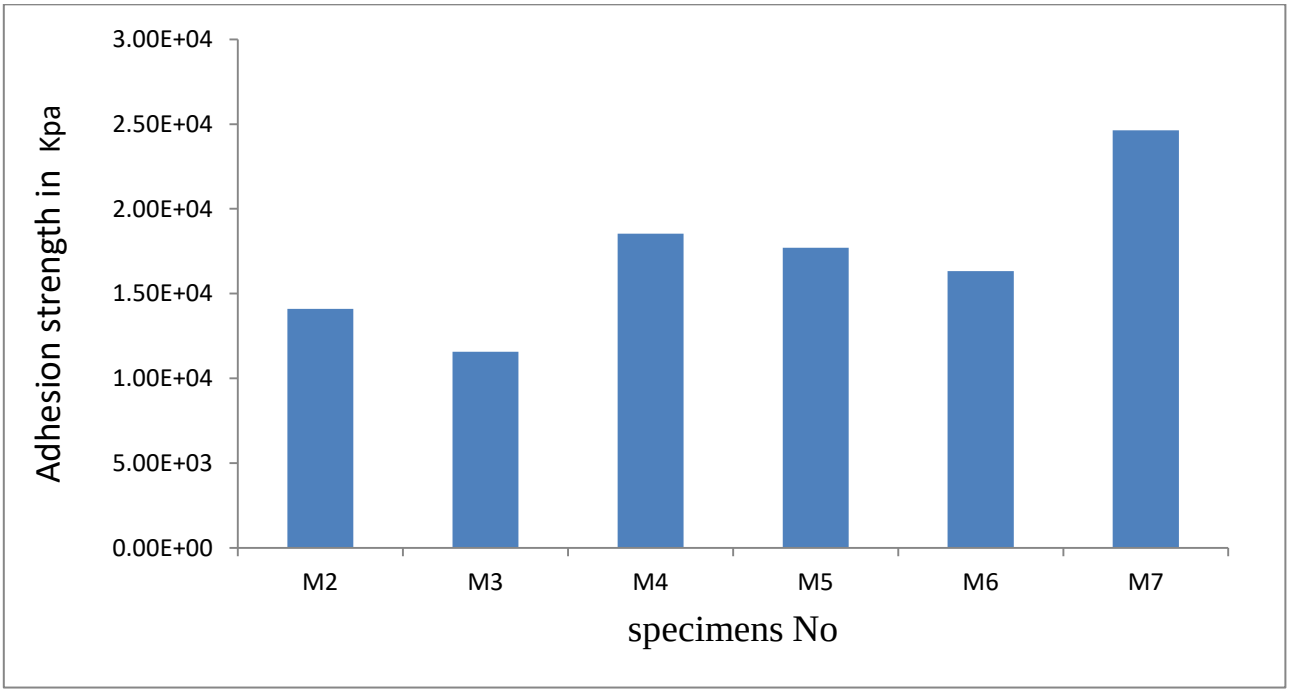

Fig 4.20 :Results of adhesion strength of six samples

4.3.3.2.Micro-hardness test results

TBC coating layer showed highest micro-hardness in all eight samples. Based on the readings explained in figure 4.20 . The two samples of interest, M4 and M7 have a close values to other samples. The TBC micro-hardness readings that were obtained depended on for each sample. Therefore, they may find some oscillating values, but in general they have high values that were ranging (600-800 HV) . The

results achieved in this study were compatible with other researchers' results that worked with YSZ [71].

The presence phases which have high hardness like Sillimanite (6.5-7.5 on mohs scale), MgSiO3(5-6 mohs), MgO(5.5) [72], and ZrSiO4 (13.7Gpa)[67] .could add another contribution in increase hardness values.

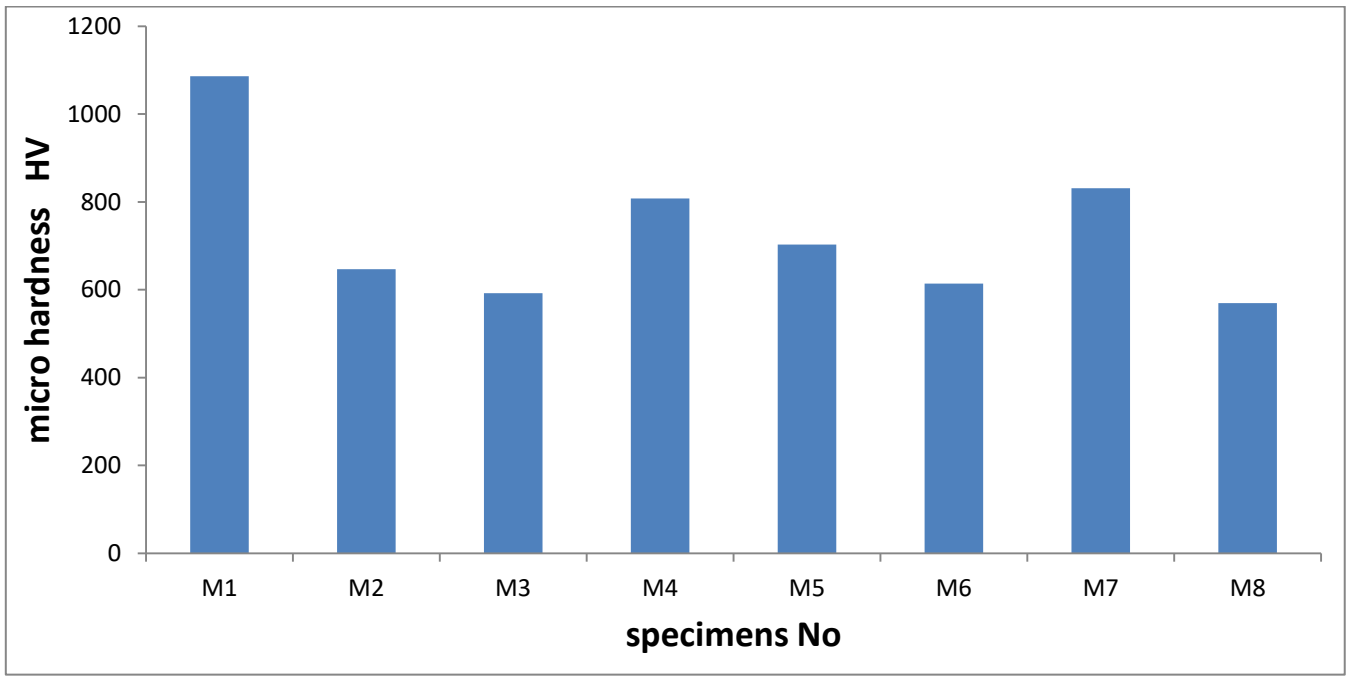

Fig 4.21 micro-hardness results of all samples

4.3.4.Physical Properties

4.3.4.1 Thickness Test

TBC formed with multilayer coating, the total thickness often doesn't exceed(500 µm) [39,73,74]. but sometimes reach until 1mm [30,45]. In this study, the thickness that reached was about 600 µm, compared with some researchers such as [58],It can be seen evidently that the highest thicknesses are for M4 and

M7 samples. This may explain why they have the highest porosity also. Because of the rapidly and non-uniformly building up of melted particles under which the pores will generate, increasing the thickness of the lamellar structure will inevitably initiate more pores under each newly formed lamella. This, in turn, will decrease the thermal conductivity as porosity is increased. However, increasing thickness and porosity have negative consequences on the mechanical characteristics of TBCs, which the thesis recommends more research into future works.

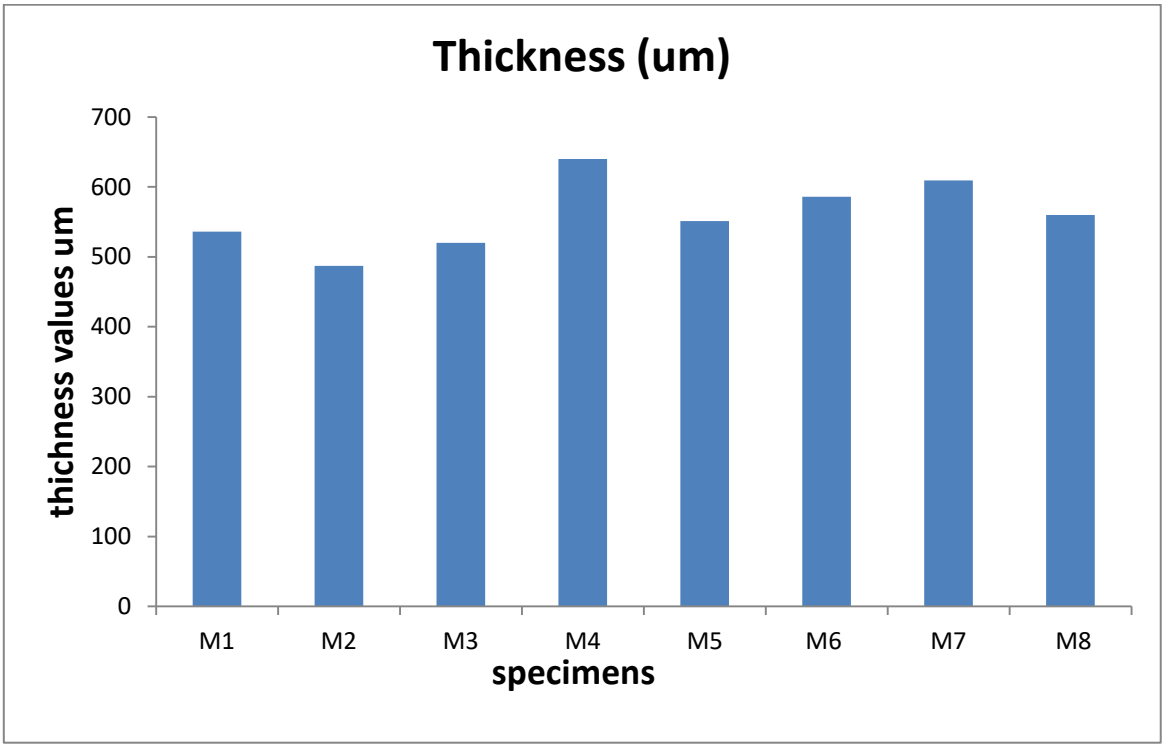

Fig 4.22 Thickness of coated Samples

4.3.4.2Roughness Test

After spraying was accomplished, the roughness of the coating layer was measured, but after coating process the test were carried out by two techniques, the profilometer device and Atomic Force Microscopy. The AFM technique gives results on a nanometer scale for a limited area of about 20 μm^2 of coating layer, The AFM readings adopted of two samples of interest, which were M4 and M7 only, The AFM readings assured profilometer measurements which determined any of the samples were rougher. the AFM test determined a feature of a limited area ($20\mu m^2$) rather than the overall area of the specimen. The roughness values shown in fig (4.23) below explain that the roughness value of coating layers is one-third to that of uncoated specimen surface. All measurements of all coated and uncoated samples revealed the building up of spraying oxide particles in valleys that found in the substrate surface, producing an excellent adhesion bond by interlocking with the base metal. The roughness values that were measured by profilometer are represented in figure 4.23 below, and the AFM characterization graphs in figures (4.17A and B, 4.18A and B) were explained.

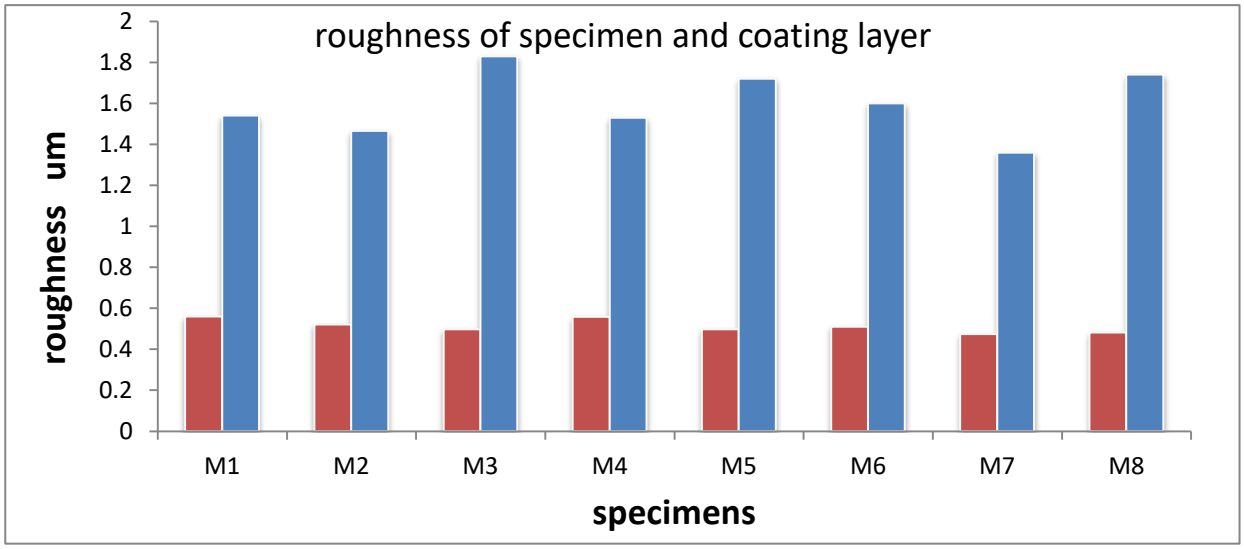

Fig 4.23 Profilometer Roughness values before and after coating (blue color before coating and others for coated specimen) .

4.3.4.3.Porosity evaluation Test

Porosity is a key feature associated with the thermal spraying process and thermal barrier coating in general. Figure 4.21 shows the percentage ratio of porosity for all samples, which clearly reveals the content was good and agrees with general content in almost all research where it was approached to (5-25)% for YSZ sprayed with air plasma spraying [6,39], and about (12-22%) for ceramic topcoat with flame spraying process[4,39]. Porosity in top coat layer within the range of (10-20%) contributes to reducing the thermal conductivity because of air confined inside, which has the lowest thermal conductivity. Besides, Due to phonon scattering at pores, thermal conductivity may generally be lowered by lowering the mean free path. Porosity content may increase or decrease based on several conditions, like particle size and shape, spraying distance, spraying angle [38], [75]. In this study, the reasons for porosity were the broad particle size distribution that caused fusion of some particles and saved others in un-melted or even semi-melted state that were laid over and solidified, creating pores. The mismatch of thermal expansion coefficient between substrate and ceramic coating layer was an essential reason for producing little micro cracks that were seen in the previous section (Fig 4.14), which work as open pores contributing in lowering the thermal conductivity of a TBC coating system. The two lowest thermal conductivity samples in this study were composed of multiphase coating layers with various CTEs with explained aforementioned reasons. These samples had porosities within the permitted range for TBC coatings applied by thermal spraying, namely (22% and 15.5%) for M4 and M7, respectively, which play a crucial role in decreasing the thermal property of the deposited coating layer.

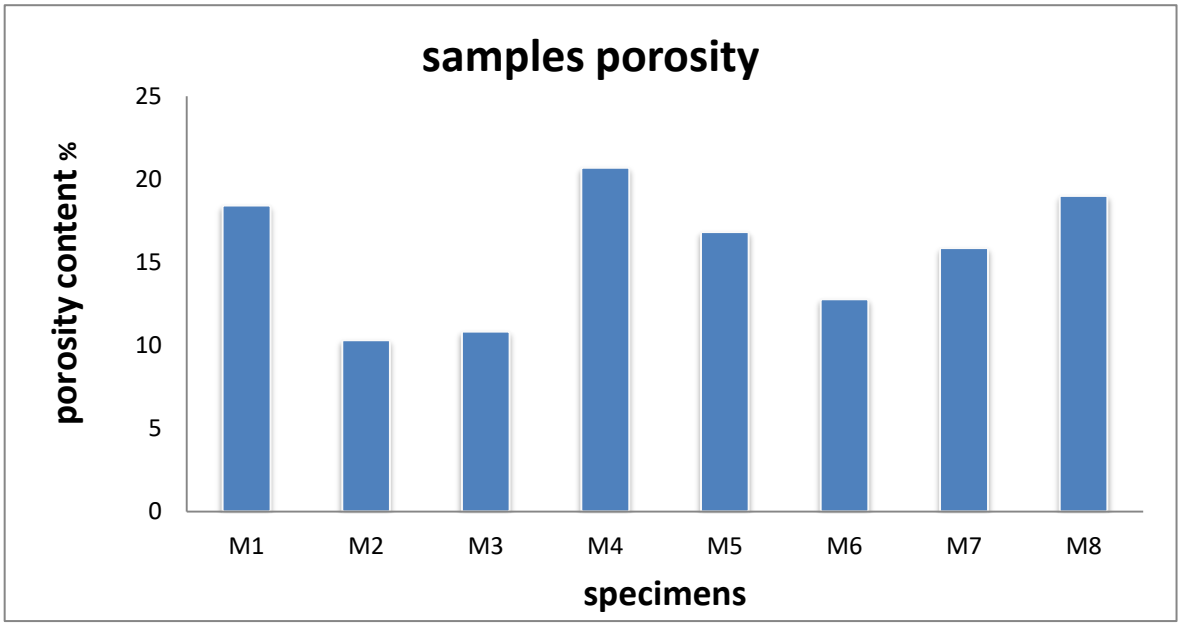

Fig 4.24 porosity content percentage of TBC layers of coated specimens

4.3.4.4. Density Test

Density is the property of a material that is related with a volume. Heat transferred through contacted bodies, therefore, thermal conductivity is related to the density by an increasing linear relationship, namely, thermal conductivity increases with density increase[76] . This is what was approved in this thesis as seen in fig (4.24) below.

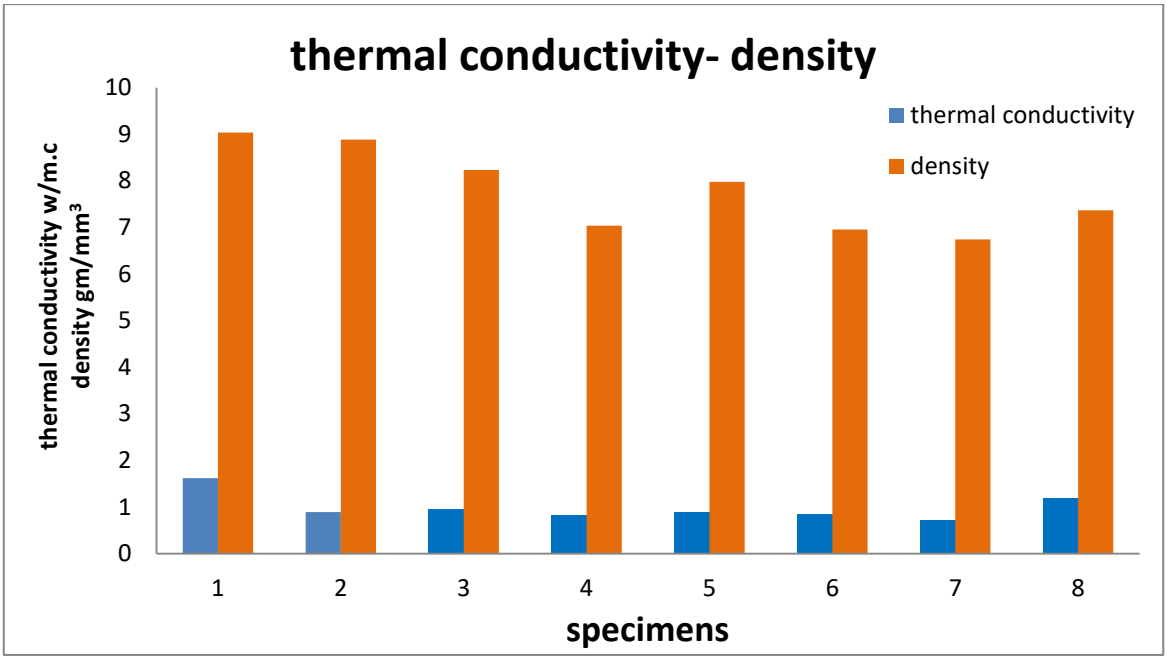

Fig 4.25: represent densities of coating layers and it's relationship with thermal conductivity of TBC coating layer.

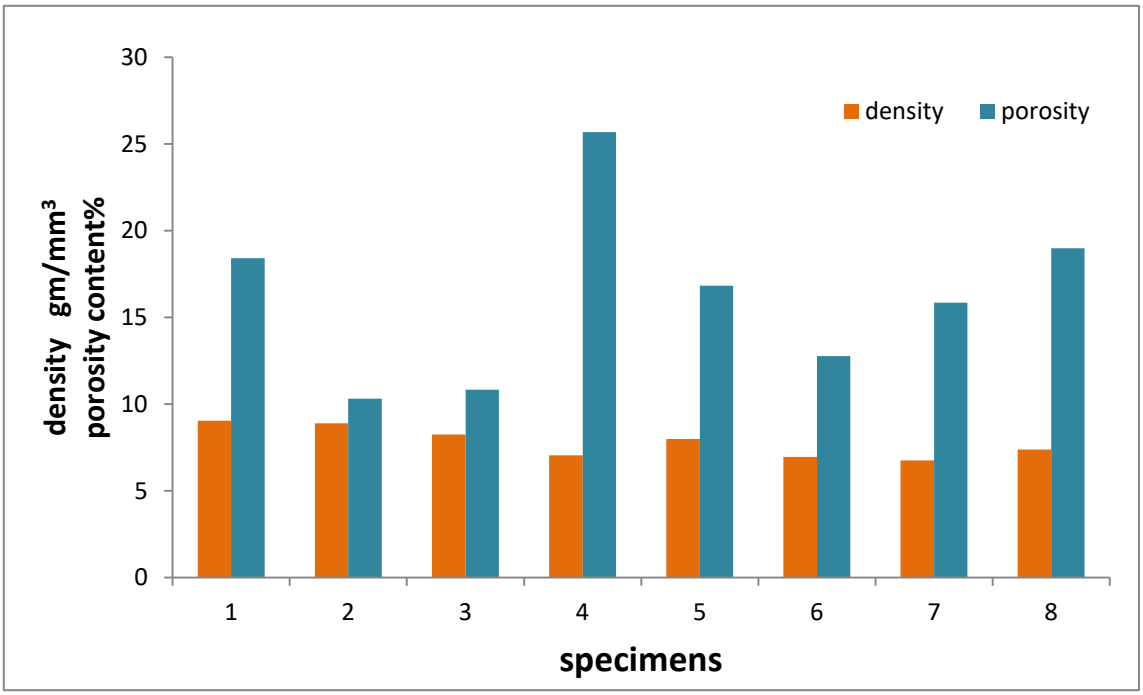

Fig 4.26: represent densities of coating layers and its relationship with porosity of TBC system

4.4.Numerical Analysis

4.4.1. Porosity analysis by Image J Program

The porosity content was measured by employing the Image J software package which is commonly used in characterization data analysis such as particle and grain size, perimeter, area …etc , depending on the distinguishable variances in color intensity(especially black and white color) of the solid features and porosity in two SEM micrographs of the coating layer of considered samples M4 and M7 were taken at different magnifications. The porosity content in each image was measured after distinguishing the intensity limits of solid phase and porosity, where the lighter color was considered a particle or solid phase[77] . The color intensity limit for digital images converted from SEM has been adjusted using the threshold option. The color intensity adjusting continues on the modified images until they reach the suitable threshold intensity that has been preferred for analyzing. The results of porosity measurements of the sample's images were close to experimental results. Fig 4.27 represents the modified images that were used to identify the porosity content of M4 and M7 coated samples, which were about (22.6 and 12.39 μm) respectively.

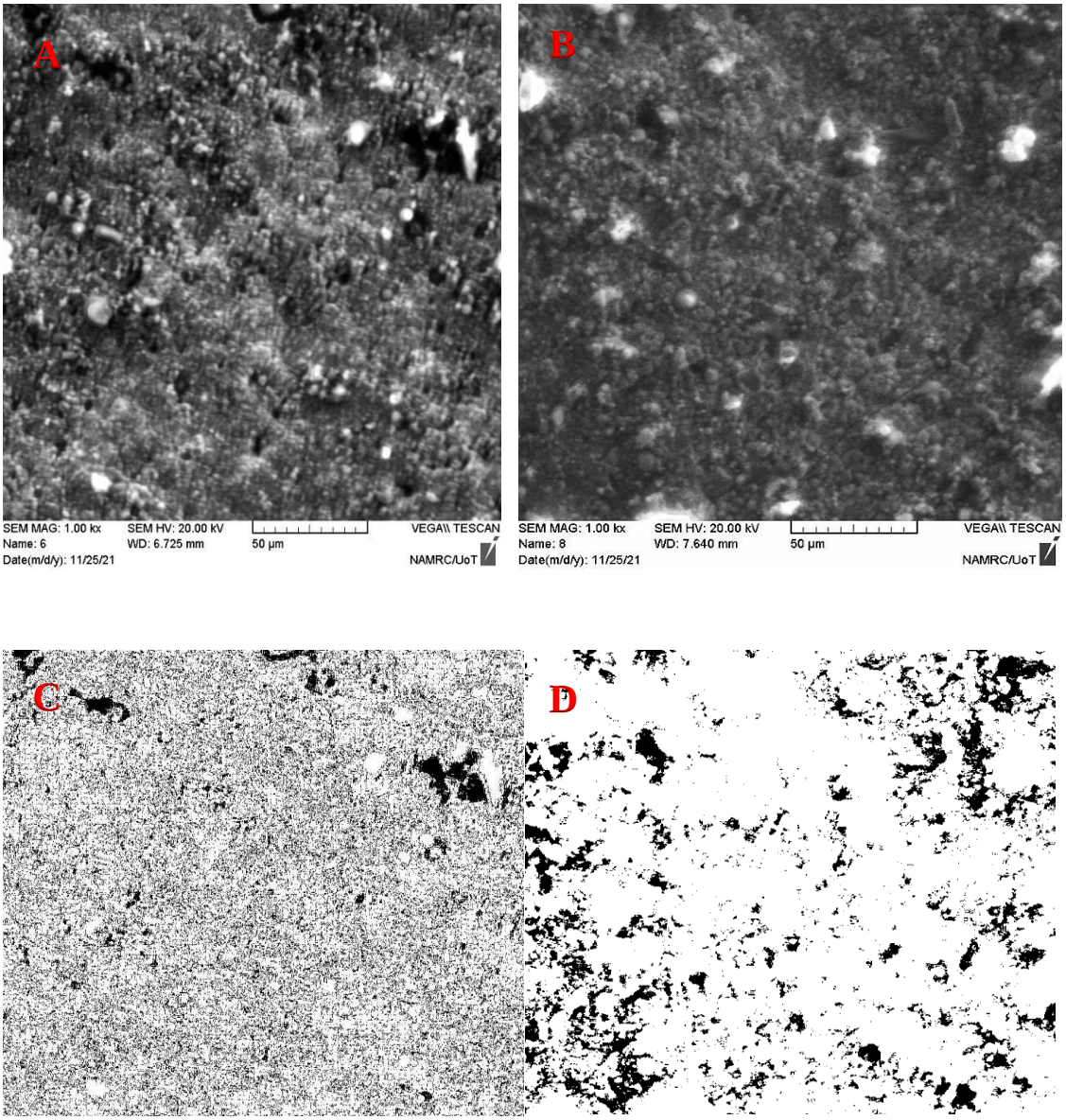

Fig 4.27 :SEM micrographs of A(M4) and B (M7) that are modified into C and D respectively to evaluate porosity by image J software.

Table 4. Porosity values taken directly from Image J program of M4 and M7

slice	Count	Total Area	Average Size	%Area	Mean	Perim.
6.jpg(M4)	21859	10026.892	0.459	22.639	253.994	2.801
Por (M7)-8	319	5428.92	317.019	12.39	251.634	25.556

4.4.2 . Analysis of simulation results

Temperature difference over piston surface is simulated by Ansys software ,steady state thermal program. based on piston and coating material properties which were entered , and boundary condition also.

The results obtained in this study was great. temperature reduction of about $190C^0$ Compared to a reduction of 75°C for the piston surface using conventional cooling mechanisms .that is , the improvement of lowering temperature of coated piston was 20% at the piston surface for tow type of coating layer . Temperature variation over the tip surface of the piston is illustrated for these cases. It has been evident from the figures 4.28, 4.29 and 4.30 that the temperature is maximum at the center of the crown surface of the piston. Figure (4.28) describes the temperature drop over the bare piston body, and Figure (4.29) represents the results of the M4 coating layer , while Figure (4.30) shows the results of the M7 coating layer, respectively. As shown in these figures the M7 for the coating ceramic materials is more efficient compare with the M4and conventional cooling mechanisms in terms of the temperature drop on the piston surface after coating.

The directional heat flux of the two coatings shown in figures (4.29b and 4.30b) indicates that the majority of the thermal energy transfers toward the surface of the coating layers, making them hotter and confirming the temperature gradient results. The results showed the thermal barrier coating system is active and successful, especially for the coating M7, which has a lower directional heat flux compared with M4, namely, 78.661 Kw/m^2 for the M7 coating layer and 81.621 Kw/m^2 for the M4 coating layer.

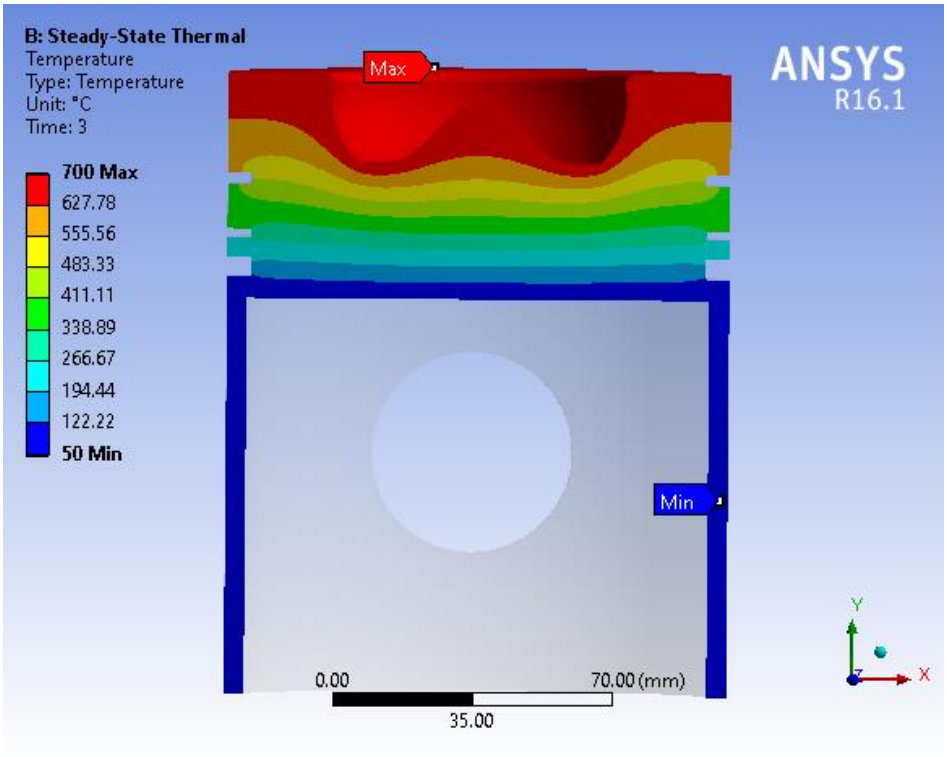

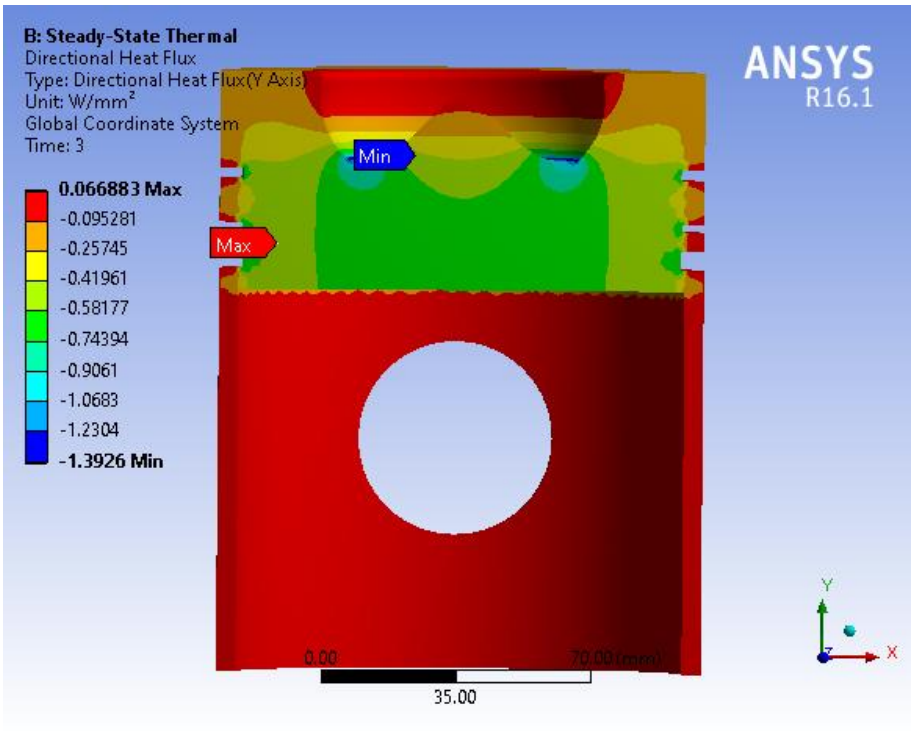

Fig 4.28 represents represent temperature gradient and directional heat flux over Y axis Of bare piston

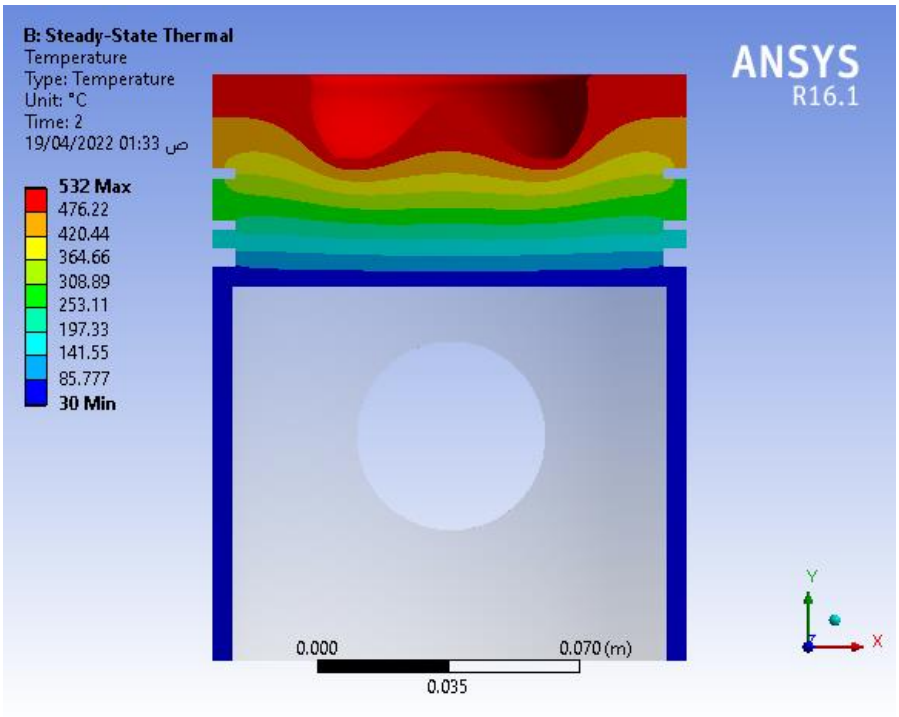

A

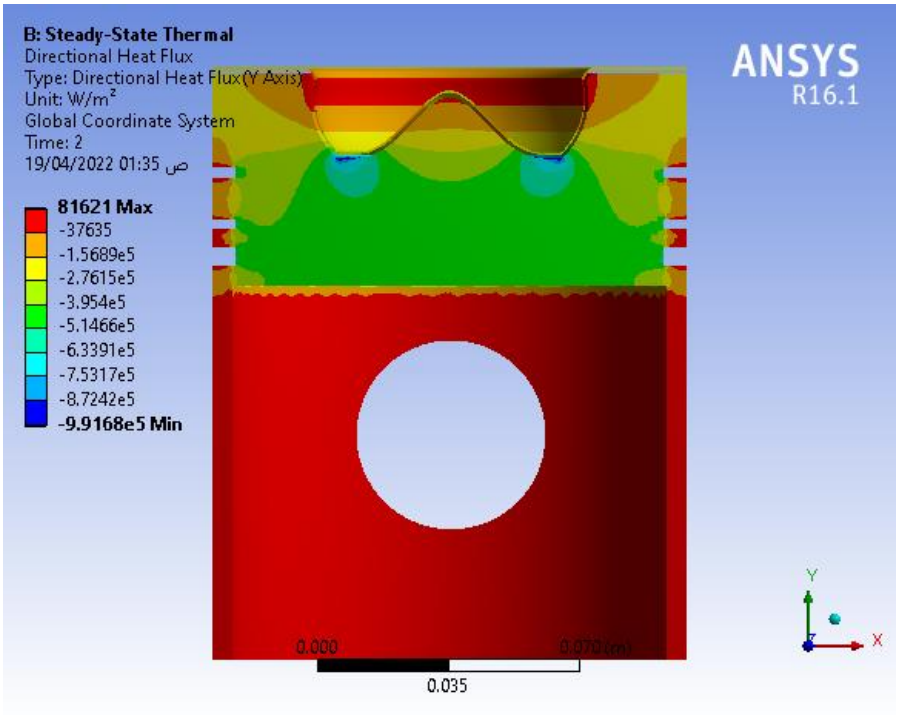

B

Figure 4. 29 represent temperature gradient and directional heat flux over Y axis Of M4 coating layer.

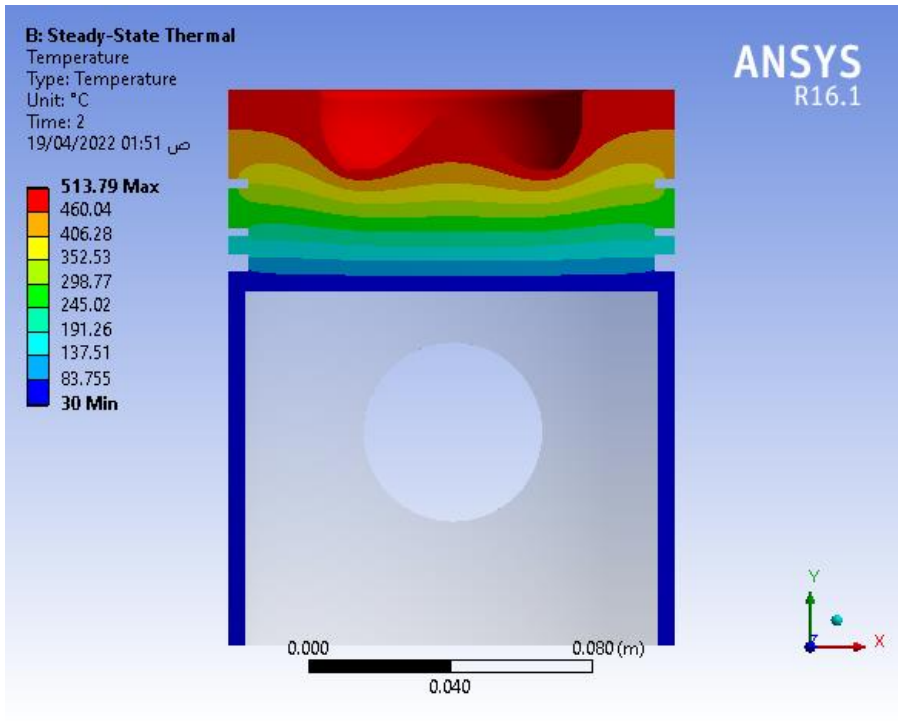

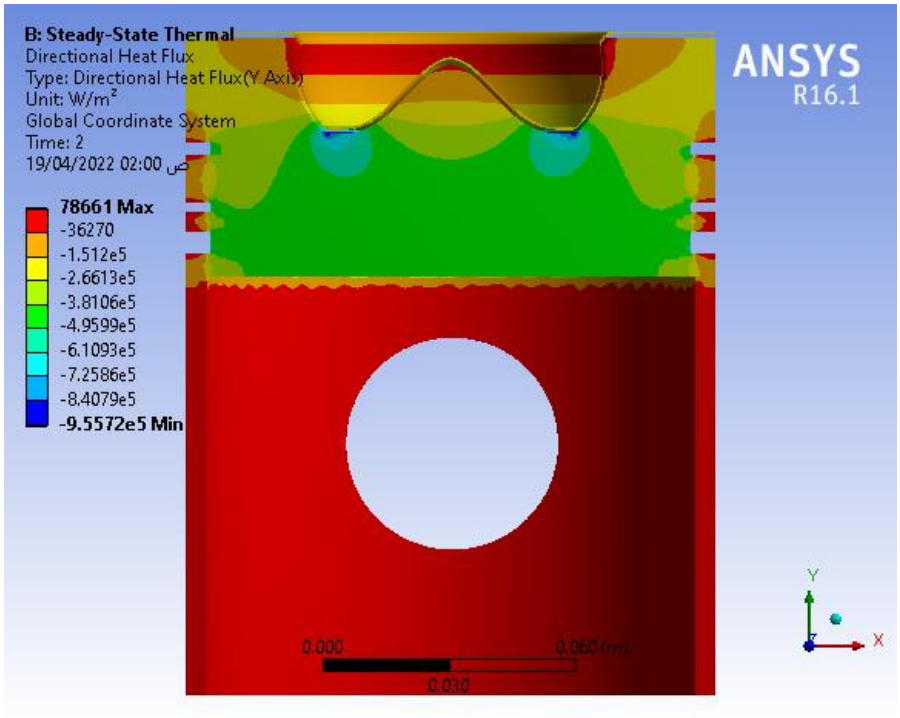

Figure 4.30 represent temperature gradient and directional heat flux over Y axis Of M7 coating layer.

Chapter Five

Conclusions and Recommendations

5.1 Conclusions

The practical results that we obtained after completing the coating using ceramic materials and thermal spraying technique, all the tests that are conducted on the coated models, as well as the simulation results using the ANSYS program for this purpose can be summarized with the following conclusions.

1. MgO using as an essential element in addition to other ceramic oxide produce a thermal barrier coating layer with lower thermal conductivity even lower than yttria stabilized zirconia .
2. The type of flame affects the composition and properties of the coating layer by the presence of a new, unremarkable element to the mixture, such as carbon or oxygen.
3. Gathering the ceramic oxides with flame spraying technique produces a thermal barrier coating with a high adhesion strength .
4. The addition of zirconia to some blends reduces the thermal conductivity of the coating layer.
5. Using ANSYS simulation software reduces the cost, time and introduces accurate results .

5.2. Recommendation and Future work

1. Study the coefficient of thermal expansion of the coating layer
2. Study the effect of particles and pores shape and size on the thermal conductivity of the coating .
3. Study of the effect of base temperature on the properties of the coating layer
4. Using other coating methods such as high-speed thermal spraying , immersion coating and Micro Arc Oxidation process.
5. Take care by using simulation software to test and confirm experimental results
6. Study the failure mechanism that may occur during service
7. This type of coating is considered recent in the automotive industry, so it can be used to improve the environmental and economic properties resulting from the use of fuel.

References

[1] Zhan Yu, Bo Song, Ping Ma, and Wenhui Fan, 'Fabrication of a Novel MgO-B2O3-SiO2-Zn Coating by Thermal Spraying', *Coatings*, vol. 11, no. 907, p. 11, 2021, doi: 7 https://doi.org/10.3390/ coatings11080907.

[2] Huibin Xu and Hongbo Guo, *THERMAL BARRIER COATING*. 80 High Street, Sawston, Cambridge CB22 3HJ, UK: Woodhead Publishing Limited, 2011. [Online]. Available: www.woodheadpublishing.com

[3] C.-G. Fei, Z.-Q. Qian, J. Ren, X.-J. Zhou, and S.-W. Zhu, 'Numerical and Experimental Research on Thermal Insulation Performance of Marine Diesel Engine Piston Based on YSZ Thermal Barrier Coating', *Coatings*, vol. 11, no. 7, p. 765, Jun. 2021, doi: 10.3390/coatings11070765.

[4] Jayant Gopal Thakare, Chandan Pandey, M. M. Mahapatra, and R. S. Mulik, 'Thermal Barrier Coatings—A State of the Art Review', *Metals and Materials International*, p. 22, Apr. 2020.

[5] M. Ranjbar-Far, J. Absi, and G. Mariaux, 'Simulation of the effect of material properties and interface roughness on the stress distribution in thermal barrier coatings using finite element method', *Materials and Design*, vol. 31, pp. 7772–781, 2010, doi: 10.1016/j.matdes.2009.08.005.

[6] S. Bose, *High temperature coatings*. Amsterdam ; Boston: Elsevier Butterworth-Heinemann, 2007.

[7] mohit Gupta, *Design of Thermal Barrier Coatings A Modelling Approach by Mohit Gupta*. University West Trollhättan , Sweden: Springer Cham Heidelberg New York Dordrecht London, 2015.

[8] M. Mathanbabu, P. Mohanraj, S. N. Krishnan, T. N. Kumar, and S. Vijay, 'DESIGN AND THERMAL ANALYSIS OF CERAMIC COATED DIESEL ENGINE PISTON (MgZrO3 & NiCrAl)', *ijser*, vol. 4, no. 1, p. 9, Apr. 2019.

[9] M. Ciniviz, M. Sahir, E. Canl, H. Kse, and zgr Solmaz, 'Ceramic Coating Applications and Research Fields for Internal Combustion Engines', in *Ceramic Coatings - Applications in Engineering*, F. Shi, Ed. InTech, 2012. doi: 10.5772/29993.

[10] P. Dechaumphai and Sucharitpwatskul, *Finite Element Analysis with ANSYS Workbench*. 2018.

[11] Esam M. Alawadhi, *Finite Element Simulations Using ANSYS*, Second. CRC Press, 2016.

[12] D. I. Satyanarayana and N. Rajyalaxmi, 'Thermal Analysis of Ceramic Coated Steel Alloy Piston Used in Diesel Engine Using FEM', vol. 3, no. 9, p. 6, 2016.

[13] Aysegul Aygun, 'NOVEL THERMAL BARRIER COATINGS (TBCs) THAT ARE RESISTANT TO HIGH TEMPERATURE ATTACK BY CaO-MgO-

Al2O3-SiO2 (CMAS) GLASSY DEPOSITS', DISSERTATION, The Ohio State University, 2008.
[14] Ashish ganvir, 'Comparative analysis of Thermal Bar-rier Coatings produced using Suspen-sion and Solution Precursor Feedstock', University West, 2014.
[15] D. R. Clarke and C. G. Levi, 'Materials Design for the Next Generation Thermal Barrier Coatings', *Annu. Rev. Mater. Res.*, vol. 33, no. 1, pp. 383–417, Aug. 2003, doi: 10.1146/annurev.matsci.33.011403.113718.
[16] ANDERS THIBBLIN, 'Thermal Barrier Coatings for Diesel Engines', KTH Royal Institute of Technology Machine Design, Stockholm, Sweden 2017, 2017.
[17] V. Sankar, 'THERMAL BARRIER COATINGS MATERIAL SELECTION, METHOD OF PREPARATION AND APPLICATIONS - REVIEW', p. 10, 2014.
[18] Sanket Shikhariya, Bhushan Shimpi, Abhishek Shinde, and Swapnil U. Deokar, 'Review on Thermal Barrier Coating in IC Engine', *JRITCC*, vol. 5, no. 6, p. 5, Jun. 2017.
[19] J.R. Davis & Associates and Daryl E. Crawmer, Eds., *Handbook of thermal spray technology*. Materials Park, OH: ASM International, 2004.
[20] X. Q. Cao, R. Vassen, and D. Stoever, 'Ceramic materials for thermal barrier coatings', *Journal of the European Ceramic Society*, vol. 24, no. 1, pp. 1–10, Jan. 2004, doi: 10.1016/S0955-2219(03)00129-8.
[21] David R. Clarke and Simon R. Phillpot, 'Thermal barrier coating materials', *Elsevier Ltd 2005*, p. 8, Jun. 2005.
[22] H. Al-Daffaie, 'Characterization of Thin Film Thermal Barrier Coating by Nanotechnology', 2020.
[23] Carter C.Barry and Norton M.Grant, *ceramic material:science and engineering*. springer, 2007.
[24] Charles A. Harper, *HANDBOOK OF CERAMICS, GLASSES, AND DIAMONDS*. McGraw-Hill, 2001.
[25] Philippe Boch and Jean-Claude Niepce, *Ceramic Materials Processes, Properties and Applications*. ISTE Ltd, 2007.
[26] S. Dhomne and A. Mahalle, 'Thermal barrier coating materials for SI engine', *Journal of Materials Research and Technology*, vol. 8, Sep. 2018, doi: 10.1016/j.jmrt.2018.08.002.
[27] C. A. Schacht, Ed., *Refractories handbook*. New York: Marcel Dekker, 2004.
[28] D. L. Perry, *Handbook of inorganic compounds*, 2nd ed. Boca Raton: Taylor & Francis, 2011.
[29] VV. D. Kingery, H.K. Bowen, and D. R.. Ublmann, *Introduction to Ceramics*, Second Edition. John Wiley and sons, 1976.

[30] H. Samadi and T. W. Coyle, 'DESIGN OF ALTERNATIVE MULTILAYER THICK THERMAL BARRIER COATINGS', in *progress in thermal barrier coating*, the american ceramic society, 2009, pp. 111–119.

[31] H.-K. Kim, 'Effect of A Rapid-Cooling Protocol on the Optical and Mechanical Properties of Dental Monolithic Zirconia Containing 3–5 mol% Y2O3', *Materials*, vol. 13, no. 8, Art. no. 8, Jan. 2020, doi: 10.3390/ma13081923.

[32] tadeusz Burakowski and tadeusz Wierzchon, *surface engineering of metals principls,equipment,technologies*. CRC Press, 1999.

[33] v.v. Sobolev, J.M. Guilemany, and J. Nutting, *High Velocity Oxy-Fuel Spraying Theory, Structure-Property Relationships and Applications*, First. W. S. Maney and Son Ltd, 2004.

[34] Z. Babiak, T. Wenz, and L. Engl, 'Fundamentals of Thermal Spraying, Flame and Arc Spraying', in *Modern Surface Technology.*, WILEY-VCH Verlag GmbH & Co. KGaA, Weinheim, 2006, pp. 119–136.

[35] Lech Pawlowski, *The Science and Engineering of Thermal Spray Coatings*, Second. The Atrium, Southern Gate, Chichester: John Wiley & Sons Ltd, 2008.

[36] Galina Xanthopoulou, Amalia Marinou, George Vekinis, Aggeliki Lekatou, and Michalis Vardavoulias, 'Ni-Al and NiO-Al Composite Coatings by Combustion-Assisted Flame Spraying', *mdpi*, vol. 4, pp. 231–252, 2014, doi: 10.3390.

[37] Bikramjit Basu and Kantesh Balani, *Advanced Structural Ceramics*. John Wiley & Sons, Inc., Hoboken, New Jersey, 2011.

[38] Lalit Thakur and Hitesh Vasudev, *thermal spray coatings*, First eddition. CRC Press, 2022.

[39] F. Fanicchia, D. Axinte, J. Kell, R. McIntyre, G. Brewster, A.D.Norton, combustion Flame Spray of CoNiCrAlY & YSZ Coatings, Surface & Coatings Technology (2017), doi:10.1016/j.surfcoat.2017.01.070

[40] M. Oksa, E. Turunen, T. Suhonen, T. Varis, and S.-P. Hannula, 'Optimization and Characterization of High Velocity Oxy-fuel Sprayed Coatings: Techniques, Materials, and Applications', *Coatings*, vol. 1, no. 1, Art. no. 1, Sep. 2011, doi: 10.3390/coatings1010017.

[41] Erich Lugscheider and lngard Kvernes, 'Thermal Barrier Coatings: Powder Spray Process and Coating Technology', in *intermetalic and ceramic coating*, Marcel Dekker, Inc., 1999, p. 498.

[42] P. Robotti and G. Zappini, 'Chapter 9 - Thermal Plasma Spray Deposition of Titanium and Hydroxyapatite on Polyaryletheretherketone Implants', in *PEEK Biomaterials Handbook*, S. M. Kurtz, Ed. Oxford: William Andrew Publishing, 2012, pp. 119–143. doi: 10.1016/B978-1-4377-4463-7.10009-0.

[43] telkar mahesh, Sunil Kumar, V.Vinay, and P.Saisrikanth Goud4, 'Temperature and Thermal Stress Analyses of a Ceramic Coated Aluminum Alloy Piston in a Diesel Engine', *IJSRD*, pp. 116–123, 2016.

[44] Silvio Memme, 'THE INFLUENCE OF THERMAL BARRIER COATING SURFACE ROUGHNESS ON SPARK-IGNITION ENGINE PERFORMANCE AND EMISSIONS', Master of Applied Science Mechanical and Industrial Engineering, University of Toronto, 2012.

[45] Ravinder Reddy Pinninti, 'Temperature and Stress Analysis of Ceramic Coated SiC-Al Alloy Piston Used in a Diesel Engine Using FEA', *ijrset*, vol. 4, no. 8, 2015.

[46] R. Thirunavukkarasu1 and S. Periyasamy2, 'Enhancing Diesel Engine Performance and Balancing Emissions with Effect and Contribution of MgO-ZrO2 and AT13 Layered Piston', *Arabian Journal for Science and Engineering*, p. 9, Aug. 2020, doi: https://doi.org/10.1007/s13369-020-04899-4.

[47] Dr. Ibtihal Al-Namie, Dr. Mahmoud A. Mashkour, A. Mashkour, and Ahmed Sabah Hameed, 'Study the Effect of Ceramic Coating on the Performance and Emissions of Diesel Engine', *Journal of Engineering*, vol. 18, p. 8, Aug. 2012.

[48] Shahanwaz Adam Havale and Prof. Santosh Wankhade2, 'DESIGN, THERMAL ANALYSIS AND OPTIMIZATION OF A PISTON USING ANSYS', *irjet*, vol. 4, no. 12, p. 7, 2017.

[49] G. AGUIRRE-RAMIREZ and J. T. ODEN, 'FINITE ELEMENT TECHNIQUE APPLIED TO HEAT CONDUCTION IN SOLIDS WITH TEMPERATURE DEPENDENT THERMAL CONDUCTIVITY', *INTERNATIONAL JOURNAL FOR NUMERICAL METHODS IN ENGINEERING*, vol. 7, p. 11, 1973.

[50] Avinash Kumar Agarwal, Dhananjay Kumar, Nikhil Sharma, and Utkarsha Sonawane, *Engine Modeling and Simulation*. springer, 2022.

[51] Raymond J. Madachy and Daniel X. Houston, *WHAT EVERY ENGINEER SHOULD KNOW ABOUT MODELING AND SIMULATION*. CRC Press ,Taylor & Francis Group, 2018.

[52] Shuo Wu, 'Review Research Progresses on Ceramic Materials of Thermal Barrier Coatings on Gas Turbine'.2021

[53] S.Balamurugan, V.Bharath, E.Boopathiraja, K.M.Boopathy, and K.Chandrasekar, 'Design and Analysis of Piston coated with Ceramic Materials', *IJARMET*, vol. 4, no. 1, p. 6, Feb. 2020.

[54] A. Rajesh and P.Navven Reddy, 'Temperature and Thermal Stress Analyses of a Ceramic-Coated Aluminum Alloy Piston Used In a Diesel Engine', *ijmetmr*, vol. 3, no. 9, p. 8, 2016.

[55] Jian-Jun Gou, Xing-Jie Ren, Yan-Jun Dai, Shuguang Li, and Wen-Quan Tao, 'Study of thermal contact resistance of rough surfaces based on the practical topography', *Computers and Fluids*, p. 10, 2016, doi: http://dx.doi.org/10.1016/j.compfluid.2016.09.018.

[56] N.Yu. Dudareva, O.P. Dombrovskiy, R.V. Kalschikov, and I.A. Butusov, 'Experimental Study of the Micro-Arc Oxide Coating Effect on Thermal Properties of an Aluminium Alloy Piston Head', in *JOURNAL OF Engineering Science and Technology Review*, Sep. 2015, p. 4. [Online]. Available: www.jestr.org

[57] Widyastuti, M. Lilis, S. Ridwan, and M. A. Putrawan, 'Al2O3 – SiO2 Coating By Flame Spray For Thermal Barrier Coating Application', *AMM*, vol. 493, pp. 691–696, Jan. 2014, doi: 10.4028/www.scientific.net/AMM.493.691.

[58] Dinesh Kumar. J, Harish. R.Sankar, and Raja R, 'Influence Of Thermal Barrier Coatings On S.I Engine Performance', *ijert*, vol. 2, no. 6, p. 6, 2013.

[59] Dr. Ibtihal Al-Namie, Dr. Mahmoud A. Mashkour, and Ali Abu Al-heel Qasim, 'The Effect of Ceramic Coating on Performance and Emission of Diesel Engine Operated on Diesel Fuel and Biodiesel Blends', *Journal of Engineering*, vol. 20, no. 6, p. 18, Jun. 2014.

[60] P. N. Shrirao1 and A. N. Pawar2, 'Experimental Investigation on Performance of Single Cylinder Diesel Engine with Mullite as Thermal Barrier Coating', *Journal of Mechanical Engineering and Technology*, vol. 3, no. 1, p. 10, Jun. 2011.

[61] Julian Heath and Nick Taylor, 'Energy Dispersive Spectroscopy', *John Wiley & Sons Ltd*, p. 32, 2015.

[62] ASTM International, 'Designation: E 384 – 05a Standard Test Method for Microindentation Hardness of Materials1'. ASTM International, Aug. 15, 2005.

[63] H. H. Schloessin and Z. DvoFBk, 'Anisotropic Lattice Thermal Conductivity in Enstatite as a Function of Pressure and Temperature', *Geophys. J. R.astr*, vol. 27, pp. 499–516, 1972.

[64] ryoichi sanadaga, fujio.p.okamura, and hirochi takida, 'X-RAY STUDY OF THE PHASE TRANSFORMATIONS', *MINERALOGICAL JOURNAL*, vol. 6, no. 1–2, pp. 110–130, 1969.

[65] Bin Liua, *et al.*, 'Advances on strategies for searching for next generation thermal barrier coating materials', *Journal of Materials Science & Technology*, vol. 35, pp. 833–851, 2019.

[66] Fei LI, Lin ZHOU, Ji-Xuan LIU, Yongcheng LIANG, and Guo-Jun ZHANG, 'High-entropy pyrochlores with low thermal conductivity for thermal barrier coating materials', *journal of adnanced ceramic*, 2019, doi: 10.1007/s40145-019-0342-4.

[67] Fumihiro Nakamori, Yuji Ohishi, Hiroaki Muta, Ken Kurosaki, and Ken-ichi, 'Mechanical and thermal properties of ZrSiO4', *Journal of Nuclear Science and Technology*, vol. 54, pp. 1267–1273, Aug. 2017.

[68] Y. Cao, C. Li, Y. Ma, H. Luo, Y. Yang, and H. Guo, 'Mechanical properties and thermal conductivities of 3YSZ-toughened fully stabilized HfO2 ceramics', *Ceramics International*, vol. 45, no. 10, pp. 12851–12859, Jul. 2019, doi: 10.1016/j.ceramint.2019.03.208.

[69] Ke Ren, Qiankun Wang, Gang Shao, Xiaofeng Zhao, and Yiguang Wang, 'Multicomponent high-entropy zirconates with comprehensive properties for advanced thermal barrier coating', *Acta Materialia Inc. Published by Elsevier Ltd.*, vol. 178, pp. 382–386, 2020, doi: https://doi.org/10.1016/j.scriptamat.2019.12.006.

[70] Satish Tailor, Nitesh Vashishtha, Ankur Modi, and S. C. Modi, 'High-Performance Al2O3 Coating by Hybrid-LVOF (Low-Velocity Oxyfuel) Process', *ASM International*, Mar. 2020, doi: 10.1007.

[71] Ruqaya A. Abbas, Sami A. Ajeel, Maryam A.Ali bash, and Mohammed J. Kadhim, 'Effect of plasma spray distance on the features and hardness reliability of YSZ thermal barrier coating', *Materials Today: Proceedings*, pp. 2553–2560, 2021, doi: 10.1016.

[72] John.W Antony, richard.A Bideaux, Kenneth.W.Bladh, and Monte .C Nichols, *handbook of mineralogy*, vol. 5. mieralogical society of America, 2015. [Online]. Available: www.handbookofmineralog.org

[73] Akio Kawaguchi, YoshifumiWakisaka, Naoki Nishikawa, and Hidemasa Kosaka, 'Thermo-swing insulation to reduce heat loss from the combustion chamber wall of a diesel engine', *international of engine research*, p. 12, 2019, doi: 10.1177.

[74] Satyapal Mahade, 'Functional Performance of Gadolinium Zirconate/Yttria Stabilized Zirconia Multi-Layered Thermal Barrier Coatings', PhD Thesis, University West SE-46186 Trollhättan Sweden +46 52022 30 00 www.hv.se, 2018. [Online]. Available: 978-91-87531-85-9

[75] Shrikant Joshi and Per Nylen, 'Review Advanced Coatings by Thermal Spray Processes', *MDPI/tecnologies*, vol. 7, no. 79, p. 14, Nov. 2019, doi: 10.3390.

[76] S. C. Stacy, X. Zhang, M. Pantoya, and B. Weeks, 'The effects of density on thermal conductivity and absorption coefficient for consolidated aluminum nanoparticles', *International Journal of Heat and Mass Transfer*, vol. 73, pp. 595–599, Jun. 2014, doi: 10.1016/j.ijheatmasstransfer.2014.02.050.

[77] Leszek Wojnar, *image analysis Applications in Materials Engineering*. CRC Press LLC, 1999.

Appendix A

Diesel piston egnine that was used in specimen set up

Part of piston after cutting to prepare specimens

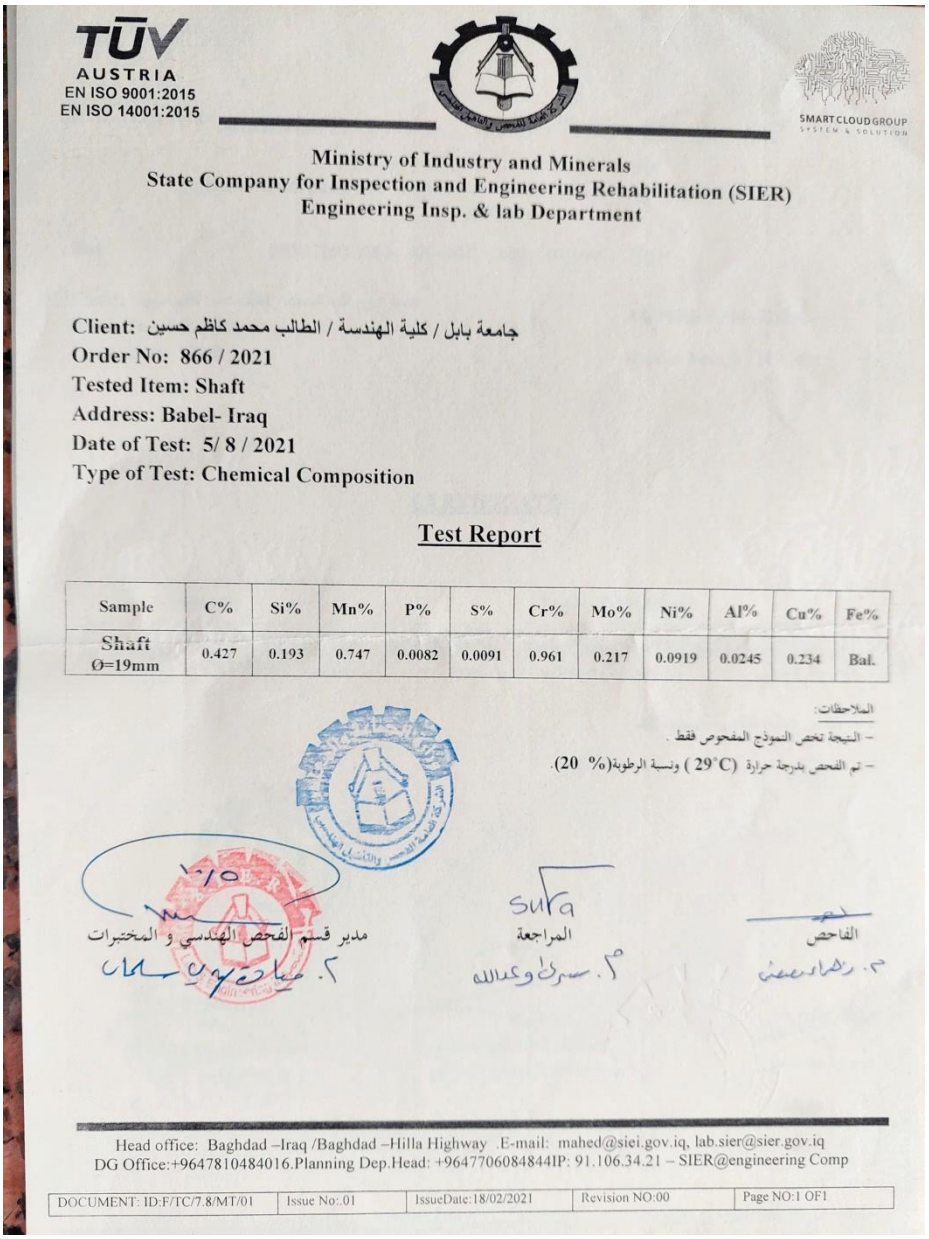

TÜV AUSTRIA
EN ISO 9001:2015
EN ISO 14001:2015

SMART CLOUD GROUP

Ministry of Industry and Minerals
State Company for Inspection and Engineering Rehabilitation (SIER)
Engineering Insp. & lab Department

Client: جامعة بابل / كلية الهندسة / الطالب محمد كاظم حسين
Order No: 866 / 2021
Tested Item: Shaft
Address: Babel- Iraq
Date of Test: 5/ 8 / 2021
Type of Test: Chemical Composition

Test Report

Sample	C%	Si%	Mn%	P%	S%	Cr%	Mo%	Ni%	Al%	Cu%	Fe%
Shaft Ø=19mm	0.427	0.193	0.747	0.0082	0.0091	0.961	0.217	0.0919	0.0245	0.234	Bal.

الملاحظات:
- النتيجة تخص النموذج المفحوص فقط .
- تم الفحص بدرجة حرارة (29°C) ونسبة الرطوبة(20 %).

مدير قسم الفحص الهندسي و المختبرات
المراجعة
الفاحص

Head office: Baghdad –Iraq /Baghdad –Hilla Highway .E-mail: mahed@siei.gov.iq, lab.sier@sier.gov.iq
DG Office:+9647810484016.Planning Dep.Head: +9647706084844IP: 91.106.34.21 – SIER@engineering Comp

DOCUMENT: ID:F/TC/7.8/MT/01	Issue No:.01	IssueDate:18/02/2021	Revision NO:00	Page NO:1 OF1

Certificate of Chemical composition of A304 4041H piston alloy steel

TÜV AUSTRIA
EN ISO 9001:2015
EN ISO 14001:2015

SMART CLOUD GROUP

Ministry of Industry and Minerals
State Company for Inspection and Engineering Rehabilitation
(SIER)

866 ISO 17025:2005 ISO 9001: 2015 ISO14001: 2015

Client:- جامعة بابل / كلية الهندسة / الطالب محمد كاظم حسين
Order No:- 866/2021
Tested Item:- Shaft

Address:- Iraq - Babel
Date of Test: 5 / 10 / 2021

CERTIFICATE

Sample	Type of Material
Shaft (Ø = 19)mm	المعدن يقع ضمن المواصفة القياسية ASTM وضمن النوعية A 304 4140H

- المطابقة من حيث الخواص الكيميائية فقط .

مسؤول شعبة المواصفات
م. تمارة نوري عبد علي

اعداد
م.مروة اياد توفيق

م. احمد ناصر هاشم
R.D.S
SIER
٥/١٠/٢٠٢١

Head office: Baghdad - Iraq /Baghdad –Karbala Highway E-mail: mahed@sier.gov.iq, lab.sier@sier.gov.iq

Identification certificate of A304 piston steel alloy

الخـــلاصـــة

تستخدم محركات الديزل في العديد من التطبيقات الصناعية بالإضافة إلى تلك المستخدمة في السيارات. يعد تطوير محركات الديزل لتكون أكثر كفاءة مع استهلاك أقل للوقود وانبعاثات غازية منخفضة وأداء عالي هدفًا للعديد من الباحثين. تم تحديد طلاء الحاجز الحراري الخزفي باعتباره أكثر الطرق الواعدة لتطوير محركات الديزل.

في هذه الدراسة ،تم طلاء (TBC) مبتكر مكون من طبقة طلاء واحدة ، في محاولة لاستبدال طلاء الزركونيا المثبت من اليتريا والذي يحتوي على ثلاث طبقات للتغلب على العديد من المشاكل مثل التشظي .بالإضافة إلى انخفاض الموصلية الحرارية, فإنه يحسن ميزات الاحتراق ، مما يؤدي إلى تعزيز الكفاءة والأداء الاقتصادي والبيئي لمحرك الديزل. تم جلب مكبس الديزل A304 المصنوع من سبائك الصلب من متاجر شركة توزيع المنتجات النفطية (OPDC) / فرع بابل. تم تحضير ثماني عينات من أجل فحص ترسيب ثمانية خلطات من مواد خزفية ، أي أكسيد المغنيسيوم (MgO) ، وأكسيد الألومنيوم (Al2O3) ، وأكسيد السيليكون (SiO2) ، وأكسيد الزركونيوم (ZrO2) ، بنسب مختلفة وتم ترقيمها (M1، M2، ... M8). يُظهر اثنان من هذه الخلطات أقل موصلية حرارية من بين الخلطات الأخرى ، وهي M4 التي تحتوي على (MgO = 30٪ ، Al2O3 = 45٪ ، SiO2 = 25٪) ، و M7 التي تحتوي على (MgO = 35٪ ، Al2O3 = 30٪ ، SiO2 = 25٪ ، ZrO2 = 10٪).

الرش باللهب هو التقنية المعتمدة باستخدام خليط الأسيتيلين والأكسجين تحت ضغط 0.6 بار و 5 بار للأسيتيلين والأكسجين ، على التوالي. علاوة على ذلك ، تم إجراء اختبارات حيود الأشعة السينية (XRD) ، والفحص المجهري الإلكتروني (SEM) ، واختبارات مجهر القوة الذرية (AFM) لتحديد وتوصيف البنية المجهرية ومورفولوجيا الطبقة المطلية. يتم أيضًا اختبار الموصلية الحرارية وسماكة طبقة الطلاء ومحتوى المسامية وقوة الالتصاق لتحديد الموصلية الحرارية لطبقة طلاء الحاجز الحراري ، والذي أكد أن الموصلية الحرارية لـ M4 و M7 كانت الأقل من بين الخلطات الأخرى ، والتي لها أدنى قيم بلغت حوالي 0.831334 W / m .c و 0.72186 W / m .c ، على التوالي. كانت سماكة طبقة الطلاء حوالي 0.6 مم مع محتوى مسامي حوالي 15-20٪ وكانت أعلى قوة التصاق للعينات حوالي 20 ميجا باسكال ، والتي كانت لخليط M7.

تم استخدام النتائج في عملية المحاكاة باستخدام برنامج محاكاة Ansys workbench 16.1 كشرط حراري ثابت. تم بناء النموذج باستخدام الأبعاد الفعلية لمكبس الديزل وطبقة الطلاء ، ثم تمت محاكاته بحالة أولية وحدودية (700 درجة مئوية كدرجة حرارة التشغيل و 30 درجة مئوية كدرجة حرارة أولية وبيئية). حتى الحصول على أفضل عدد من العناصر وهو (213514) عنصر و (303548) عقد بالشكل التربيعي. أكدت النتائج المتحصل عليها انخفاض درجة الحرارة على سطح تاج المكبس بعد الطلاء إلى (534 Co و 513 Co) لعينات M4 و M7 المطلية على التوالي. وهذا يعني أن درجات الحرارة المنخفضة تراوحت بين 165 درجة مئوية و 190 درجة مئوية.

.

.

وزارة التعليم العالي والبحث العلمي
جـــــامعة بـــــابـــــل
كـــــلية هندســـــة المـــواد
قـــسم السيرامـــيك ومواد البناء

استقصاء الخواص الحرارية للمواد السيراميكية الاوكسيدية كطبقة طلاء لمكابس محركات الديزل

رسالة

مقدمة الى قسم السيراميك ومواد البناء في كلية هندسة المواد / جامعة بابل

كجزء من متطلبات نيل درجة الماجستير في هندسة المواد/ السيراميك

من قبل الباحث
محمد كاظم حسين علوان
بكالوريوس هندسة مواد 2002

بإشراف
أ. د. الهام عبد المجيد
أ. د. حيدر كريدي راشد